DOCTORAL THESIS

Mechanochemical Approach to Biotin-Containing Hemicucurbiturils

Elina Suut-Tuule

TALLINNA TEHNIKAÜLIKOOL
TALLINN UNIVERSITY OF TECHNOLOGY
TALLINN 2026

TALLINN UNIVERSITY OF TECHNOLOGY
DOCTORAL THESIS
47/2026

Mechanochemical Approach to Biotin-Containing Hemicucurbiturils

ELINA SUUT-TUULE

TAL TECH PRESS

TALLINN UNIVERSITY OF TECHNOLOGY
School of Science
Department of Chemistry and Biotechnology
This dissertation was accepted for the defence of the degree of Doctor of Philosophy in Chemistry 22/07/2026

Supervisor: Prof. Riina Aav
School of Science
Tallinn University of Technology
Tallinn, Estonia

Co-supervisor: Dr. Dzmitry Kananovich
School of Science
Tallinn University of Technology
Tallinn, Estonia

Opponents: Prof. Agnieszka Szumna
Institute of Organic Chemistry
Polish Academy of Science
Warsaw, Poland

Dr. Dominik Lungerich
CEMES-CNRS (Centre for Materials Elaboration and Structural Studies, French National Centre for Scientific Research)
University of Toulouse
Toulouse, France

Defence of the thesis: 26/08/2026, Tallinn

Declaration:
Hereby I declare that this doctoral thesis, my original investigation and achievement, submitted for the doctoral degree at Tallinn University of Technology has not been submitted for doctoral or equivalent academic degree.

Elina Suut-Tuule

---
signature

European Union
European Regional
Development Fund

Investing
in your future

ISSN 2585-6898 (paperback)
ISBN 978-9916-80-531-2 (paperback)
ISSN 2585-6901 (PDF)
ISBN 978-9916-80-532-9 (PDF)
https://doi.org/10.23658/taltech.47/2026

Suut-Tuule, E. (2026). *Mechanochemical Approach to Biotin-containing Hemicucurbiturils* [TalTech Press]. https://doi.org/10.23658/taltech.47/2026

TALLINNA TEHNIKAÜLIKOOL
DOKTORITÖÖ
47/2026

Biotiini sisaldavate hemikukurbituriilide mehhanokeemiline süntees

ELINA SUUT-TUULE

TAL TECH
KIRJASTUS

Contents

List of Publications

The list of author's publications, on the basis of which the thesis has been prepared:

I **E. Suut-Tuule**[‡], T. Jarg[‡], P. Tikker, K.-M. Lootus, J. Martõnova, R. Reitalu, L. Ustrnul, J. S. Ward, V. Rjabovs, K. Shubin, J. V. Nallaparaju, M. Vendelin, S. Preis, M. Öeren, K. Rissanen, D. Kananovich, R. Aav. Mechanochemically Driven Covalent Self-Assembly of a Chiral Mono-Biotinylated Hemicucurbit[8]uril. *Cell Reports Physical Science*, **2024**, 5, 102161.

II T. Jarg, J. Tamm, **E. Suut-Tuule**, K.-M. Lootus, D. Kananovich, R. Aav. How reliable is internal standard method in monitoring mechanochemical synthesis? A case study of triphenylmethane in HPLC-UV-MS analysis of hemicucurbit[n]urils. *RSC Mechanochemistry,* **2025**, 2, 507-515.

III **E. Suut-Tuule**, E. Schults, T. Jarg, J. Adamson, D. Kananovich, R. Aav. Scalable mechanochemical synthesis of biotin[6]uril. *ChemSusChem*, **2025**, e202402354.

Note [‡] – shared first authorship.

Author's Contribution to the Publications

Contribution to the papers in this thesis are:

I The author had a major role in the method development, synthesis and characterisation of compounds used in the study. The author had a major role in the compilation of the supporting material and significant role in the preparation of the manuscript.

II The author was responsible of conducting synthesis experiments used in this study. The author participated in the preparation of the manuscript.

III The author had a major role in the method development, synthesis and characterisation of compounds used in the study. The author had a major role in the compilation of the supporting material and significant role in the preparation of the manuscript.

Author's Other Publications and Conference Presentations

Other publications:

1. Šakarašvili, M., Ustrnul, L., **Suut, E.**, Nallarapaju, J. V., Mishra, K. A., Konrad, N., Adamson, J., Borokov, V., Aav, R. Self-Assembly of Chiral Cyclohexanohemicucurbit[n]urils with Biz(Zn Porphyrin): Size, Shape, and Time-Dependent Binding. *Molecules* **2022**, 27, 937.

Patent application:

1. Method of preparation of chimeric hemicucurbit[n]urils, derivatives, and uses thereof; Tallinn University of Technology, School of Science, Department of Chemistry and Biotechnology; Riina Aav, Elina Suut-Tuule, Tatsiana Jarg, Tatsiana Nikonovich, Dzmitry Kananovich, Lukaš Ustrnul; Priority number: EP23181344.5; Priority date: 26.06.2023, International Application number: PCT/IB2024/056236, Publication number: WO/2025/003925

Conference presentations:

1. Suut-Tuule, E.; Konrad, N.; Schults, E.; Allik, T. P.; Kananovich, D.; Aav, R. Scalable Mechanochemical Synthesis of Biotin[6]uril and Selective Lanthanide Recognition by Its Derivatives. Balticum Organicum Syntheticum (BOS), 28 June – 1 July **2026**, Tallinn, Estonia. (Poster)
2. Suut-Tuule, E.; Schults, E.; Jarg, T.; Kananovich, D.; Aav, R. Scalable Mechanochemical Synthesis of Biotin[6]uril. 11th International Conference on Mechanochemistry and Mechanical Alloying (INCOME), 14 – 18 September **2025**, Berlin, Germany. (Poster)
3. Suut-Tuule, E.; Schults, E.; Jarg, T.; Kananovich, D.; Aav, R. Mechanochemical synthesis of biotin[6]uril. Book of Abstracts: Summer School on Organic Synthesis under Non-classical Conditions, 2 – 6 September **2024**, Poland, Warsaw. (Poster)
4. Suut, E.; Shalima, T.; Kananovich, D.; Aav, R. Mechanochemical Synthesis of New Mono-Functionalized Cyclohexanohemicucurbit[8]uril. Balticum Organicum Syntheticum (BOS), 3 – 6 July **2022**, Vilnius, Lithuania. (Poster)

Introduction

A major challenge in chemistry is sustainable access to molecules with specific functions. Macrocyclic cavitands are complex molecules, often with molecular weights exceeding 1000 Daltons, with important roles in constructing functional supramolecular systems, such as molecular machines and selective sensing materials. Hemicucurbiturils (HCs) are a family of macrocyclic cavitands renowned for their anion-binding properties, which are relevant in chiral recognition,[1–3] environmental science for sensing and removing pollutants,[4,5] and transmembrane transport.[6–8] HCs are traditionally synthesised in solution by polycondensation of urea monomers with formaldehyde in a one-pot reaction via dynamic covalent chemistry (DCC). HC synthesis is controlled by anion templation, which determines the size of macrocyclic cavitands and thereby establishes their anion-binding properties. While most HCs comprise one type of repeating monomer, introducing additional functional monomers into the macrocycle scaffold can enhance the chemical diversity of these cavitands and therefore their versatility for supramolecular applications.

Solvent-based synthesis of HCs can be labour-intensive, deliver moderate yields, and rely on large volumes of mineral acid solution, which poses significant scalability and environmental challenges. Additionally, assembling a non-uniformly composed macrocycle in a single step can be extremely difficult due to the vast array of possible linear and cyclic intermediates. A more sustainable alternative to traditional solution-based synthesis is mechanochemistry. Its advantages include reduced solvent usage, a concentrated reaction environment and faster reaction rates, resulting in higher conversions, yields and time economy. However, only a limited number of macrocyclic cavitands have been synthesised in the solid state.[9–17]

Advancing knowledge in this area is vital for developing new sustainable synthetic methods for macrocyclic cavitands and enabling the discovery of new applications. Accordingly, this thesis contributes to the solid-state synthesis of HCs.

This doctoral thesis begins with an overview of the HC family of macrocyclic cavitands and their synthesis strategies. This is followed by a brief overview of mechanochemistry, highlighting the instrumentation and variable parameters and shedding light to the advantages and disadvantages of this method.

The primary aim of this research was to investigate new solid-state methods for the synthesis of D-biotin-containing HCs. In the first publication, a chimeric enantiopure mono-biotinylated cyclohexanohemicucurbit[8]uril (mixHC[8]) was synthesised *via* mechanochemistry and its anion-binding properties were evaluated (Publication I). This macrocycle comprised two different urea monomers, involving a diverse range of possible intermediates, making the selective synthesis challenging. Furthermore, as the macrocycle contained a carboxylic functional group, it was covalently immobilised on 3-aminopropyl-functionalised silica gel. The resulting functionalised material was used for the selective capture of perchlorate. A quantitative analytical method was developed to enable reliable monitoring of the composition of the mechanochemical reaction mixtures (Publication II).

Scaling up reactions can be difficult in solution-based and mechanochemical synthesis. Thus, the next part of the thesis focuses on developing a scalable mechanochemical approach to obtain biotin[6]uril (Publication III), which was previously synthesised in strongly acidic solution (7M HCl) in moderate 40–60% yields. The goal was to develop a practical mechanochemical protocol to obtain biotin[6]uril at the decagram scale in high

yield and purity. Optimisation studies in a shaker mill were successfully followed by scale-up in a planetary mill. The new mechanochemical method produces biotin[6]uril in a high 92% yield, reduces the process mass intensity (PMI) by nearly 60-fold and reduces the mineral acid consumption by 190-fold.

Through these results, the thesis emphasises the synthetic potential of mechanochemistry. The chemical industry is notorious for its waste generation; however, mechanochemistry is a valuable tool for reducing this waste generation and overall carbon footprint. In addition to publishing the results in peer-reviewed journals, the results have been presented at various international conferences in Lithuania, Estonia, Poland and Germany.

Abbreviations and Pictograms

AE	atom economy
API	active pharmaceutical ingredient
APS	3-aminopropyl silica gel
BaU[*n*]	bambus[*n*]uril
BO	bayesian optimisation
B[6]U	biotin[6]uril
CB	cucurbituril
CDI	carbonyldiimidazole
cycHC[*n*]	cyclohexanohemicucurbit[*n*]uril
DCC	dynamic covalent chemistry
DCL	dynamic covalent library
DFT	density functional theory
DoE	design of experiments
DOSY	diffusion-ordered spectroscopy
DP	degree of polymerisation
HC[*n*]	Hemicucurbit[*n*]uril
HPLC-UV-MS	high-performance liquid chromatography-ultraviolet-mass-spectrometry
IBX	2-iodoxybenzoic acid
ITC	isothermal titration calorimetry
IUPAC	International Union of Pure and Applied Chemistry
LAG	liquid-assisted grinding
mixHC[8]	mono-biotinylated cyclohexanohemicucurbit[8]uril
MOF	metal-organic framework
NMR	nuclear magnetic resonance
OFAT	one-factor-at-a-time
PFAS	per- and polyfluoroalkyl substances
PMI	process mass intensity
PMMA	poly(methyl methacrylate)
PTFE	polytetrafluoroethylene
RAE	real atom economy
RAM	resonant acoustic mixing
RME	reaction mass efficiency
RSD	relative standard deviation
RSM	response surface methodology
SC-XRD	single-crystal X-ray diffraction
TBA	tetrabutylammonium
TCR	total carbon dioxide release
TFA	trifluoroacetic acid
TPM	triphenylmethane

TSE	twin-screw extruder
ZIF	zeolitic imidazolate framework
	ball milling
	aging

1 Literature Overview

1.1 Supramolecular chemistry

Supramolecular chemistry, also known as "chemistry beyond the molecule", studies molecular recognition and complex assemblies organised through non-covalent interactions.[18] The term "host-guest chemistry" was proposed by D. J. Cram with J. M. Cram, where the host is the larger molecule (often a macrocycle) from the binding pair and the guest is a smaller species recognised and enclosed by the host through its binding sites.[19] Host-guest chemistry is a part of supramolecular chemistry and its complexes are typically stabilised by non-covalent interactions, such as hydrogen bonding, electrostatic interactions, π-π stacking, hydrophobic effects, and van der Waals forces. Although these interactions are individually weak, their cumulative contribution can provide substantial stabilisation of the host-guest complex.

Macrocyclic molecules are among the most widely used host systems, with applications in molecular recognition and anion binding,[20–22] transmembrane anion transport,[6–8] chiral recognition,[1,23] sensing and removal of pollutants.[4,5] Given the range of applications, supramolecular chemistry, covering the preparation and application of host molecules, is an interdisciplinary field encompassing organic chemistry, physical chemistry, coordination chemistry and material and biological science. Macrocyclic host molecules are commonly constructed from smaller molecular building units and can subsequently form supramolecular complexes or assemblies with suitable guests. These macrocyclic structures are often difficult to synthesise using traditional solution-based synthetic approaches but can be prepared more readily through templated synthesis, in which a guest molecule or ion acts as a template, exploiting host-guest binding interactions.

The advantage was first discovered by Charles J. Pedersen, who developed the potassium-cation-templated synthesis of crown ethers in 1967.[24] This work was expanded by Jean-Marie Lehn, who developed three-dimensional cryptands,[25] and Donald J. Cram, who contributed to investigating the molecular recognition of these two cyclic molecules.[26] In 1987, Charles J. Pedersen, Jean-Marie Lehn and Donald J. Cram were jointly awarded the Nobel prize in chemistry "for development and use of molecules with structure-specific interactions of high-selectivity" (Figure 1A).[27] Following these discoveries, more complex structures were developed. Jean-Pierre Sauvage succeeded in synthesising catenanes, structures where two ring-shaped molecules are linked to form a chain.[28] Sir J. Fraser Stoddart developed rotaxanes, ring-shaped molecules which are mechanically attached to an axle and able to move along it.[29] Bernard L. Feringa designed the first light-driven molecular motors, which were mechanically constructed to spin in the same direction.[30] In 2016, Jean-Pierre Sauvage, Sir J. Fraser Stoddart and Bernard L. Feringa were awarded a joint Nobel prize in chemistry "for the design and synthesis of molecular machines" (Figure 1B).[31] Finally, in 2025, the chemistry Nobel prize was awarded to Susumu Kitagawa, Richard Robson and Omar M. Yagi "for the development of metal-organic frameworks" (Figure 1C).[32] These metal-organic frameworks (MOFs) are porous functional materials bearing large cavities which can capture and adsorb smaller molecules, such as water,[33] hydrogen,[34] carbon dioxide,[35] other gases[36] and even per- and polyfluoroalkyl substances (PFAS).[37] The need for sustainable methods for preparing porous materials has attracted the use of mechanochemistry for MOF synthesis during the last 20 years.[38,39]

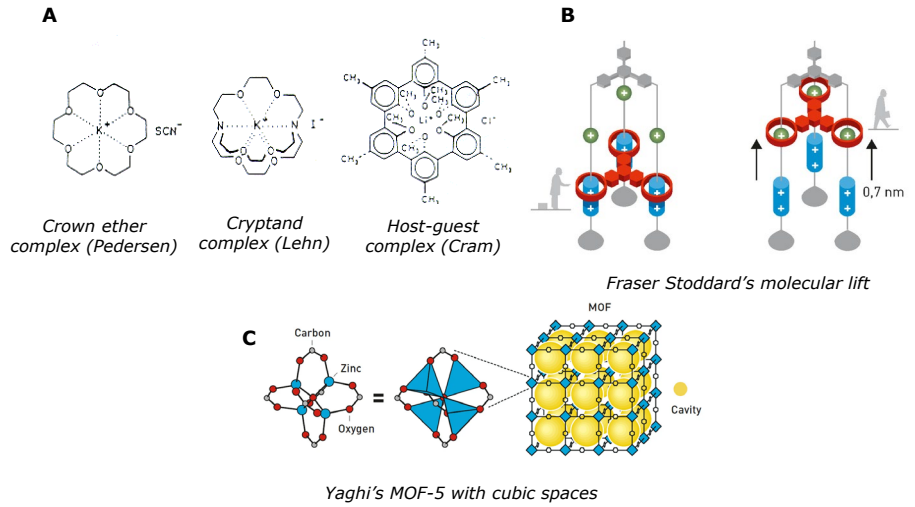

Figure 1. Highlights of chemistry Nobel prizes in supramolecular chemistry: (A) 1987 Nobel prize,[27] (B) 2016 Nobel prize[31] and (C) 2025 Nobel prize.[32] Reproduced from respective Nobel prize press releases and popular science backgrounds; (B) and (C) illustrations: ©Johan Jarnestad/The Royal Swedish Academy of Sciences.

1.2 Hemicucurbiturils

HCs (HC[*n*]s)[40] are macrocyclic compounds composed of covalently linked urea moieties; they are a subclass of a larger family of doubly bridged cucurbituril (CB) macrocycles.[41] HC[*n*]s contain an even number of monomeric units, typically 6 to 12, where [*n*] in the name denotes the number of monomers connected by methylene bridges. In contrast to CBs, the monomers in HC[*n*] are connected through a single methylene bridge, making them more conformationally flexible and resulting in electron-rich portals and hydrophobic, electron-deficient cavities. These molecules are synthesised *via* a thermodynamically driven, template-assisted acid-catalysed polycondensation reaction between urea monomers and formaldehyde, during which carbon-nitrogen bonds are formed.[40]

The first unsubstituted HC[*n*]s, comprising solely of ethylene urea monomers, were reported by Miyahara and colleagues in 2004 (Figure 2).[42] Inspired by this work, numerous substituted HC[*n*]s have been synthesised using different types and numbers of monomers. These include bambus[*n*]urils (BaU[*n*]) and their derivatives, such as semithio- and semiazabambusurils (semithio-BaU[*n*] and semiaza-BaU[*n*]), as well as cyclohexanohemicucurbit[*n*]urils (cycHC[*n*]) and biotin[6]urils (B[6]U), which are all discussed below.

The general approach to synthesising HCs in the solution phase is broadly similar across the different HC subclasses. Urea monomers and formaldehyde (or its polymeric form, paraformaldehyde) are stirred in the presence of a strong Brønsted acid catalyst. Formaldehyde forms methylene bridges, while the anion of the Brønsted acid serves as an essential template for macrocyclic cavitand formation. Although the general reaction conditions are similar, variations arise from the choice of monomers, the type and concentration of acid, and the reaction time.

1.2.1 Hemicucurbituril derivatives, their solvent-based synthesis, properties and applications

The first reported HC[6] was prepared by condensation of ethylene urea and formaldehyde in 4 M HCl solution at room temperature, resulting in a 94% yield after 30 min (Figure 2). Reducing the concentration of HCl to 1 M enabled the synthesis of the larger HC[12] in 93% yield at 55 °C after 3 h. The obtained single-crystal X-ray diffraction (SC-XRD) structures revealed the formation of an HCl adduct, indicating the Cl^- anion position at the centre of the obtained macrocycle. It was also seen that the monomers were in alternating orientation in the macrocycle and half of the C–H bonds in ethylene urea pointed into the cavity, creating an electron-deficient cavity. This property is very favourable for the HC[6] interactions with anions through C–H···anion interactions, including Cl^-,[42] SCN^- and I^-.[43] Moreover, the host-guest interaction between HC[6] and ferrocene was shown to be driven by the formation of hydrogen bonding between the aromatic hydrogen atoms of ferrocene and carbonyl groups on HC[6].[44]

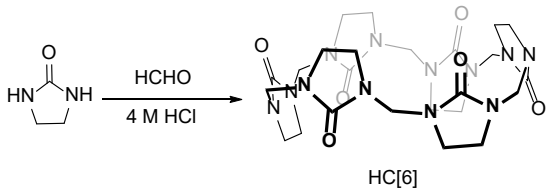

Figure 2. Synthesis of HC[6].

Unsubstituted HC[6] has been employed as a supramolecular catalyst. For example, HC[6] has been successfully used as a catalyst in the esterification of conjugated carboxylic acids, where the host provided a catalytic reaction site and host-guest interactions were monitored by nuclear magnetic resonance (NMR) spectroscopy.[45] Additionally, HC[6] can induce aerobic oxidation of heterocyclic compounds (including furan, 2-methylfuran and thiophene) in aqueous solution. According to the proposed mechanism, host-guest complexation occurs between the furan and HC[6], followed by oxygen attack on an α-carbon of furan and subsequent proton transfer, resulting in the introduction of hydroxyl groups to the furan ring. HC[6] further stabilises the unstable hydroxylated product via encapsulation.[46] Moreover, HC[6] can be used for the selective oxidation of hydroxybenzyl alcohols by acting as a supramolecular protecting agent. HC[6] forms a host-guest complex with the substrate through hydrogen bonding, effectively shielding the phenolic hydroxy groups, rendering them chemically inert and protecting them from oxidation by 2-iodoxybenzoic acid (IBX). IBX then selectively oxidises the benzylic hydroxy group into an aldehyde.[47] In addition to their catalytic properties, HC[6] and HC[12] have been used as molecular carriers to extract several amino acids (including leucine, cysteine, valine, phenylalanine and serine) from the aqueous phase into chloroform.[48] Collectively, these examples highlight the potential of HCs for diverse applications mediated by host-guest interactions.

Bambus[*n*]urils (BaU[*n*]) were first reported by Šindelar and co-workers in 2010 (Figure 3), and the trivial name was given because the structure resembles a bamboo stem. The synthesis procedure is similar to that for HC; 2,4-dimethylglycouril and formaldehyde are stirred in 5.4 M HCl solution, affording 30% of BaU[6]. The 2,4-substituted glycouril monomers are connected by a single methylene bridge.[49]

In 2011, three analogues of BaU[6] were reported – dodecabenzylbambus[6]uril, dodecapropylbambus[6]uril and octabenzylbambus[4]uril.[50] In the first two, the 12 methyl groups in the B[6]U structure were replaced by benzyl or propyl groups. The smaller 4-membered derivative was obtained even in the absence of a template, bearing too small a cavity to accommodate anions. While the first reported BaU[6] was synthesised in aqueous solution, these examples highlight the ability to obtain BaU[*n*] derivatives in organic solvents. Šindelar's group made the first water-soluble BaU[6] by changing the benzyl groups on dodecabenzylbambus[6]uril to 4-carboxybenzyl.[20] Subsequently, they prepared other water-soluble BaUs, using amino,[51] carboxyalkyl[52] and 3,6,9-trioxadecyl[53] groups. Water-soluble receptors attract much interest in medicinal and analytical chemistry. Heck and co-workers further expanded the BaU[*n*] family by synthesising several 4- and 6-membered allylbambus[*n*]urils, one of which was subsequently used in a cross-metathesis reaction with hexene to yield the first mono-functionalised bambusuril.[54] Complex formation between bambusurils and inorganic anions is slow on the ^{1}H NMR time scale; therefore, the complexations are easily visible. Complexes with different anions show distinct chemical shifts, which makes these receptors highly suitable for anion sensing in different solvents.[55] This was demonstrated by the identification of nine different anions and quantification of five of them through encapsulation in dodecabenzylbambus[6]uril by real-time analysis.[56] Moreover, the same bambusuril was used as a carrier in electromembrane extraction, where anions were transported from one aqueous solution to another through a layer of organic solvent-supported membrane.[57] Fluorine-containing benzylated BaU[6]s demonstrated an ability to function as a Cl^-/HCO_3^- carriers.[7]

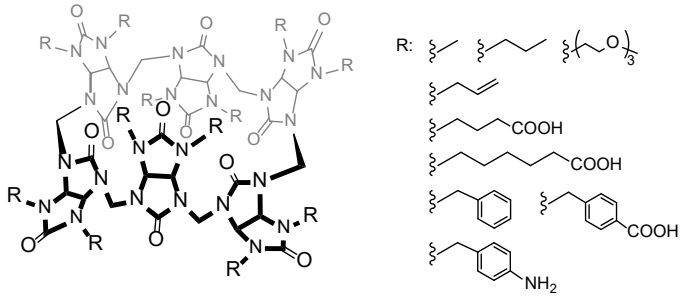

Figure 3. Bambus[6]uril and its derivatives.

In 2015, the first sulphur-containing analogues of BaU[4,6] were described by Reany and co-workers (Figure 4).[58] Like other 6-membered BaU derivatives, semithio-BaU[6] could also bind anions (such as chloride, bromide, iodide or tetrafluoroborate anion) within the macrocyclic cavity; however, the binding affinity was stronger than in oxygen-containing BaU[6]. The smaller semithio-BaU[4] could bind metal cations (Hg^{2+} and Pd^{2+}) through the sulphur atoms located at the portals, as shown by ^{1}H NMR and SC-XRD structures. This introduced new opportunities for dual functionality, as while the cavity is suitable for anion encapsulation, the portal carbonyl groups had previously appeared to be irrelevant to binding. Subsequently, the same group synthesised semiaza-BaU[*n*]s from semithio-BaU[*n*]s *via* a two-step one-pot synthesis.[59] This resulted in a semiaza-BaU[6] with a larger cavity size, able to accommodate multiple anions: two triflates and bromide or iodide between them. These anions were positioned at a short distance of approximately 4 Å, rendering them efficient anion channels.

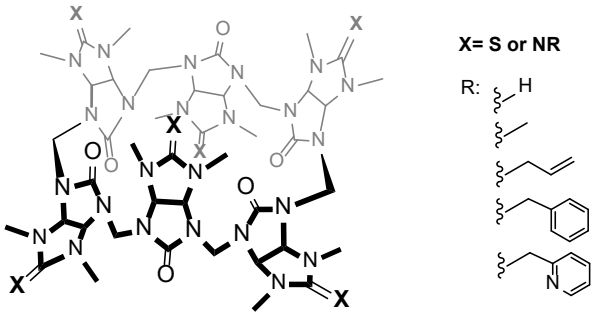

Figure 4. Semithio- and semiaza-BaU[6] derivatives.

Biotin[6]uril (B[6]U), as the first water-soluble HC in the ethylene urea family, was described by Pittelkow and co-workers in 2014 (Figure 5). B[6]U comprises D-biotin (vitamin B7) monomers and can be synthesised using various conditions, but the highest yields were obtained when D-biotin and paraformaldehyde were stirred for 2 days in 3.5 M H_2SO_4 with 5 M NaBr as the template, affording a single isomer in 63% yield. D-biotin has non-equivalent nitrogen atoms; therefore, nine different B[6]U regioisomers are possible, but only one forms selectively.[60] The isolation of a dimeric D-biotin intermediate showed that the two biotin monomers were linked at the nitrogen atoms opposite the carboxylate-containing alkyl chains. Accordingly, the macrocyclisation to B[6]U could be considered as trimerisation of these dimers. This hypothesis was tested by subjecting the dimer to the same reaction conditions used to form B[6]U, and the same conversion to B[6]U was observed. This observation helped rationalise the high regioselectivity. The investigation of the anion-binding properties of B[6]U showed good affinity towards halide anions (iodide > bromide > chloride) in aqueous media with 1:1 binding stoichiometry.

Carboxylic acid side chains were converted into the respective methyl, ethyl and butyl esters to increase the B[6]U solubility in organic solvents. This was achieved using a simple Fischer esterification strategy on B[6]U with the respective alcohols and a catalytic amount of HCl. The B[6]U hexaesters showed good transmembrane anion transport ability.[6]

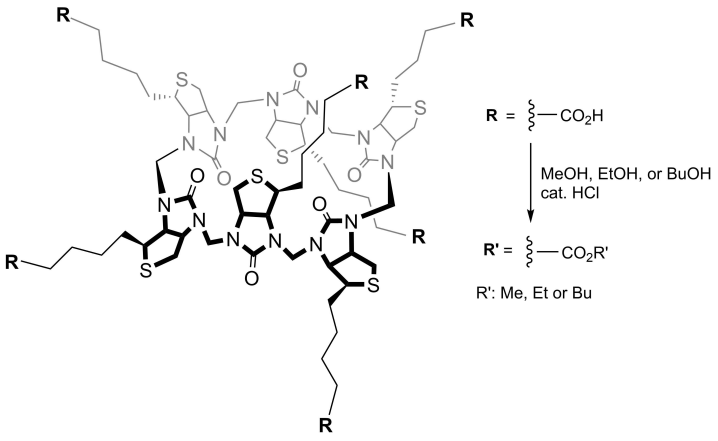

Figure 5. Biotin[6]uril and the corresponding hexaesters.

Additionally, Pittelkow's group reported that the sulphur atoms in B[6]U (and the corresponding hexaesters) could be diastereoselectively oxidised to yield biotin-L-sulphoxide[6]uril using a stoichiometric amount of H_2O_2 in glacial acidic acid, achieving a 72% product yield.[21] Moreover, the carboxylate units in the side chains were amidated *via* a mechanochemical coupling reaction by Aav's research group.[61] In this synthesis, B[6]U underwent a sixfold amidation with L-phenylalanine methyl ester, using uronium-based coupling reagents, to yield hexaamide-B[6]U in high yield and purity.

The first cyclohexanohemicucurbituril (cycHC[*n*]), namely (*R,S*)-cycHC[6], was synthesised in 2009 by Wu and co-workers using an achiral *cis*-cyclohexaneurea monomer. Analogously to the general synthesis of other HCs, the (*R,S*)-cyclohexaneurea monomer and paraformaldehyde were heated in 4 M HCl solution for 4 h and the product was isolated in 78% yield.[62]

The first enantiomerically pure cycHC[6]s were described by Aav and co-workers in 2013; (*S,S*)-cycHC[6] and (*R,R*)-cycHC[6] were prepared (Figure 6) by stirring enantiopure cyclohexaneurea monomers and paraformaldehyde at 80 °C in 4 M HCl or HBr, affording 85% and 64% yields, respectively, after simple filtration of the precipitate.[23] In contrast to *cis*-cycHC[6] and HC[6] where 12 C–H groups of the ethyleneurea moiety face into the cavity, (*S,S*)- and (*R,R*)-cycHC[6] only have six such groups in the *trans*-configuration of the monomer, determined by SC-XRD structures.

Two years later, Aav and co-workers described the synthesis of the cycHC[8] macrocycle (Figure 6) using anions (HCO_2^-, $CF_3CO_2^-$ or PF_6^-) larger than chloride.[63] It was shown that templates must have a suitable size and shape to maximise the favourable interactions between the templating anion and the macrocycle. For example, the acetate anion was insufficient for the cycHC[6] or cycHC[8] formation, while PF_6^- had the appropriate octahedral size and shape to facilitate cycHC[8] formation. Interconversion between cycHC[6] and cycHC[8] is also possible. For example, trifluoroacetic acid can promote cycHC[8] formation, whereas chloride anions can drive the reverse process to cycHC[6] at elevated temperatures. This demonstrates the dynamic nature of acylaminal bond formation under acidic conditions. Differences in cavity size among HC systems are extremely appealing for expanding the applications in host-guest chemistry. Comprehensive investigation of cycHC[8] complexation showed exclusive 1:1 complex formation with anions in the gas phase, in solution and in solid state. Crystallographic studies revealed that the cycHC[8] fits octahedral anions (such as SbF_6^-, PF_6^-) particularly well, whereas tetrahedral guests (like BF_4^- or ClO_4^-) exhibited various degrees of disorder due to the larger space available inside the cavity.[64] In 2020, a 12-membered cycHC[12] macrocycle was isolated with an extremely low yield of 1%.[65] CycHC[*n*]s were also the first chiral HCs synthesised in the solid state (see Chapter 1.3.5 for further discussion).[17]

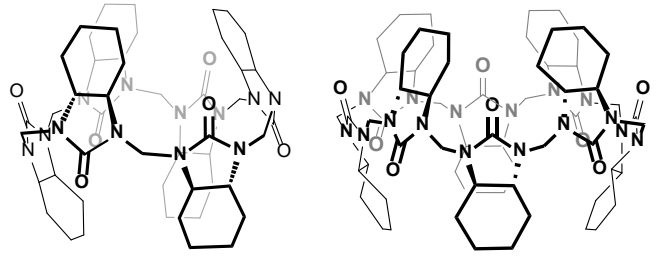

Figure 6. Chiral (R,R)-cycHC[6] and (R,R)-cycHC[8].

In 2019, another member of the cycHC[*n*] family, the thermodynamically unfavoured inverted-*cis*-cycHC[6], was synthesised and isolated by Aav's group.[66] By repeating the reaction for the previously known (*R,S*)-cycHC[6],[62] inverted-cycHC[6] was formed alongside the expected (*R,S*)-cycHC[6] in equal amounts. In this molecule, one of the monomers was in an inverted configuration.

So far, cycHC[*n*]s have been used in the encapsulation of various anions (such as halides, SbF_6^-, PF_6^-, ClO_4^- and others)[23,64] and small electron-rich guests (such as various sulphur- and oxygen-containing heterocycles and other organic guests)[4,67] within their cavities due to the electron deficiency of these cavities. Moreover, it is possible to bind metallo-porphyrins to the outward-facing carbonyl groups, inducing chiral distortion in planar porphyrins, as evidenced by circular dichroism spectroscopy.[68,69]

All previously discussed HCs comprised one type of monomer only, making them homomeric macrocycles. In contrast, several examples of heteromeric ("chimeric") HCs have also been reported, in which different types of monomers are incorporated into a single HC macrocycle. These examples are discussed in Chapter 1.2.3.

1.2.2 Dynamic covalent chemistry approach to hemicucurbituril synthesis

HCs are prepared using DCC, a strategy exploiting the advantages of reversible chemical reactions, in which covalent bonds can reversibly form and break, making them dynamic. Using DCC, given sufficient time, the most thermodynamically stable product will form, and the product distribution depends on the differences in the Gibbs free energies of the final product(s). The equilibrium position can be influenced in two ways: by removing a reaction product or adding an excess of a starting material. Additionally, starting materials can be chosen with specific constitutional characteristics that determine their steric or electronic features, favouring the formation of the most thermodynamically stable product by shifting the equilibrium towards it.[70–72]

Common dynamic covalent bonds include carbon-oxygen, carbon-sulphur, sulphur-sulphur, boron-oxygen and finally carbon-nitrogen bonds, which are present in the methylene bridges of HCs.[73] One of the oldest transformations involving dynamic carbon-nitrogen bonds is the reversible condensation of aldehydes and amines to form imines (Schiff bases), which was discovered by Hugo Schiff in 1864[71,74] and has established the formation of C=N bonds among the most exploited in DCC (Scheme 1).[71] Considering the reversibility of imine bond formation, the reaction could be driven forward by removing the formed water, physically by separation or chemically by adding a drying agent or molecular sieves, which adsorb water from the reaction mixture. However, if additional water is added, the imine bond will undergo hydrolytic cleavage to form the starting amine and carbonyl compound.[71] Moreover, DCC is used to produce hydrazones,[75] aminals,[76] hemiaminals[77] and others.[70,71]

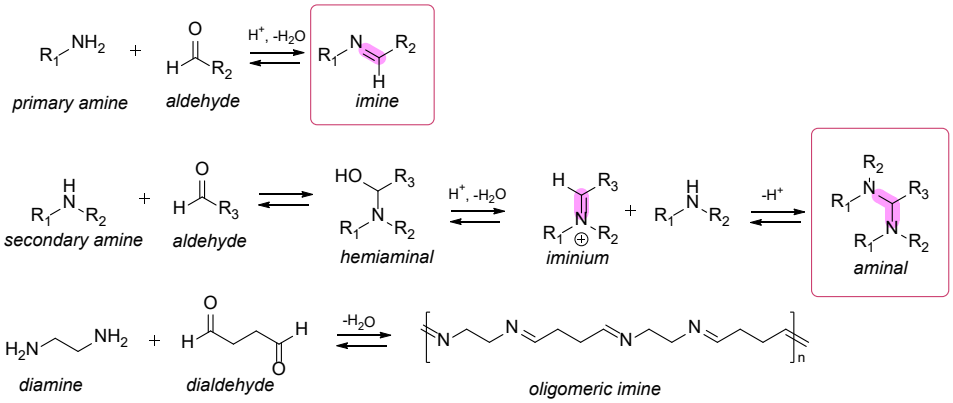

Scheme 1. Formation of imines, aminals and oligomeric imines.

If molecules contain at least two amino- and aldehyde groups, oligomeric imines can be formed, which can be further used for macrocycle formation. Via a reversible covalent bond formation approach to the synthesis of complex molecules, the starting monomers react with one another through DCC, generating dynamic covalent libraries (DCLs) of intermediates that are a mixture of oligomers. Various external parameters can affect the equilibrium of DCC, including the choice of solvent, which affects the solubility and non-covalent interactions, pH, temperature, concentration of monomers, steric and electronic factors. Additionally, introducing a template (such as a metal ion, anion, or small molecule) into the DCL shifts the equilibria towards the most thermodynamically stable product.[70–73]

Monomers in HCs, having a urea moiety, are connected through acylaminal linkages formed following the DCC principles (Scheme 2). Urea monomers react with formaldehyde via a Brønsted acid-catalysed polycondensation reaction. Under these conditions, the formaldehyde oxygen is protonated, making the carbonyl carbon more electrophilic; this is then attacked by urea's weak nucleophilic nitrogen, resulting in water elimination and formation of an iminium intermediate. This extremely reactive intermediate readily reacts with the available nitrogen atom of another monomer, forming an ammonium intermediate; after deprotonation, a neutral acylaminal is formed. Continuous formation of these acylaminal linkages creates oligomers, and the whole oligomerisation process is reversible because, under acidic conditions these linkages can undergo hydrolysis to the iminium species through the protonation of the neighbouring nitrogen or oxygen of the acyl group.[78] The same acid-catalysed polymerisation reaction process occurs to connect monomers via acylaminal linkers, regardless of whether the starting monomer is ethylene urea, biotin or cyclohexaneurea, to form HCs, B[6]U or cycHC[*n*], respectively. Therefore, it is possible to produce heteromeric HCs in a one-pot synthesis due to the same urea moiety and functional group availability.

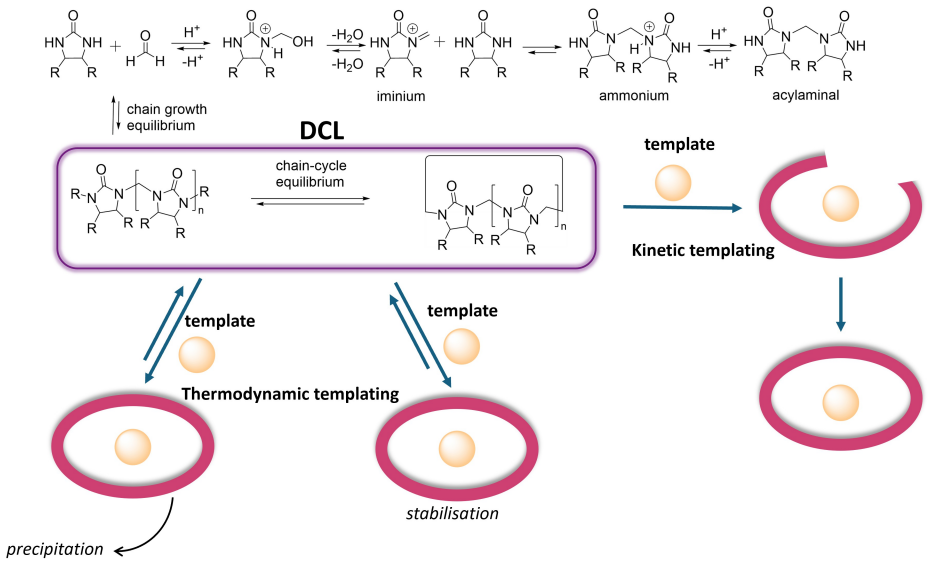

Scheme 2. Acylaminal linkage formation and templation effects in HC synthesis via DCL.

Templated synthesis of HCs includes three reversible processes – chain growth, chain-macrocycle equilibrium and product stabilisation through templating or precipitation, all of which can be influenced by the external parameters mentioned above. A range of oligomers of different lengths is formed by a reversible polycondensation reaction of the respective monomers, and the polymerisation degree (DP) and oligomeric abundance are determined by the chain growth equilibrium. HC formation is determined by chain-cycle equilibrium, which must promote the accumulation of the cyclic product. Inter- and intramolecular reactions are important, the former is responsible for the growth of oligomers, whereas the latter terminates chain growth by macrocyclisation.[78] Anionic templates were found to be among the most important factors promoting HC formation.[40,55,79] The obtained products are stabilised by precipitation from acidic solution or host-guest complex formation.[78]

In a simple classification, templates can have a kinetic or a thermodynamic effect. If **kinetic templating** occurs, the template will attach to the linear oligomer in the DCL through non-covalent interactions, bringing the two chain ends closer to each other. This accelerates the rate of macrocyclisation for a particular product. In the case of **thermodynamic templation**, the template binds to the macrocycle, forming a complex, which is the lowest energy species in the mixture. These processes result in the formation of various macrocycles, but the equilibrium is shifted towards the thermodynamically most preferred product. The equilibrium can also be influenced if a template forms a complex with a certain component of the dynamic mixture (usually a macrocycle), changing its solubility. If the complex is removed from the mixture (*e.g.* via precipitation), this process drives the DCL to produce more of it according to Le Chatelier's principle. Under these conditions, even thermodynamically unfavoured products can be amplified, as removal of the complexed component is controlled by solubility equilibrium.[70,78] One example of a thermodynamically unfavoured product is the synthesis of inverted-*cis*-cycHC[6], where one monomer in the cycHC[6] is inverted. During the synthesis, using DCC principles, *cis*-cycHC[6] and inverted-*cis*-cycHC[6] were produced. However, as the

cis product was the thermodynamically favoured product, the inverted macrocycle was obtained via kinetic trapping due to low solubility.[66]

1.2.3 Synthetic approaches to functionalised hemicucurbiturils

As described earlier, homomeric HCs are usually synthesised under very similar conditions – monomers and formaldehyde are stirred in an acid solution and heated, yielding the target HC. However, synthesising heteromeric HCs containing different types of monomers can be extremely difficult because many linear and cyclic oligomers could form. Only a few examples exist of HCs formed from two or more distinct monomers.

In 2020, Šindelar's group published the first example of mono-functionalised benzylated BaU[6]s (Figure 7).[80] The primary monomer was 2,4-dibenzylglycouril, and then asymmetrically substituted glycouril monomers bearing a carboxylic acid functional group. The idea was to add a functional group to allow the selective addition of other chemical entities into the structure of the cavitand without altering the core supramolecular properties. Macrocyclisation was conducted via the condensation reaction of monomers with paraformaldehyde in dioxane in the presence of sulphuric acid as a catalyst and an anionic template at 80 °C for several hours. Based on a binomial distribution model, it was calculated that if monomers were used in a stochiometric ratio of 1:5, a maximum of 40.2% of mono-functionalised BaU[6] would be produced, with significant amounts of doubly (20.1%) and triply (5.4%) substituted macrocycles, making the purification very complex. Therefore, the symmetrical 2,4-dibenzylglycouril was used in a large excess (98:2) to minimise the formation of doubly and triply functionalised BaU[6]s. Mono-functionalised bambusurils **1a** was obtained in 31% yield and **1b** in 41% yield.

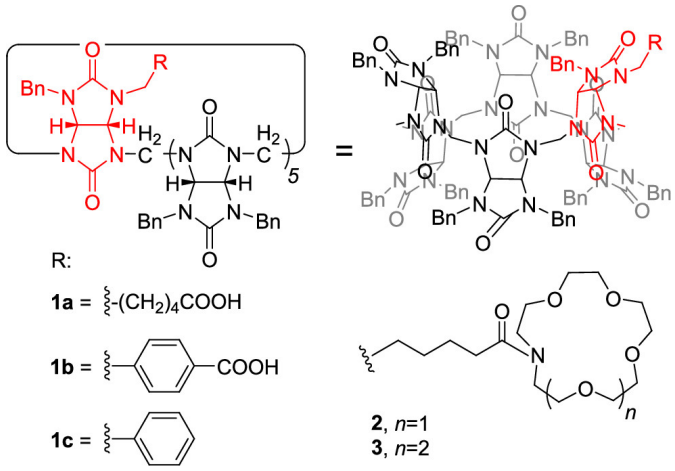

Figure 7. Mono-functionalised BaU[6]s and their conjugates. Reprinted from reference 80 with permission from American Chemical Society.

The presence of a carboxylic acid group allowed further selective amide-coupling of two aza crown ethers with different ring sizes to mono-functionalised BaU[6]. This yielded heteroditopic receptors, combining anion- and cation-binding properties in a single host molecule. While bambusurils are known for their anion-binding affinity, crown ethers bind small cations. Therefore, these BaU[6]-crown ether conjugates were successfully applied in liquid-liquid extraction of inorganic salts (such as NaI or NaBr) from water to chloroform. The conjugates showed good extraction efficiency with Br^-

and I^- anions, regardless of the counter-cation and crown ether size. However, fluoride salts were not extracted due to the high hydration of the anion. Chloride salt extraction depended on the counter-cation, as well as the crown ether attached to BaU[6]; 15-crown-5 showed very little extraction efficiency (below 5% receptor occupancy) compared to larger 18-crown-6 (13%–76%). Moreover, new conjugates were more efficient than the corresponding mixture of BaU[6] and crown ethers, suggesting a cooperative effect in the binding of ion pairs.[80]

Building on previous work with fluorinated BaU[6][7] and mono-functionalised BaU[6],[80] the same research group synthesised mono-functionalised fluorinated BaU[6]s (Figure 8).[81] Again, one monomer bearing a carboxylic moiety was introduced to the structure of fluorinated BaU[6], and the synthesis was similar to that of the first mono-functionalised BaU[6].[80] Similarly to before, based on binomial distribution estimation, the highest amount of mono-functionalised 6-membered macrocycle could be obtained with a 1:5 monomer ratio. However, in this example, a large excess of monomers was avoided, and monomers were used in a 1:6 ratio to reduce the amount of unwanted doubly and triply functionalised derivatives. Fluorinated 2,4-substituted glycouril, (*1S,5R*)-2-(4-carboxybenzyl)-4-methyl-glycoluril and paraformaldehyde were heated in 1,4-dioxane at 80 °C in the presence of sulphuric acid; as an acid catalyst and template (HSO_4^-). Mono-functionalised macrocycle **2a** from 2,4-bis(3,5-bis(trifluoromethyl)-benzyl)glycouril monomer was isolated in 11% yield and **2b** from 2,4-bis(4-((trifluoromethyl)sulphanyl)benzyl)glycoluril in 12% yield.

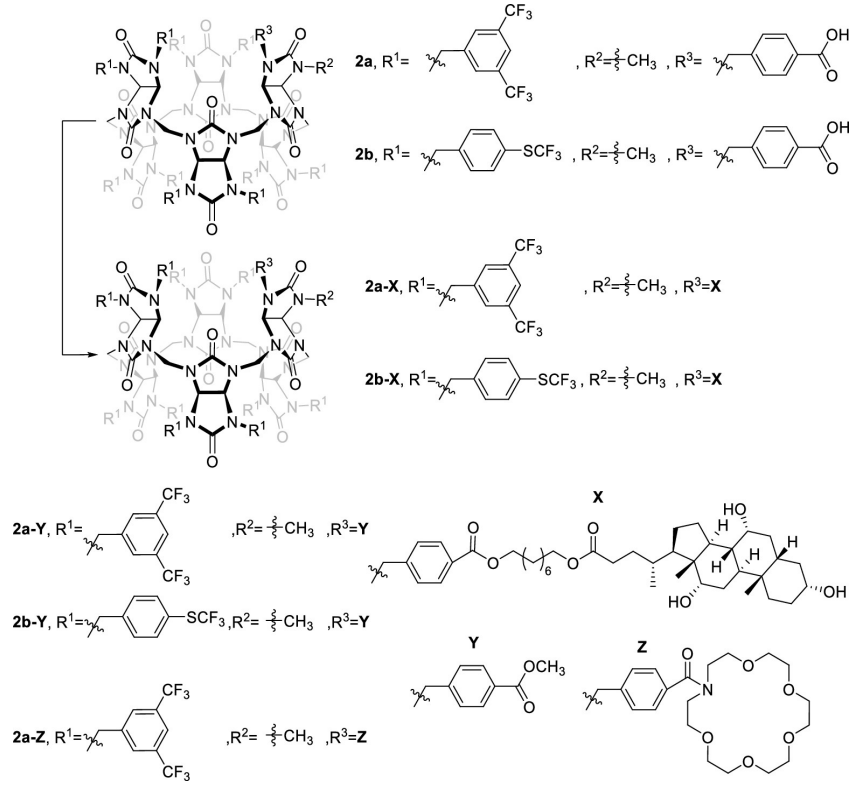

Figure 8. Fluorinated mono-functionalised bambusurils and their respective conjugates. Reprinted from reference 81 with permission from the American Chemical Society.

The new fluorinated mono-functionalised BaU[6]s were coupled through esterification or amidation. Conjugates of BaU[6] with cholesterol unit and aza-crown ethers were obtained and used in the transmembrane anion transport and in the extraction of inorganic salts. Notably, all the conjugates showed similar transport activities of Cl^-/HCO_3^- with the parent fluorinated BaU[6]s, indicating that the rate-limiting step is binding and the release of anions at the membrane, rather than the speed of diffusion of complexes across the lipid layer.[81]

In 2024, D-biotin was incorporated into the BaU[6] structure to obtain an enantiomerically pure macrocycle containing one biotin and five 2,4-dibenzylglycouril monomers (Figure 9).[82] Preparing enantiomerically pure glycouril monomers is challenging; thus, the authors used D-biotin as a commercially available alternative to add chirality in the macrocycle. Similarly to 2,4-dibenzylglycourea, D-biotin is a urea derivative, enabling its incorporation directly into the macrocycle, and the D-biotin provides a single carboxylic acid group for further derivatisations.

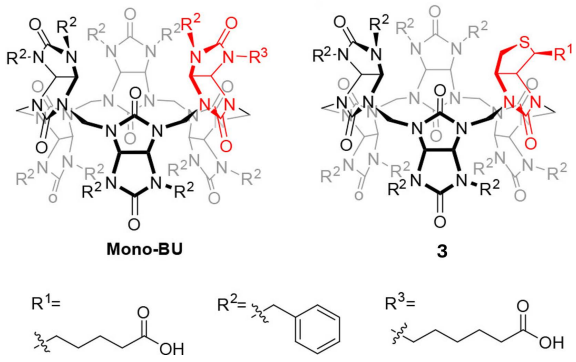

Figure 9. Mono-functionalised and mono-biotinylated BaU[6]s. Adapted from reference 82 under the terms of the Creative Commons Attribution 4.0 International Licence (CC-BY-4.0).

The synthesis conditions were again similar to previous works with mono-functionalised BaU[6]s,[80,81] involving heating a mixture of monomers with paraformaldehyde in dioxane with sulphuric acid at 80 °C for several hours. Biotin and glycouril monomers were used in a stoichiometric 1:5 ratio. Notably, only one mono-functionalised macrocycle (35% yield) was produced along with homomeric dodecabenzyl-BaU[6]. This differed from their first mono-functionalised BaU[6], where a mixture of mono-, di- and tri- substituted BaU[6]s were obtained.[80] It was shown that the binding affinities of anions of the new mono-biotinylated BaU[6] **1** were similar to those of benzylated BaU[6]; therefore, the D-biotin incorporation into the BaU structure did not significantly influence the anion-binding efficiency. The obtained mono-biotinylated BaU[6] was used to construct a rotaxane via reversible covalent bonds, showing its usability in building mechanically interlocked molecules.[82]

While the examples discussed above are mono-functionalised derivatives, it is also possible to introduce chromophores and other functional groups to further expand the diversity of HCs, making hybrid derivatives (Figure 10). In 2014, Keian and co-workers reported the synthesis of multifarenes (Figure 10A), where the macrocycle comprises alternating ethylene urea or ethylene thiourea and phenol-derivative building blocks.[83] It was shown that the obtained hybrid macrocycles bind palladium cations at the portals through sulphur-mediated interactions.

In 2019, Šindelar and colleagues attempted to produce a BaU[*n*] derivative containing alternating m-xylene and glycouril units (Figure 10B).[84] However, in this one-pot nucleophilic substitution reaction, the main product was a 4-membered macrocycle. Unfortunately, its cavity appeared too small to bind any anions, and it was therefore unsuitable as a receptor.

In 2021, a 6-membered aminobenzene-containing HC (Figure 10C) was synthesised by Liu and co-workers.[85] They envisioned that amino groups could provide reactive sites for derivatisation, while also allowing the coordination of hydrogen-bonding interactions with guests, and that the aminobenzene unit would act as a chromophore to improve optical properties. The macrocycle was constructed by using a fragment-coupling strategy involving a nucleophilic substitution reaction, followed by the reduction of nitro groups, to produce an aminobenzene-containing HC[6], which was shown to bind Fe^{3+} and Cu^{2+} cations.

In 2022, the same group attempted to synthesise an all-thiohemicucurbituril (thio-HC) from commercially available ethylene thiourea monomer, following the same fragment coupling strategy. Neither the direct condensation of thiourea and formaldehyde in acidic conditions nor the coupling of oligomeric fragments worked to obtain an all-thioHC. However, cyclic HC[6]s containing up to three thiourea motifs were obtained (Figure 10D) via fragment-coupling.[86]

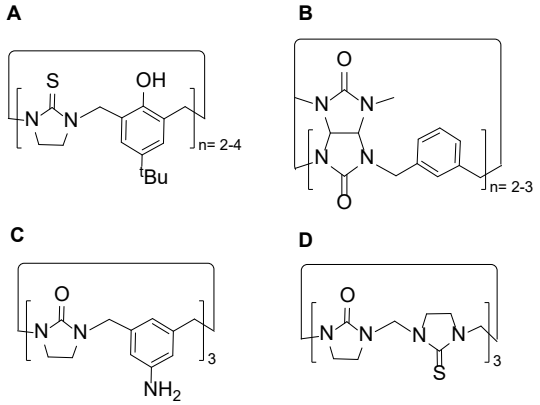

Figure 10. Hybrid HCs: (A) Multifarenes, (B) m-xylene-containing BaU, (C) aminobenzene-containing HC[6] and (D) thio-HC[6] containing three thiourea motifs.

Post-functionalisation is an attractive approach to derivatising and modifying macrocycles without altering the key supramolecular properties of the macrocycle. It relies on the availability of accessible functional groups (some examples were given above). This approach can be appealing but may present challenges in selective mono-functionalisation, or partial or full functionalisation. Examples exist of other macrocycle classes that have been mono-functionalised, such as calixarenes,[87,88] crown ethers[89] and CBs.[90] However, this is not thoroughly demonstrated with HC[*n*]s.

1.3 Mechanochemistry as an enabling sustainable synthetic technique

Mechanochemistry is an age-old synthetic technique that has experienced a resurgence over the years as a powerful tool for sustainable synthesis. The International Union of Pure and Applied Chemistry (IUPAC) has defined a mechanochemical reaction as a

"chemical reaction that is induced by the direct absorption of mechanical energy".[91] From a practical standpoint, the significance of mechanochemistry lies in its ability to induce chemical transformations in powdered solids without using excessive amounts of solvents, making it a greener approach in organic synthesis.

The first documented example of a mechanochemical reaction was described by Theophrastus of Eresus in 315 B.C. in the book entitled "On Stones". Theophrastus wrote that if a red-coloured cinnabar (mercury(II)sulphide, HgS) was ground with a copper or bronze mortar and pestle, it formed elemental mercury (quicksilver; Scheme 3). It was also mentioned that a small amount of vinegar accelerated the reaction.[92,93] This is a reference to a modern technique called liquid-assisted grinding (LAG; see Chapter 1.3.2). It also demonstrates that the milling equipment can participate in mechanochemical reactions.

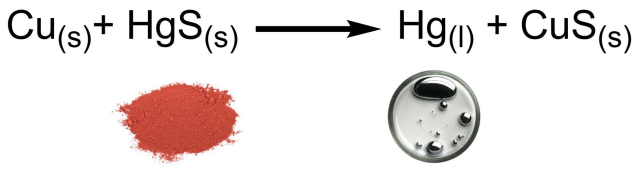

Scheme 3. The earliest documented mechanochemical reaction between copper and cinnabar.

1.3.1 Mechanochemical instrumentation and scalability

The earliest reactions were conducted using a pestle and mortar, by manually grinding solids together. However, this approach has several limitations, including poor control over the reaction and limited reproducibility. This stems from variations in the mechanical energy input, which depends solely on the physical abilities of the person performing the reaction. Therefore, modern laboratories use automated milling devices to conduct mechanochemical reactions. Many instruments are available to induce chemical transformations in solids, including ball mills, extruders, resonant acoustic mixers, and others. The choice of mechanochemical instrument depends on several factors, including the desired reaction scale, type of mechanical action applied and physical states of reactants.[94]

The most used milling devices in modern laboratories are shaker (or mixer) mills and planetary ball mills (Figure 11A and B), but their modes of mechanical agitation differ. In shaker ball mills, the jars oscillate back and forth on a horizontal axis at a desired frequency.[95] In planetary mills, the jars rotate around a central axis while simultaneously spinning around their own axes, creating a so-called planetary movement; mimicking the motion of the planets around the Sun. Planetary mills are usually used for scale-up purposes and can serve as a bridge to industrial-scale production.[96]

Bead mills, which use small milling beads, are also available, such as Dyno®-mill (Figure 11E), which offers further scale-up and can operate in batch or continuous mode, highlighting the effectiveness of the wet milling process.[97] Compared to conventional batch set-ups, the continuous Dyno®-mill operation offers improved particle-size reduction, enhanced mixing capability and increased production efficiency.[94] Another technology enabling continuous mechanochemical reactions is twin-screw extrusion (TSE, Figure 11D). In this instrument, the reactants are continuously processed between two parallel screws. Various parameters can be varied, including temperature, screw speed and residence time, all of which help optimise the product yield.[94,98] TSE has been

used efficiently in large-scale synthesis for different organic transformations, active pharmaceutical ingredient (API) co-crystal[99] and MOF synthesis.[100]

All mixer and planetary ball mills use milling balls. When milling balls collide with reactants, mechanical energy is transferred to the reactants, and chemical reactions occur. However, it is possible to perform reactions with no milling media, using resonant acoustic mixing (RAM, Figure 11C) technology. No milling media (e.g. balls or screws) are required, and the reactants are simply mixed at a certain acoustic frequency, inducing chemical and morphological changes. It can be scaled up and used continuously, and no product contamination occurs due to the absence of milling media.[94,101]

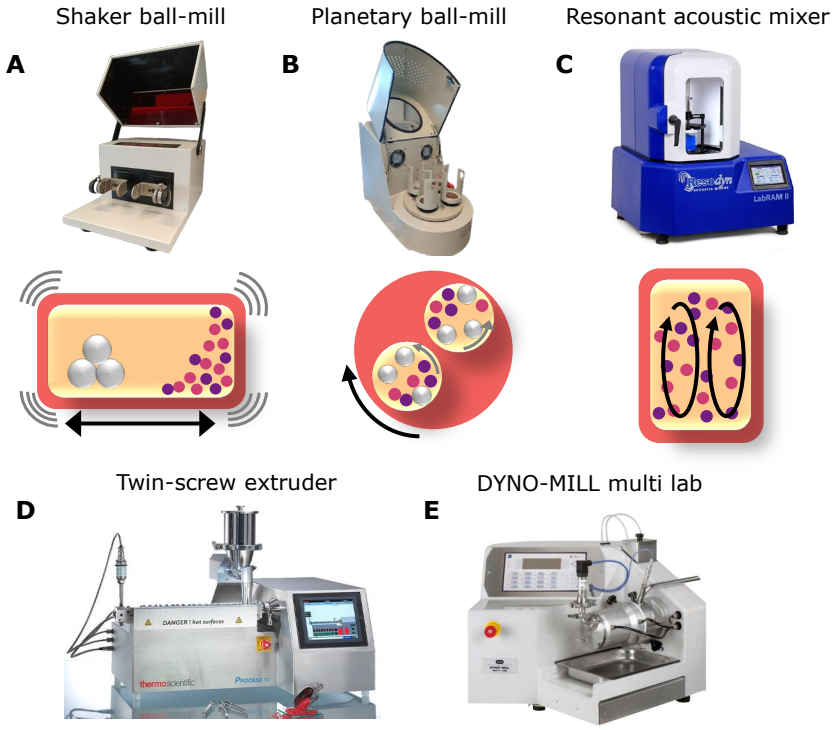

Figure 11. (A) FTS-1000 shaker mill, Form-Tech Scientific, (B) ND2L planetary ball mill, Torrey Hills Technologies, (C) LabRAM II Resonant Acoustic mixer, Resodyn (image reproduced from https://resodynmixers.com/products) and their representative motions applied, (D) Process 11 Twin-screw extruder, Thermo Scientific (image reproduced from https://www.thermofisher.com) and (E) WAB-GROUP DYNO-mill multi lab (image reproduced from https://www.wab-group.com/en/products)

The energy input into the mechanochemical system can be influenced by varying the milling devices, vessels and media (see discussion in Chapter 1.3.3). The mechanochemical reaction scale in a laboratory setting can vary depending on whether shaker or planetary mills are used. For daily small-scale reactions, shaker mills find more use, where the reaction scale is usually up to a few grams. The jar internal volumes can vary from 1.5 to 125 mL, using milling balls with diameters of 1 to 70 mm. Planetary mills bridge the gap between small-scale reactions and larger production. They can be implemented for small-scale reactions; however, they are useful for scaling up the

reactions (up to 1 kg) because the jar volumes range from 40 to 900 mL, with ball diameters extending from 0.1 to 40 mm.[101]

Various materials are used for milling vessels (or jars) and milling media (or balls). Typical materials used are zirconium dioxide (ZrO_2, zirconia, Figure 12), stainless steel, tungsten carbide, or plastics such as polytetrafluoroethylene (PTFE, or Teflon) and poly(methyl methacrylate) (PMMA). These materials are chemically inert, varying in density and hardness, enabling direct control of the energy input and therefore reactivity.[93,102–104] Plastic jars (density 2.7 g/mL, hardness 100 for agate and 2.1 g/mL density for Teflon) offer the least energy input;[104] however, PMMA jars are extremely useful for *in-situ* reaction monitoring, which can provide valuable insights into reaction kinetics and mechanisms.[105] Stainless steel jars (density 7.8–7.9 g/mL, hardness 550–750)[104] are most commonly used; however, on extensive use, leaching of different metals, including iron, nickel and chromium, can be observed, which could influence the reaction outcomes.[106,107] Additionally, exposure to strong acids leads to the corrosion of stainless steel jars.[93] An excellent alternative to overcome these problems is zirconium oxide jars, which offer a similar density (density 5.9 g/mL, hardness 1200) to stainless steel jars.[103,104] Tungsten carbide exhibits the highest density of all the mentioned materials and provides high energy input (density 14.8 g/mL, hardness 1200);[104] it is a relatively fragile and brittle material, which usually have to be stabilised by cobalt, which can in turn lead to unwanted contamination.[103]

Figure 12. Various ZrO_2 jars for shaker and planetary mills available in our laboratory and used in the current work.

Milling media can provide greater versatility, and examples exist where the milling material is selected to participate in the reactions for catalytic purposes.[108–110] Mack and co-workers showed an example of Sonogashira coupling of para-substituted aryl-halides with trimethylsilylacetylene in the solid state, where the reaction still required palladium as a catalyst but the co-catalyst was copper-coated milling balls. Copper iodide is

normally used as a co-catalyst; however, this was unnecessary in this case. This approach simplified the work-up, and the obtained yields with copper material were similar to those obtained when copper iodide was used in solution-based synthesis.[111] In 2019, the first study using palladium milling balls as catalyst in a mechanochemical Suzuki reaction was published by Borchardt and co-workers. Suzuki polymerisation occurred at the surface of the milling balls. This was the first time the term "direct mechanocatalysis" was proposed.[112]

In solution-based synthesis, control of the reaction temperature is usually achieved using heating baths. However, during mechanochemical reactions, the temperature cannot be controlled and due to repeated collisions and impacts, it may rise because of friction, ball impacts, and heat release during reaction.[101,113] Additionally, if the temperature rises during milling, it is difficult to understand whether the reaction is driven by mechanochemical forces or heat. However, there are examples of custom-made reactors where temperature control is available through modified milling jars, in which thermal fluids are circulated around the jacket.[114,115] Additionally, cryo-mills offer external cooling.[116] Retch has recently released a milling device, which allows regulation of the temperature between −100 and +100 °C with thermal plates.

1.3.2 Assisted grinding and post-treatment

LAG is a concept used in mechanochemistry when a minute amount of liquid is added to a mechanochemical reaction.[102,103,117] LAG is characterised with the parameter η (µL/mg) and represents the ratio of the liquid additive volume (in µL) to the total mass (in mg) of the solids in the reaction (Equation 1).[117]

$$\eta = \frac{V\ (\text{liquid}, \mu\text{L})}{m\ (\text{solid}, \text{mg})} \tag{1}$$

If η is 0 µL/mg, this indicates neat-grinding conditions, where no liquid additives are used. If η is between 0 and 2 µL/mg, this corresponds to LAG conditions. Slurry reactions are characterised by η values between 2 and 10 µL/mg, and if η exceeds 10, this indicates traditional solution-based reactions (Figure 13).

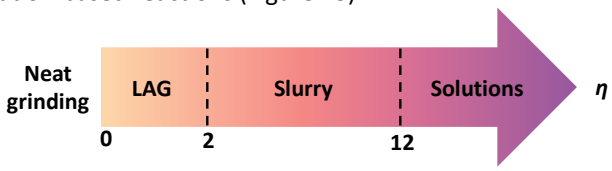

Figure 13. LAG scale.

While the reactivity is less dependent on the solubility of reagents under LAG conditions, in slurry reactions, the influence of solubility becomes more pronounced, whereas in solution-phase synthesis, reactivity is controlled by the solubilities of the reactants and products. Therefore, the small and controlled amount of LAG additive is a simple yet powerful tool for accelerating solid-state reactions. It accelerates the reaction even under the static conditions of aging and provides an additional dimension for the optimisation of mechanochemical reactions (LAG amount, aging time, or temperature).[102,117]

LAG aims to accelerate reactions through multiple mechanisms. LAG can facilitate the mass transfer of the reactants through enhanced mixing and dispersion, mediating

enhanced interparticle interactions and promoting dissolution. Additionally, liquid additives can function as chemical modulators, polarising substrates or stabilising polar transition states and reactive intermediates through solvation. These effects lower the activation barriers for covalent bond formation. In metal-catalysed reactions, the LAG additive can interact with metal centres to tune electronic and steric properties under nearly solvent-free conditions. LAG additives can also directly participate as stochiometric reagents in bond-forming processes or proton transfer steps.[118] In aging-driven reactions, such as the solid-state synthesis of cycHC[*n*]s, one role of LAG is to accelerate the rate of molecular diffusion.[17]

The concept of LAG was originally studied in mechanochemical co-crystallisation, where it was shown to influence the co-crystallisation process.[119,117] However, it is now widely used in mechanosynthesis, as LAG is not only a "greener" synthetic approach but also an enabling strategy for obtaining products inaccessible under solution-based or neat-grinding conditions.

Another means to control mechanochemical reactions is using inert **grinding auxiliaries**, such as silica, alumina or other inorganic salts. This becomes particularly important when liquid reactants are used, as they can negatively affect the rheology of a reaction mixture, resulting in soft and sticky products and inhibiting proper energy and mass transfer. In such cases, adding auxiliary solids can improve the powder-like rheology of reaction mixtures, which is also important for efficient mechanical energy transfer and improving homogeneity. Solid additives can also be used to dilute the reaction mixtures in mechanochemical reactions. Liquid reagents adsorb onto the solid, which can restrict the movement of liquids away from the position of impact, thus enhancing the energy transfer.[93,95,120] The differences in reaction mixture rheology can result in different reaction kinetics.[121] These solid additives are usually chemically inert towards the reaction; however, they can have a chemically important role in some cases.[122,123]

The concept of **aging** in mechanochemical reactions was developed by Friščić and co-workers.[124] It refers to a process in which, after a brief mechanical activation step, chemical transformations proceed under diffusion-controlled static conditions, while minimising energy and solvent consumption.[124,125] Reactivity can be accelerated by mild heating, exposure to different solvent vapours,[126] moisture[127] or even liquid additives. As aging is diffusion-based, liquid or its vapours are required to facilitate the reaction, as solid reactants have very limited mobility. A short milling period is crucial for the homogenisation of reaction components, reduction of particle size to increase the reaction rates through a greater accessible surface area, and amorphisation, which may be important for reactivity in some cases.[124] Aging has been shown to be beneficial in the solid-state synthesis of cycHC[*n*]s, where the templating effect becomes pronounced during the aging step (see below for detailed discussion).[17]

Templ and Borchardt recently highlighted the correlation between single-impact energies delivered to the reaction mixture and aging. They showed that the Finkelstein halogen-exchange reaction was impact-triggered, meaning that after brief milling, the reaction continued during aging without further mechanical input. In contrast, the Wittig olefination reaction proved to be impact-complete, proceeding via active ball impacts and correlating with the total cumulative energy.[128] Determining whether reactions are impact-triggered could avoid equipment depreciation and unnecessary energy consumption, and could facilitate the use of alternative instruments for scale-up. Aging is currently less widespread in organic mechanochemistry, although related approaches

have long been used by geologists and crystallographers[124] and was also used in the early examples of solvent-free organic synthesis.[129–131]

1.3.3 Parameters affecting mechanochemical reactions

In a mechanochemical reaction occurring in a ball mill, the mechanical energy is primarily transferred to the reactants through high-energy impacts and collisions within the milling vessel and depends on the following variables: the kinetic energy of milling balls before collision, how the energy is transferred to the reactants and the collision frequency. The kinetic energy of milling balls, which they possess before the collision, determines the maximum energy transferable to the reagents. However, the outcome of a reaction is influenced by how the energy is transferred to the reactant during the collision. A higher milling frequency increases the kinetic energy via increased velocities of milling balls, which can enhance the reaction rates.[95]

In solvent-based reactions, collisions between reactant molecules are achieved by diffusion, affinity and molecular charge properties. In mechanochemistry, the mechanical energy applied to the system induces collisions between the solid particles, so the reaction occurs on the surface of colliding particles or, if present, in a concentrated liquid phase (LAG), thereby overcoming diffusion barriers and promoting intermolecular interactions.[132]

Mechanical force promotes a more effective collision probability through mixing and more uniform mass transfer. The Knoevenagel reaction between vanillin and barbituric acid appeared to be affected by proper mixing, surface area generation and mass transfer, rather than by high energy input.[133] Breaking larger particles into smaller ones increases the surface area and the number of collisions. Mechanical agitation induces structural deformations at collision sites, creating lattice defects and surface activation. These defects offer high-energy sites that lower the activation barriers of solid reactants. As mechanical agitation continues, the accumulation of lattice defects leads to the amorphisation of crystalline solids. This further enhances reactivity by creating more disordered, high-energy states. Mechanical energy can also cleave covalent bonds in polymers, assisting in polymer degradation.[134]

Mechanical energy can also dissipate. A portion of energy can be lost through friction between particles and milling media, as well as through heat generation. Some energy can be absorbed by the vessel walls through elastic and plastic deformations. Energy transfer is also sensitive to the fill ratio; if the jar is overfilled, the reactant mixture can cause damping effects that absorb the kinetic energy before it can reach the reactants efficiently. Additionally, increasing the milling frequency can lead to lower efficiency, as energy may dissipate as non-productive heat rather than facilitating chemical bond formation. Moreover, the energy dissipation as heat can complicate distinguishing between mechanochemical and thermally assisted pathways.[133,135]

Controllable parameters affect the energy input to the reaction mixture – milling device type, milling time, frequency, amount (and size) of the milling balls and filling degree of the jar.

The choice of a **milling device** determines the motion of grinding balls within the jars, which determines the type of forces applied to the reaction. In mixer mills, the dominating force employed for the reaction is impact force, and in planetary mills it is shear forces; however, both types of forces are encountered in both devices.[95]

Milling frequency is a straightforward parameter to control and adjust, as it can be set on the milling device interfaces. Increasing the milling frequency increases the velocity of the milling balls and consequently the impact energy delivered to the reactant. Point impact energy (E_{impact}, Equation 2) arises from the collisions between the milling ball and reactants

and must exceed a threshold energy for the reaction to occur.[136] E_{impact} depends on the mass of the ball (m_b) and its impact velocity ($v_{effective}$), which can be influenced by changing the milling frequency or milling ball weight.[95,135,136]

$$E_{impact} = \frac{1}{2} m_b {v_{effective}}^2 \quad (2)$$

Prolonging the **milling time** directly increases the total cumulative energy (E_{total}), which is transferred to the system during the whole milling process.[95,136] As shown in Equation 3, E_{total} depends on E_{impact}, the empirical filling degree φ, the total number of balls N_b, the frequency of collisions f_b and the milling time t.

$$E_{total} = \varphi E_{impact} N_b f_b t \quad (3)$$

E_{impact} and E_{total} for shaker or planetary mill reactions can be conveniently calculated using a Ball-mill Calculator developed by Lungerich's group.[136] By combining the work of Lungerich and co-workers[136] with the research of Templ and Borchardt,[128] valuable insight can be gained into whether a mechanochemical reaction depends primarily on impact energy (E_{impact}) or the total cumulative energy input (E_{total}), corresponding to impact-triggered and impact-complete behaviour, respectively.

The **amount, size and mass of milling balls** are easy parameters to control and are usually chosen based on the jar volume. Energy transferred to the reactants increases with the number of milling balls. However, an excessive number of balls can occupy a substantial fraction of the milling jar volume, increasing the filling degree (see below) and thereby restricting ball movement and velocity; consequently, the kinetic energy transferred to the reactants is reduced. Mechanical energy delivered to the system can be regulated using a smaller number of heavier balls, which possess higher kinetic energy and therefore deliver higher energy to the reactants in a single impact.[103,137] Additionally, the literature on mechanocatalysis contains examples of the advantages of modified milling balls.[138] The energy transfer is usually closely linked to the mass and surface area of the milling balls, as increasing the ball size changes the mass and available surface area, which affects the impact and total energies. In contrast, hollow milling balls enable the effects of ball mass and surface area to be studied independently. They deliver less impact energy due to their lower mass, while offering the same surface area as a solid ball of the same size. However, if the reaction occurs at the ball surface, no additional energy input is required, leading to higher energy-normalised efficiency. Moreover, corrugated milling balls can also be advantageous.[139] The ridges on the surface of the balls provide more contact points, which allow more efficient kinetic energy transfer, ensuring homogeneous mass transfer by breaking up clumps and generating more uniform heat distribution, which can lead to more efficient product formation.

Finally, the **filling degree** is also an important variable to consider. Essentially, this parameter describes how much volume the reactants and milling balls occupy compared to the total volume of the jar. This has a significant role in the trajectories of the moving milling balls therefore energy transfer and mixing. If the jar is too overloaded with reactants, the impact forces will be reduced, which can lead to poor results.[95,133]

All the mentioned parameters are crucial for tuning the parameters of mechanosynthesis (Figure 14). However, if the time comes to up-scale the reactions from one device to another, problems can occur. Transferring a mechanochemical reaction from one milling device to another can be complex, especially if a protocol involves moving from a shaker mill to a planetary mill, as the motion of milling and the forces applied are different. Reporting only

the milling time and frequency is insufficient to ensure reproducibility. Additionally, even minor changes in planetary ball mill geometry (such as jar radius and sun wheel dimensions) can cause significant variation in energy, despite using the same number of balls or exactly the same milling speed. This concern could be addressed by calculating the total cumulative energy using a kinematic model to ensure that the total energy remains constant while using different milling devices.[136] It is also notable that merely increasing the milling frequency does not always lead to better results but can lead to diminishing returns due to energy being consumed as non-productive heat rather than promoting chemical reactions.[133]

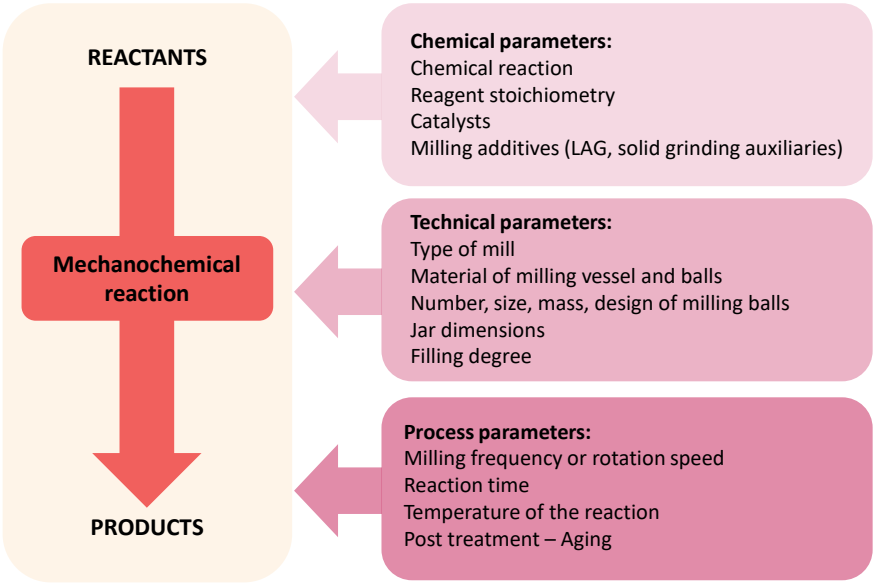

Figure 14. Summary of different parameters affecting the mechanochemical reactions discussed above in different chapters.

1.3.3.1 Data-driven optimisation

As discussed in previous chapters, numerous instrument and chemistry specific variables affect mechanochemical reactions. Several optimisation methods are available and depending on the approach used, the number of experiments can increase substantially.

In chemistry, including mechanochemistry, the most widely used approach is varying one factor at a time (OFAT). In OFAT, one experimental parameter is varied while all the others are kept constant to study its individual effect on the reaction outcome. Although effective, this approach is time-consuming, and important interactions between variables can be missed, leaving the optimal reaction conditions unexplored.[140,141]

An alternative to OFAT is the design of experiments (DoE), which can advance the multi-factor optimisation process.[140] DoE is a statistical strategy, in which multiple experimental factors are explored simultaneously, reducing the number of reactions required. While OFAT can miss interactions between variables, these can be explored with DoE. Parameter selection and the ranges used must be defined in advance by the researcher. This selection must be made carefully, so the parameter ranges are not too narrow and relevant trends are not overlooked.

Bayesian optimisation (BO) is a machine-learning-based strategy that uses information gathered from previously conducted experiments. BO can further expand the experimental reaction space and help predict high-yielding reaction conditions with even fewer

experiments.[141,142] By employing these optimisation methods, the number of experiments can be reduced, requiring less starting materials, time, and operation resources, which support sustainable chemistry.

1.3.4 Sustainability assessment of mechanochemical processes

In 1998, Paul Anastas and John Warner introduced the 12 principles of green chemistry to provide a framework for transitioning the chemical industry towards sustainable chemistry (Figure 15).[143] These guidelines were designed to encourage the development of chemical processes and products that minimise pollution, reduce risks to human health, and eliminate the generation of hazardous waste. Mechanochemistry is aligned with this framework, as its applications follow several of these principles.[144,145]

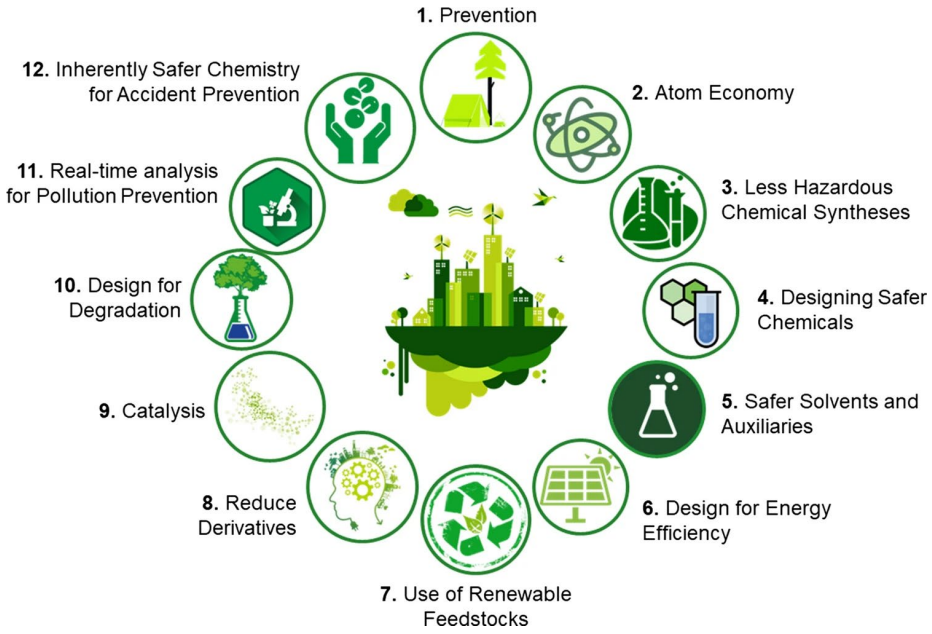

Figure 15. The 12 principles of green chemistry.[143,146] Reprinted from reference 146 with permission from Springer Nature.

Waste prevention is perhaps the most important principle, as it emphasises that preventing waste generation is more beneficial than the treatment or clean up afterwards. In conventional solvent-based synthesis, 80–90% of mass utilisation is attributed to solvents, making them the primary source of waste.[147] Mechanochemistry directly addresses this principle by avoiding bulk solvent usage, reducing the environmental footprint.[144,145]

Atom economy (AE) and *real atom economy* (RAE) focus on maximising the incorporation of all starting materials into the final product, thereby minimising by-product formation and waste.[148] In conventional solvent-based synthesis, an excess of reagents is often required to force the reaction to completion; this is frequently accompanied by the formation of side products, which increases waste generation. Mechanochemistry often provides faster reaction rates and precise stochiometric control of the reagents, where equimolar ratios of starting materials are sufficient, resulting in higher selectivity and yields.[144,145,149] The synthesis of the zeolitic imidazolate framework ZIF-62 was found to be

more efficient under mechanochemical conditions, using zinc oxide as precursor and producing only water as a by-product, instead of acids. This method demonstrated a high RAE of 92% compared with the conventional solvothermal method (RAE 2.2%).[150]

Safer solvents and auxiliaries should be used whenever possible. Beyond waste, many solvents pose safety risks due to toxicity (such as benzene, dichloromethane) and flammability (such as diethyl ether). While mechanochemistry reduces the need for solvents and thereby mitigates safety concerns, the LAG approach still requires small amounts of liquid. This is for catalytic purposes rather than as a reaction medium, although work-up and purification steps still require solvent use. Therefore, replacing hazardous solvents with more sustainable alternatives is highly recommended.[144,145] Amide synthesis is typically conducted in toxic solvents, like dichloromethane or dimethylformamide.[151] However, mechanochemical amide synthesis has been shown to proceed without solvent using *N,N'*-carbonyldiimidazole (CDI) as a coupling reagent.[152]

Chemical processes should be designed to maximise *energy efficiency* by operating at ambient temperatures and pressures. Mechanochemical reactions often proceed without external heating and can reach completion faster due to shorter reaction times, resulting in lower energy consumption.[144,145] Suzuki-Miyaura coupling *via* ball-milling proved to be more energy efficient than microwave and ultrasound activation.[153] Iron-catalysed synthesis of ammonia from hydrogen and nitrogen was achieved in a ball mill at a mild temperature of 45 °C and 1 bar of pressure,[154] whereas the standard Haber-Bosch type industrial process requires 450 °C and 200 bar.[155]

Green chemistry metrics offer quantitative evaluation of the sustainability of chemical processes through toolkits, such as the CHEM21 metrics toolkit[156] and the DOZN 2.0 green chemistry evaluator.[157] These metrics help assess the performance and sustainability of chemical processes and enable systematic comparison between methods. Important metrics include the yield, conversion, selectivity, AE, RAE or reaction mass efficiency (RME), E factor or process mass intensity (PMI), as defined in Equations 4–8.[145,149] Additionally, the total carbon dioxide release (TCR) can be calculated to estimate the carbon footprint in a process. For TCR calculation, PMI values for organic compounds, leading to organic waste, and water, originating from incineration of water waste, are used and multiplied by the appropriate factor (Equation 9).[158] Although this metric is designed for the pharmaceutical industry, it can still provide useful insight into reaction sustainability.

$$\mathrm{AE} = \frac{\text{molecular mass of product}}{\text{sum of molecular masses of all reactants}} \times 100\% \tag{4}$$

$$\mathrm{RME} = \frac{\text{mass of isolated product}}{\text{sum of masses of reactants}} \times 100\% \tag{5}$$

$$\text{E factor} = \frac{\text{total mass of waste}}{\text{mass of product}} \tag{6}$$

$$\mathrm{PMI} = \frac{\text{total mass in a process}}{\text{mass of product}} \tag{7}$$

$$\mathrm{PMI} = \text{E factor} + 1 \tag{8}$$

$$\mathrm{TCR} = (\text{PMI organic} \times 2.3 + \text{PMI water} \times 0.63) \tag{9}$$

AE is a simple theoretical metric that describes how many atoms from the starting materials are incorporated into the final product. However, it does not consider the reaction stoichiometry and assumes 100% yields. The RME (or RAE) is similar to AE but reflects the actual efficiency of reactant use because it also accounts for the stoichiometry and product yield. Currently, PMI is probably the most widely used metric, as it reflects the total amount of input materials (including all the reagents, solvents, catalysts and work-up chemicals) required to synthesise a product, while also considering the yields and stoichiometry. The PMI is therefore a useful indicator for comparing processes and identifying areas requiring improvement during process development. The E factor is closely related to the PMI but focuses on the evaluation of waste generation. The closer the E factor is to 0 (and PMI to 1), the less waste-intensive the chemical process is.[145,149]

The CHEM21 toolkit and DOZN 2.0 evaluator include qualitative parameters, such as solvent selection, catalyst use, energy consumption and health and safety concerns. These parameters are categorised as "preferred" (green flag), "acceptable" (amber flag) and "undesirable" (red flag), indicating how well a process aligns with sustainability principles and highlighting areas requiring improvement.

1.3.5 Advantages of mechanochemistry

Besides the sustainability benefits of mechanochemistry (discussed in the previous chapter), this method can often outperform solution-based approaches in several ways. Neat-grinding or solvent-minimised environments help overcome the solubility limitations of the reactants. In conventional solvent-based chemistry, reagents must be dissolved in specific solvents to react, which often limits the choice of starting materials due to solvent incompatibility. Moreover, the absence of bulk solvents avoids solvent conditioning steps (such as distillation or drying), which can be time- and energy-intensive. Mechanochemical reactions are generally conducted under ambient conditions, whereas some solution-based protocols require inert atmospheres, necessitating the use of a glovebox or nitrogen atmosphere.[102,144,145] Notable examples include the ability to conduct Grignard[159] or Barbier[160] reactions without the need for dry solvents or inert atmospheres. Due to the high concentration of reagents in mechanochemical systems, reactions often proceed with faster reaction rates, resulting in improved yields, shorter reaction times, lower catalyst loadings, and reactivity inaccessible under solvent-based conditions.[102,144,145]

Mechanochemistry can also produce unexpected reaction outcomes, which may not be accessible in solution-based synthesis. An early example is the dimerisation of C_{60} fullerene. It was initially expected that milling with potassium cyanide (KCN) would produce a hydrocyanation product; however, a dumbbell-shaped C_{120} product was obtained instead.[161]

Although mechanochemistry offers many advantages, areas remain where it cannot solve all synthetic challenges. For example, scale-up and control of the kinetics of highly exothermic reactions can be problematic. Producing a homogeneous reaction mixture can sometimes be challenging, and additional elucidating measures, such as adding solid grinding auxiliaries or LAG additives to improve homogenisation, may therefore be required. Understanding reaction kinetics also requires more specialised equipment for *in-situ* measurements. Furthermore, the solvent cannot be fully avoided because mechanochemical reactions often yield crude mixtures requiring work-up or purification

to isolate the target product. Mechanochemistry therefore complements solution-based techniques by compensating for some limitations of the latter.

1.3.5.1 Mechanochemical synthesis of cyclohexanohemicucurbiturils

Solid-state synthesis can be beneficial for preparing molecules less favoured in solution, including HCs. In 2019, Aav's group demonstrated for the first time that chiral (*R,R*)-cycHC[6] and (*R,R*)-cycHC[8] can be quantitatively synthesised in the solid state.[17] This acid-catalysed, template-directed polycondensation reaction proceeds *via* two major steps, in which the LAG additive serves as the acid catalyst source and template. First, mechanical agitation of the reactants produces a mixture of solid oligomers and macrocycles. Second, during prolonged aging, template-assisted self-assembly of oligomers into (*R,R*)-cycHC[6] and (*R,R*)-cycHC[8] occurs. The macrocycle formed depends on the template used; HCl is used to selectively form cycHC[6], and $HClO_4$ is used to form cycHC[8].

Using diluted HCl did not produce quantitative yields of cycHC[6], presumably due to the lower concentration of chloride anions. Additionally, manual grinding was insufficient due to the evaporation of HCl. Therefore, using concentrated aq. HCl proved to be the best approach, providing quantitative yields of cycHC[6] after milling and aging.[17]

Trifluoroacetic acid (TFA) is used as a template source in the solution-based synthesis of cycHC[8]; however, this was ineffective in the solid state, as the trifluoroacetate binds weakly with the macrocycle (K_a < 10 M^{-1}).[64] Replacing the TFA with $HClO_4$ enabled full conversion to cycHC[8] in solid state due to the stronger binding affinity of the perchlorate anion (K_a = 470 ± 20 M^{-1}).[64] It was observed that the solid state formation of cycHC[8] proceeded faster (in 1 day) and at lower temperatures (as low as 45 °C) compared to cycHC[6] (3 days at 60 °C). This was attributed to the higher acidity of $HClO_4$, as the ratio of acid to the obtained products remained constant.[17]

Very recently, thio analogues of HC[6] and cycHC[8] were synthesised by Reany, Keinan and co-workers (Figure 16) using a mechanochemical approach similar to that used for cycHC[*n*] synthesis.[16] This process also involved the mechanochemical agitation of reactants, followed by thermal aging.

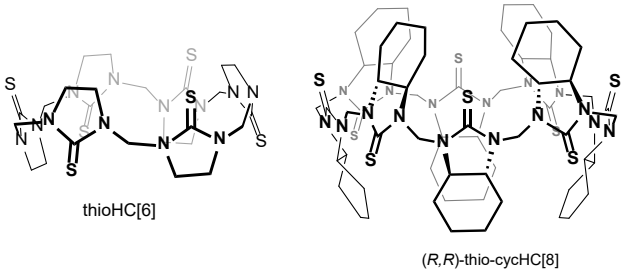

Figure 16. ThioHC[6] and (R,R)-thio-cycHC[8].

Solution-based synthesis with the monomer ((*R,R*)-octahydro-2H-benzimidazol-2-thione) proved unfavourable because, it is acid-sensitive, leading to a mixture of oligomers or decomposition products. Therefore, they adopted a similar mechanochemical approach to that used for cycHC[*n*]s. Notably, the first reaction, carried out under similar conditions to cycHC[6] synthesis with conc. HCl, showed that thio-cycHC[8] was favoured over thio-cycHC[6], which could not be obtained. Different tetrabutylammonium (TBA) salts of templating anions, with conc. HCl as an acid catalyst,

were screened. These included BF_4^-, ClO_4^-, PF_6^-, TfO^-, I_3^-, and I^-, affording thio-cycHC[8] in 62–92% isolated yields.

Although thio-cycHC[6] was not obtained in this system, a 6-membered thio analogue was successfully synthesised from ethylene thiourea, whereas the corresponding solution-based approach was unsuccessful.[86] Here, mechanochemistry provided an advantage. Thio-HC[6] was synthesised using conc. HCl as acid and different TBA salts (Cl^-, Br^- and I^-), giving thio-HC[6] in 75–90% isolated yields.

The formed thio-cycHC[8] analogue showed almost twice the anion-binding affinity compared to cycHC[8],[64] possibly due to the higher polarisability of sulphur compared to oxygen in cycHC[8]. However, the binding order was the same for both the oxo and thio analogues of cycHC[8]: PF_6^- > ClO_4^- >TfO^-. Thio-HC[6] showed the binding order I^- > Cl^- > Br^-.[16]

2 Motivation and Aims for the Present Work

The primary motivation of this research stems from the inherent limitations of traditional solution-based synthesis for complex macrocyclic HC-type cavitands, which prompted the exploration of a mechanochemical synthesis approach. The specific aims of the thesis were as follows:

- Selective assembly of chimeric mono-biotinylated hemicucurbit[8]uril (mixHC[8]). Navigate through different chemical parameters to selectively amplify the generation of a mono-functionalised macrocycle. Investigate how different chemical and mechanical parameters affect the yields of mixHC[8].
- Contribute to the development of a general and reliable methodology to quantify yields in mechanochemical syntheses of HCs as a prerequisite for using data-driven optimisation algorithms.
- Develop scalable and high-yielding mechanochemical synthesis of biotin[6]uril. Achieve decagram-scale production of biotin[6]uril after optimisation studies, including the transition from a shaker to a planetary ball mill.

3 Results and Discussion

3.1 Covalent assembly of cycHC[8] and mixHC[8] in solid state (Publications I and II)

Based on previous research on the solid-state synthesis of cycHC[*n*],[17] the idea arose to incorporate D-biotin into the cycHC[8] structure in order to expand the versatility of the receptor molecule. For example, in sensing applications, this functionality enables immobilisation on solid supports and post-functionalisation via amide coupling to prepare receptor molecules.[2] Moreover, esterification of biotin[6]uril resulted in hydrophobic analogues for transmembrane anion transport carriers.[6] The D-biotin monomer (B) was chosen because it bears a urea moiety that enables macrocycle formation, is commercially available and contains a carboxylic group which is appealing for further derivatisation purposes.

The selective generation of mono-biotin containing cyclohexanohemicucurbituril from a complex mixture is a major challenge, as the number of possible linear and cyclic species increases with the number of monomeric units added. As the biotin monomer is non-symmetric, it can be incorporated in different orientations within the oligomer structures, which further complicates the mixture and increases the number of plausible intermediates. According to a combinatorial assessment conducted by Marko Vendelin, approximately 50,000 possible linear and cyclic oligomers (2 to 10 monomeric units) can form. However, template-assisted cyclisation reduces the number of possible products. Only 498 distinct 8-membered cyclic products are possible when accounting for the number of biotin and cyclohexa-1,2-diylurea (CU) monomers, the possible orientations of the asymmetric biotin unit, and the monomer sequence (Figure 17).

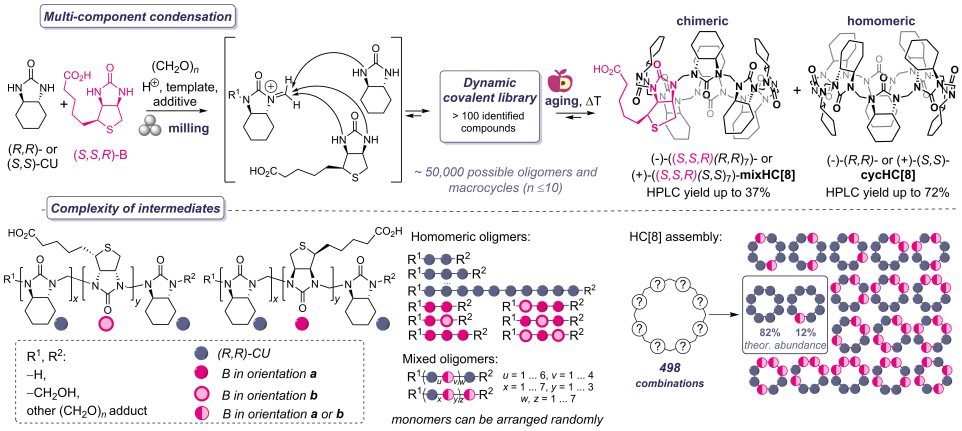

Figure 17. Synthetic scheme and complexity of intermediates involved in the formation of HC[8]s investigated in this work.

The first attempts to synthesise mono-functionalised mixHC[8] in acetonitrile solution, following the known protocol for cycHC[8],[63] were promising. B and CU monomers were used in a stoichiometric 1:7 molar ratio and mixed with paraformaldehyde, using TFA as a Brønsted acid catalyst and templating agent. MixHC[8] was obtained in 9% yield, along with cycHC[8] as the major product (38% yield), that is, in a ca. 1:4 ratio. This product ratio did not reflect the expected statistical distribution of 1:7 based on the starting

monomers, suggesting a dependence on the reaction conditions, such as acid, solvent, concentration, temperature or other experimental variables.

In solution-phase synthesis, the compatibility of the solvent with reagents determines the efficient diffusion and mixing of starting materials, intermediates and products, thereby influencing their reactivity. Poor solubility can hinder reactions, especially in DCC, by limiting the exchange between the reactants. Therefore, we envisaged that mixHC[8] could be assembled more efficiently in the solid state, where solubility is not a limiting factor, non-covalent interactions are not obstructed by solvent molecules and templation is enhanced due to the high concentration of reactants.[162] Previous studies with cycHC[8] mechanosynthesis[17] have demonstrated that covalent self-assembly in the solid state requires only minimal amounts of liquid additive[103,117,163] to facilitate proton transfer, mediate anionic template delivery and promote conformational flexibility.

According to the combinatorial analysis, complete conversion of a 1:7 molar ratio of B:CU into HC[8] products is assumed to direct 498 possible 8-membered cyclic combinations to a 12% yield of mixHC[8] and an 82% yield of cycHC[8], resulting in a ratio of 1:6.8. The above-mentioned deviation from the statistical distribution (1:7) of mixHC[8] and cycHC[8] in solution-phase synthesis motivated us to investigate whether the selectivity of mono-biotinylated mixHC[8] formation could be enhanced by mechanosynthesis.

3.1.1 Condition screening and optimisation studies

Reaction mixtures produced by mechanochemistry are generally heterogeneous and consist of liquid and various solid phases, including crystalline, amorphous and polymorphic solids. Mixture homogeneity (that is, uniform composition) depends on the amount of LAG additive and may display substantial variations in chemical composition. Thus, accurate quantification of products requires a reliable analytical method. NMR analysis is insufficient for this purpose because the reaction mixture is highly complex, containing oligomers and various products with overlapping signals in the ^{1}H NMR spectra. In contrast, high-performance liquid chromatography coupled with ultraviolet and mass spectrometric detection (HPLC-UV-MS) offers separation of mixHC[8] and cycHC[8], as well as identification and quantification based on their calibration graphs. However, accurate analysis is further complicated by mass fluctuations caused by evaporation of water or its absorption from the air. This influences the concentration of solids and the reaction mixture inhomogeneity (i.e. uneven distribution of components in the solid reaction mixture). Although the use of an internal standard for yield determination in homogeneous solvent-based synthesis is well established, its application in solid-state synthesis has not been thoroughly validated.

The condensation reaction between urea monomers and formaldehyde produces water as a side product, thereby changing the liquid-to-solid ratio in the reaction mixture during milling and aging. Therefore, triphenylmethane (TPM) was used as a solid internal standard and introduced to the reaction mixture before the milling step to mitigate the issue with uncontrollable water evaporation throughout the whole reaction process. TPM was chosen due to its chemical inertness (it is unreactive towards strong acids, monomers and macrocyclic products), stability and strong UV absorbance, which allowed the use of very small amounts of standard (usually ca. 3% w/w) without interfering with the mechanochemical reaction. A single-point measurement approach was used for the analysis of mechanochemical mixtures, meaning that random sampling was done from

different parts of the milling jar and parallel HPLC samples were prepared and analysed. The analytical method was developed and the analysis performed by Tatsiana Jarg.

Several parameters affecting the TPM distribution were investigated, including the amount of LAG, milling duration, TPM loading and total mass of solid reactants. TPM was shown to be distributed uniformly in the reaction mixture during the mixHC[8] synthesis, except when $\eta > 0.5$ µL/mg. Similar trends were observed for the distribution of mixHC[8] and cycHC[8] within the reaction mixtures, demonstrating increased inhomogeneity at higher LAG amounts (Figure 18). Importantly, product distribution depends on the reaction outcome. Reactions carried out under unfavourable conditions resulted in poor yields and consequently greater variation between replicate measurements. The importance of the milling time was also demonstrated. Although a short 5-min milling time was enough to distribute the small amount of internal standard uniformly throughout the mixture, it was insufficient for homogeneous mixing of other reaction components. Increasing the number of parallel measurements can improve the reliability of the results.

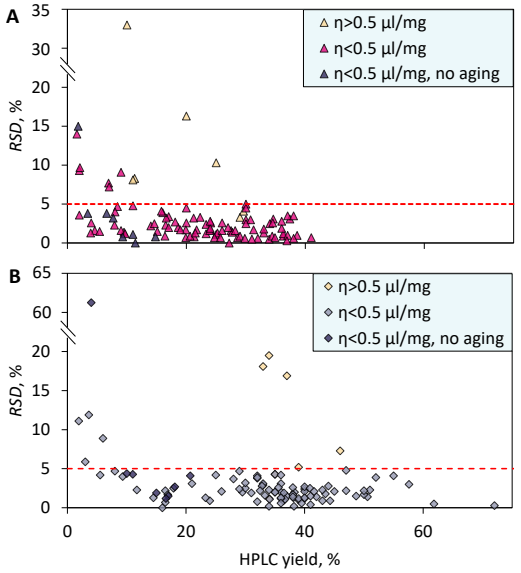

Figure 18. Distribution of mixHC[8] (A) and cycHC[8] (B) in crude reaction mixtures under different conditions, expressed as relative standard deviation (RSD) of corresponding peak areas from replicate samples (n=3). RSD ≤ 5%: acceptance criteria for sufficient homogeneity.

Based on the variability in component distribution in the reaction mixtures, single-point measurements for mechanochemical reaction yield determination must be properly investigated and validated to ensure accurate results representing the whole reaction mixture.

Once a reliable analysis method for yield determination was developed, optimisation studies were conducted. Response surface methodology (RSM) was used for the design of experiments and screening of reaction conditions to explore the influence of multiple reaction parameters on the formation of 8-membered macrocycles simultaneously.[164] The HPLC yields of mixHC[8] and cycHC[8], which were determined after the aging step, were visualised as 3D response surfaces, identifying the favourable conditions for the assembly of mixHC[8] over cycHC[8]. The ratio of monomers, amount of aqueous mineral

acid ($HClO_4$), milling duration and aging temperature, all of which influence the macrocyclisation of cycHCs,[78] were investigated at the same time. The goal was to determine the optimal reaction conditions to maximise the mixHC[8] yield.

The monomer ratio (B:CU) was varied between *1:5 and 1:15 equiv*. to evaluate its effect on the selectivity of the self-assembly process and macrocycle composition, as the ratio of monomers could affect the number of biotin units incorporated into the macrocyclic structure. An excess of biotin could be beneficial if it reacted more slowly than CU monomer, whereas an excess of CU could suppress the formation of polybiotinylated side products. **The acid loading** ranged from *0.5 to 4 equiv*. This parameter accounts for the number of templating anions, protons required for the condensation and cyclisation reactions and water for the liquid grinding additive, while the maximal loading was capped to remain within the LAG conditions and the minimal loading was close to neat grinding. **The milling duration** was between *10 and 60 min*, during which mechanical energy was added to the system and the polycondensation reaction and monomer shuffling occurred. It was previously shown that 30–60 min is sufficient to provide quantitative yields for cycHC[*n*]s,[17] and we wanted to determine whether the milling time could be decreased, while ensuring sufficient mixing of reagents and mechanical energy transfer. Finally, **the aging temperature** range was between *35 and 75 °C*; at this step, the self-assembly of oligomers to macrocyclic products takes place and it was previously shown that elevated temperatures accelerated the formation of macrocycles.[17]

After selecting the variable parameters, experiments were planned in Design-Expert 13 software[165] using an optimal (custom) design for four numeric factors with a polynomial model with a quadric process order. 23 experiments were conducted and reaction mixture content was analysed after the aging step. Based on HPLC results, response surfaces were plotted and analysed.

The analysis of 3D response surfaces revealed that the formation of mixHC[8] and cycHC[8] was sensitive to the monomer ratio and acid loading (Figure 19). Changing the monomer ratio did not significantly impact the yield of mixHC[8]; however, using excess CU monomer led to a clear increase in the generation of homomeric cycHC[8]. The amount of $HClO_4$ was the most vital parameter influencing chimeric mixHC[8] formation. The highest yields for mixHC[8] were obtained within the specific range of 1.2 to 3.0 equiv. of $HClO_4$, while cycHC[8] was less sensitive to the acid loading. This finding emphasises the differences in mixHC[8] and cycHC[8] generation in response to changes in reaction conditions. The milling duration and aging time were less significant, although the optimal aging temperature for mixHC[8] ripening was determined to be between 40 and 65 °C. This RSM study helped achieve a 20% yield for mixHC[8] under the following conditions: 3 equiv. of template, 1 h of milling and 24 h of aging at 60 °C, which were selected for further optimisation studies.

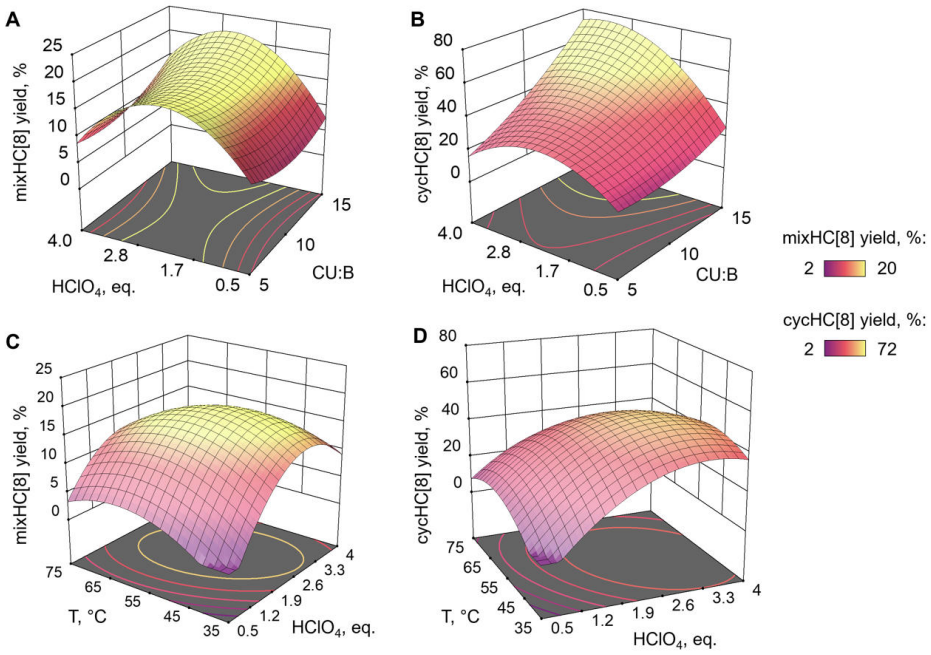

Figure 19. 3D response surfaces displaying the effects of monomer ratio and acid loading on the HPLC yields of (A) mixHC[8] and (B) cycHC[8], and the effects of aging temperature and loading of acid on the HPLC yields of (C) mixHC[8] and (D) cycHC[8].

Building on previously established conditions using perchloric acid, we further investigated alternative templating systems, the role of salt additives, and specific kinetic requirements of milling and aging to achieve the highest possible yields.

Previous binding studies with cycHC[8] showed good affinity towards hexafluorophosphate (PF_6^-),[64] and this has been used as an efficient template for cycHC[8] synthesis in solution.[63] Based on this information, HPF_6 was selected as an alternative reagent to mediate the solid-state formation of mixHC[8] (Figure 20A).

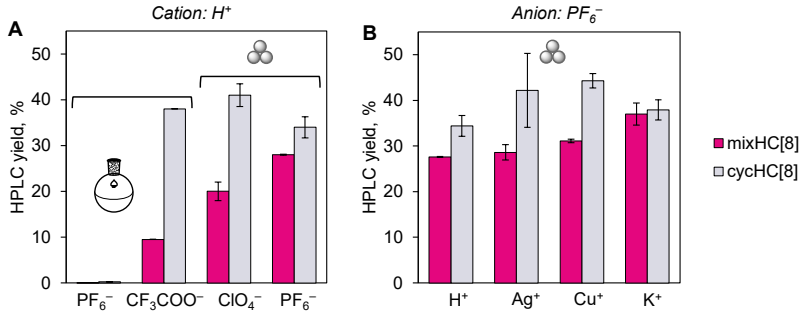

Figure 20. Bar charts describing the effect of acid anions in solution-phase synthesis and in the solid-state (A) and hexafluorophosphate salt cations in the solid state (B) on the yields of mixHC[8] (magenta) and cycHC[8] (grey). Error bars express the standard deviation of HPLC yields between the reproduced reactions (n = 2–8).

Notably, replacing $HClO_4$ with HPF_6 increased the yield of mixHC[8] to 28% and reduced the formation of cycHC[8]. Since mixHC[8] formation was sensitive to the acid loading, three hexafluorophosphate salts ($AgPF_6$, $[Cu(CH_3CN)_4]PF_6$ and KPF_6) were tested as additives to partially substitute the acid while maintaining a constant concentration of templating anion (Figure 20B). It was also assumed that Ag^+ and Cu^+ cations could potentially promote mixHC[8] formation due to their affinity for biotin's sulphur atom, thus promoting its incorporation into the macrocycle.[166–168] However, the addition of Ag^+ and Cu^+ salts had minimal effect on mixHC[8] formation while increasing the yield of cycHC[8] compared to the HPF_6-only system. This suggests a reduction in CU-rich mixed oligomers, which can reorganise and provide free CU for the formation of cycHC[8]. Among the tested salt additives, KPF_6 provided the best results, yielding 37% mixHC[8] alongside 38% cycHC[8]. Additional optimisation with RSM with KPF_6/HPF_6 did not improve the mixHC[8] yields.

With the best templating combination (2 equiv. HPF_6 and 1 equiv. KPF_6), the monomer ratio, milling time and aging duration were additionally optimised. Monomer ratios of 1:5, 1:7 and 1:15 were checked. A stochiometric ratio of 1:7 proved to be the best (Table 1).

Table 1. Screening monomer ratio.

Entry	Monomer molar ratio	HPLC yield, %	
		mixHC[8]	cycHC[8]
1[a]	1:5	34	30
2[b]	1:7	37±2	38±2
3[c]	1:15	27	62

HPLC yields are provided as mean value ± standard deviation for the reaction reproduced 4 times for [b] and [a, c] are single experiments. The deviation between triplicate HPLC measurements did not exceed 0.7%.

The milling time was varied from 5 to 90 min (Table 2). A mixHC[8] yield of 37% was achieved after 20 min. However, a milling time of 60 min was selected to ensure efficient mixing and distribution of intermediates. Increasing the milling time to 90 min did not improve the yields. Shorter milling times also did not benefit the yield of mixHC[8] and required a longer aging time (Table 3).

Table 2. Screening milling times.

Entry	Milling time, min	mixHC[8] HPLC yield[a], %	cycHC[8] HPLC yield[a], %
1	5	15.5±0.4	55±3
2	10	23.9±0.2	39±3
3	20	37±1	39±1
4	30	33±4	32±3
5	45	26±4	29±4
6	60	37±2	38±2
7	90	34±1	32±1

The deviation between parallel measurements did not exceed 3.1%; [a] Average HPLC yields expressed as the mean value ± standard deviation between reactions reproduced *n* times (*n* = 2–4).

The aging duration was varied from 0 to 24 h (Table 3). It was found that the aging time could be substantially shortened to 3 h. When the reaction was milled for 20 min and aged for 3 h, a lower yield of mixHC[8] was obtained compared with the reaction milled for 60 min. Therefore, the optimal aging duration for a 60-min milled reaction was 3 h.

Table 3. Screening aging duration.

Entry	Aging time, hr	mixHC[8] HPLC yield[a], %	cycHC[8] HPLC yield[a], %
1	0	13±3	18±4
2	3	38±1	34±2
3	6	38±1	35.3±0.1
4	12	32.1±0.5	33±2
5	24	37±2	38±2
6	3[b]	30.1±0.3	31.7±0.2

The deviation between parallel measurements did not exceed 1.5%; [a] Average HPLC yields expressed as the mean value ± standard deviation between reactions reproduced n times (n = 2–4). [b] Reaction mixture was milled for 20 min.

After optimisation of the key parameters, the highest yield of mixHC[8] was 38% after a total reaction time of 4 h, representing an approximately fourfold improvement over the initial results obtained in solution-phase synthesis. Careful fine-tuning of the chemical environment and mechanical parameters helped efficiently direct the covalent self-assembly from a complex library of ca. 50,000 possible members towards two major products, homomeric cycHC[8] and new chimeric mixHC[8].

3.1.2 Overview of self-assembly mechanism

The synthesis of mono-biotinylated mixHC[8] via mechanochemistry is a complex example of DCC, where the final product distribution is governed by the interconversion of thousands of intermediates. The synthesis is carried out in two stages. Firstly, milling of the reactants generates a rich DCL of numerous linear and cyclic intermediates via an acid-catalysed polycondensation reaction between the monomers and paraformaldehyde. Secondly, during subsequent aging of the crude reaction mixture, DCL intermediates self-assemble into stable macrocyclic products around the anionic template.

HPLC-MS analysis, conducted by Tatsiana Jarg, revealed that coupling between CU monomers is kinetically preferred. This occurs at the initial phase of the polycondensation reaction after only 5 min of milling before CU-CU dimers begin to decay as they are incorporated into longer oligomer chains. Conversely, the condensation of biotin monomers is significantly slower, and B-B dimer decay was absent in this case; however, even for biotin monomers, the maximum amount was reached after 5 min.

The composition of the reaction mixture changes between the end of milling and after aging (Figure 21). Directly after the milling stage, the yields of macrocycles remained below 20% but increased noticeably after aging. This could be attributed to the high entropy during milling, which prevents steady interaction between the template and macrocycle, which is necessary for cyclisation.[17,64] The duration of milling determines what will occur after aging. If the reaction mixture is milled for a short time (5 min) and contains mainly CU oligomers, then after aging, the dominant product is cycHC[8] with a 55% yield, along with a minor amount of mixHC[8] (16% yield). However, milling for 60

min further allows the rapid C-N bond formation and cleavage, causing dynamic changes in the DCL profile with a random distribution of biotin units in the oligomeric structure. This significantly increases the HPLC yield for mixHC[8] from 16% to 37%, with a concurrent decrease in cycHC[8] yields to 38% after aging, resulting in a 1:1 product ratio.

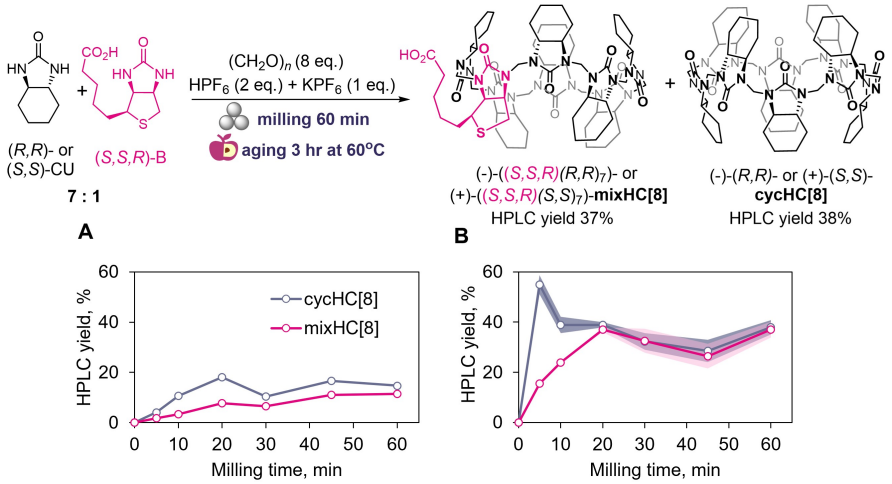

Figure 21. Best reaction conditions for mixHC[8] mechanosynthesis and HPLC yields of mixHC[8] (pink) and cycHC[8] (grey) after only milling (A) and after aging (B).

3.1.3 Preparative synthesis and green metrics evaluation

After establishing the optimal reaction conditions, the procedure was repeated several times to produce 2.6 g of crude reaction mixture with each mixHC[8] diastereoisomer. The resulting crude reaction mixture required a multistep purification procedure to separate mixHC[8] from cycHC[8] and oligomeric by-products. First, the dry crude reaction mixture was treated with 5% KOH in methanol for 45 min to convert the mixHC[8] to its potassium salt. The methanol and water were removed by three successive azeotropic evaporations with toluene until a dry mixture formed. Next, solid-liquid extraction with toluene was performed to remove the majority of the more soluble cycHC[8]. The remaining solid was then dissolved in water, resulting in a milky suspension, which was subsequently acidified with HCl until the pH was 2-3, causing the formation of a white precipitate. The solid was then filtered and dried in air. Finally, the remaining dry solid was purified via flash column chromatography to yield pure mixHC[8]. CycHC[8] and oligomers were also obtained but were not separated by this approach.

This procedure afforded 225 mg of (+)-mixHC[8] (11% yield and 90% NMR purity) and 320 g of (−)-mixHC[8] (16% yield and 88% NMR purity). Detailed characterisation of the products is provided in the corresponding article supporting information.

Depending on the CU monomer used, two different enantiopure diastereoisomers were obtained, each showing slight conformational differences. A density functional theory (DFT) study, performed by Rauno Reitalu and Mario Öeren, revealed that the mixHC[8]s, predominantly composed of CU units, are altered mainly by the biotin position. The sulphur atom in the biotin monomer is oriented toward the inside or outside of the macrocycle cavity. As a result, the two diastereoisomers give distinct NMR spectra with the most pronounced differences observed for the biotin envelope moiety (Figure 22).

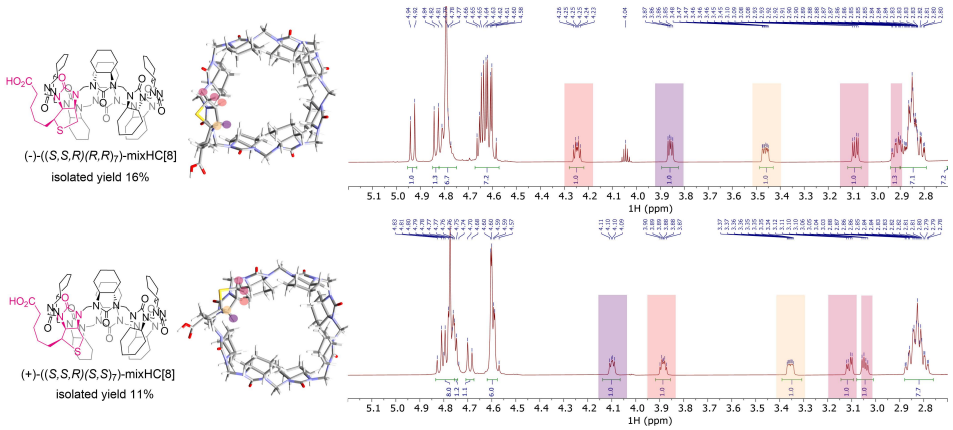

Figure 22. MixHC[8] diastereoisomers, their DFT models and respective ^{1}H NMR spectra.

Solvent-free synthesis of mixHC[8] showed a much lower reaction PMI (= 4) than the reaction carried out in acetonitrile solution (PMI = 306), reflecting the higher yields and conversion to products. PMI values were calculated based on the HPLC yields obtained after the aging step. For these calculations, all the input reactants were summed and divided by the product mass calculated from the HPLC result. Although the solution-based synthesis was not optimised and the isolation procedures were not compared, it is reasonable to assume that they would be similar.

3.1.4 Anion-binding properties and applicability

As mentioned, mixHC[8] diastereoisomers have different conformations due to different biotin monomer positions. Anion-binding studies with both mixHC[8] diastereoisomers were performed using isothermal titration calorimetry (ITC), performed by Tatsiana Jarg, and the cycHC[8] data was available from a previous study (Figure 23).[64]

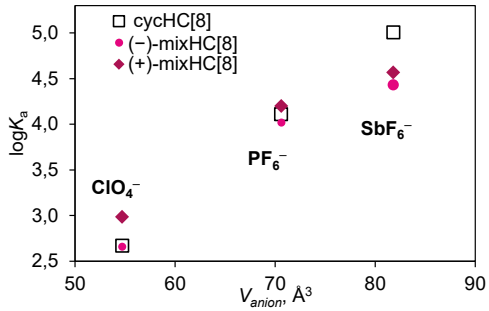

Figure 23. Correlation between association constants and anion volumes obtained from ITC analysis.

The mono-biotinylated macrocycles formed complexes with chaotropic anions (ClO_4^-, PF_6^- and SbF_6^-) in methanol and a methanol-water mixture (1:1) through an exothermic, enthalpy-driven process. The (+)-mixHC[8] showed higher binding affinities than its (−)-diastereoisomer across all anions, and for perchlorate, the binding efficiency was almost twice as high as for (+)-mixHC[8] and cycHC[8]. The association constants for PF_6^- were higher than those of ClO_4^- in both media, supporting its enhanced templating effect in the mechanosynthesis of mixHC[8]. The differences in binding affinity among all three

macrocycles were least pronounced for PF_6^-, whereas SbF_6^- and ClO_4^- exhibited stronger binding to cycHC[8] and (+)-mixHC[8], respectively. These observed differences reflect the variations in cavity properties and steric features, highlighting their relevance to tailored applications and selective guest binding.

The carboxylate side chain of mixHC[8] was used to covalently immobilise it on the surface of 3-aminopropyl silica gel (APS), resulting in a functional material. This material was further used to selectively capture perchlorate anions from solution. When mixHC[8] is covalently bound to APS, the macrocycle remains in the solid phase even in solvents in which it is soluble, such as dichloromethane or methanol, and can therefore be used in solid-liquid extractions. Functionalisation and perchlorate removal experiments were conducted by Tatsiana Jarg.

3.2 Scalable mechanochemical synthesis of biotin[6]uril (Publication III)

As discussed in Chapter 1.2.1 of the literature overview, the solution-based procedure for B[6]U delivers moderate yields of 40–60%, requires a long reaction time (48 h) and synthesis is limited to gram-scale (Figure 24). Additionally, substantial hazardous waste is generated, primarily due to the large amount of strong mineral acids used and the process is labour-intensive. Building on previous work on cycHC[*n*][17] and mixHC[8][5] in the solid state, we therefore focused on developing a practical mechanochemical approach to the large-scale synthesis of B[6]U with high purity. This approach enables a drastic decrease in the consumption of toxic solvents and affords higher yields, both of which contribute to a lower environmental impact compared with the solution-based method.

The mechanochemical approach to B[6]U is similar to that in previous works[5,16,17] and involves two steps. First, a dynamic covalent library of oligomers is generated via the mechanochemical acid-catalysed polycondensation reaction between the D-biotin monomer and paraformaldehyde during the milling stage. Second, template-assisted covalent self-assembly is promoted during aging at 60 °C, yielding the macrocyclic product B[6]U.

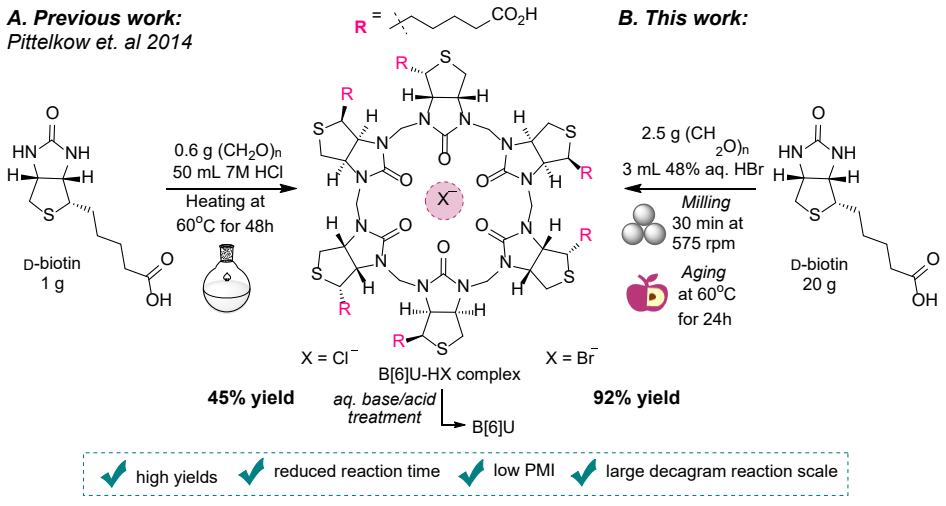

Figure 24. (A) Solvent-based synthesis of B[6]U (previous work)[60] and (B) mechanochemical approach to B[6]U (this work).

The investigation began with optimisation studies in a shaker mill to determine the most suitable templating agent and aging duration to maximise product formation. This was followed by the scale-up in the shaker mill. The procedure was later adapted for the planetary mill to produce decagram quantities of the product. Finally, the developed method was compared with solution-based synthesis by green chemistry metrics.

HPLC yields for B[6]U were calculated similarly to mixHC[8]. The analysis was conducted after the aging step, and calibration graphs were constructed for the B[6]U standard and TPM as an internal standard. Reaction mixtures were sampled *n* times (*n* = 2–5). Careful sampling and analysis enabled monitoring of the inhomogeneity of reaction mixtures, which is induced by insufficient mixing of reactants or incomplete condensation reaction. The reactions were carried out together with Eve Schults.

3.2.1 Optimisation experiments in a shaker mill

Screening reactions were performed on a 1 mmol scale, based on D-biotin, by milling the reactants in 15 mL ZrO_2-coated grinding jars for 1 h at 30 Hz using a single milling ball. After milling, the reaction mixture was transferred to a capped glass vial and aged at 60 °C for several hours, followed by HPLC analysis. During optimisation, the primary focus was on identifying the most effective templating additive and aging time, as these are the two key parameters impacting the product yield. The milling time was kept constant at 60 min. This time was selected to ensure the completion of the condensation reaction between the biotin monomers and paraformaldehyde, as well as a homogeneous distribution of templating agent.[5,17]

Anionic templates govern the self-assembly process and stabilise the forming macrocycle; thus, determining the best template is crucial. Anions with stronger binding affinities usually serve as more effective templates.[5,78] Chloride and bromide anions were shown to be effective templates in solution-based synthesis;[60] thus, the first attempts were performed with 38% aq. HCl and 48% aq. HBr (0.5 equiv.). Under mechanochemical conditions (Figure 25) with 38% HCl, B[6]U formed with a 64% HPLC yield, while 48% yield was achieved in solution-based approach. The best results in mechanosynthesis were achieved with 48% aq. HBr (91% HPLC yield), but decreasing the amount of HBr to 0.3 equiv. further increased the HPLC yield to 95%. This outcome is consistent with the significantly higher binding affinity constant of bromide (K_a = 540 M^{-1}) to chloride (K_a = 55 M^{-1}) for B[6]U.[60] This shows that in the solid-state, the choice of template (Br^- or Cl^-) has a stronger effect on the yield of the product (>91% vs 64%) than in solution (63% vs 48%),[60] probably due to the stronger interactions with the templating anion in the concentrated reaction media, which are not affected by solvent molecules.[5,162] During the optimisation of mixHC[8] synthesis, it was found that the combination of solid and liquid templating agents resulted in the best outcomes.[5] Therefore, the combination of 48% aq. HBr with solid NaBr (0.3 + 0.2 equiv.) was attempted, but was found to be ineffective in this case. A combination of 50% aq. H_2SO_4 with solid NaBr salt (0.5 equiv.) also produced only 55% B[6]U. Mechanochemical reactions under LAG conditions can be sensitive to the amount and properties of LAG additives.[117,163] The LAG additive in the B[6]U synthesis was water, and η remained in the range of 0.13–0.21 µL/mg. This range is relatively small compared to the addition of solid NaBr or sulphate anion to the templating media, which both appear to hinder the self-assembly of B[6]U under these conditions.

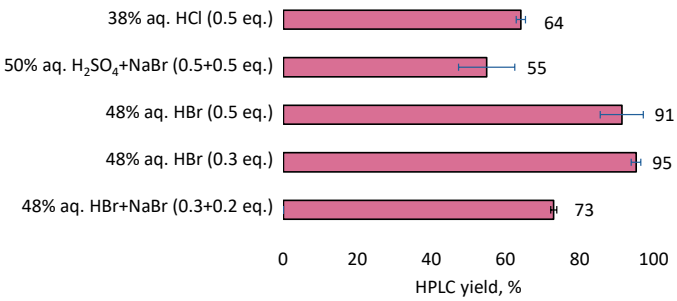

Figure 25. Screening different templates. General reaction conditions: 1 mmol biotin, 1 h of milling at 30 Hz and 24 h aging at 60 °C. HPLC yields were determined via multiple sampling (n = 3) of the reaction mixture, containing TPM as internal standard. Black error bar expresses the standard deviation of replicate measurements, and blue error bars show total error, including within- and between-reaction variance.

Various aging durations were evaluated across all tested templating agents, to optimise the aging time (Figure 26).

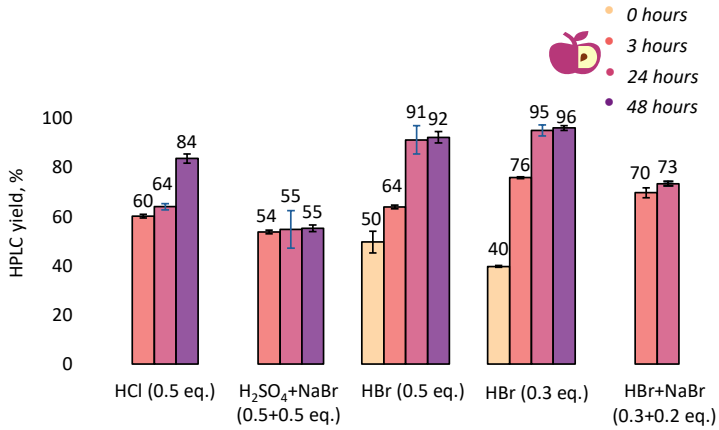

Figure 26. Screening aging duration. General conditions: 1 mmol reaction scale, 1 h milling at 30 Hz. HPLC yields were determined via multiple sampling (n = 2–3) of the reaction mixture, containing TPM as internal standard. Black error bar expresses the standard deviation of replicate measurements, and blue error bars show total error, including within- and between-reaction variance.

A shorter aging time of 3 h consistently produced lower yields (54–76%), demonstrating that insufficient aging results in incomplete product formation. Increasing the aging duration to 48 h generally improved the yields. The most noticeable increase was observed with 38% aq. HCl, from 64% to 84% B[6]U. However, with the optimal template (0.3 equiv. HBr), the yield remained comparable to that with the 24 h aging time. This shows that the self-organisation is faster with the HBr template, which is consistent with the stronger affinity of B[6]U towards the bromide ion.[60] Generally, 24 h aging appeared to be the optimal aging duration for the HBr template and aging was found to be an important step for macrocycle formation. Without the aging step and with milling only, the HPLC yield dropped significantly from 95% to 40%, where most of the

mixture remained as oligomers of various lengths. This aligns with previous studies,[5,17] confirming that the additional aging step is crucial for effective amplification of the target macrocycle, thereby reducing the need for further lengthy purification from linear oligomers.

In conclusion, during the optimisation studies, the optimal conditions for B[6]U mechanosynthesis were determined to be 48% aq. HBr (0.3 equiv.) with 1 h of milling at 30 Hz, followed by aging at 60 °C for 24 h, providing B[6]U in high 95% yield.

3.2.2 Scaling up in a shaker mill

The next step was to scale up the developed process while maintaining high yields. We started with upscaling in a shaker mill with the 15 mL ZrO_2-coated milling jars used previously. However, the jar loading was increased stepwise, while maintaining the established optimal reaction conditions (Figure 27A). Increasing the milling load from 1 to 4 mmol (ca. from 250 mg to 1 g) led to a progressive decrease in HPLC yields from 95% to 84%. This tendency is common in mechanochemical reactions and has been reported before when using shaker mills,[160,169,170] since the same amount of mechanical energy is distributed across a larger amount of reactants.

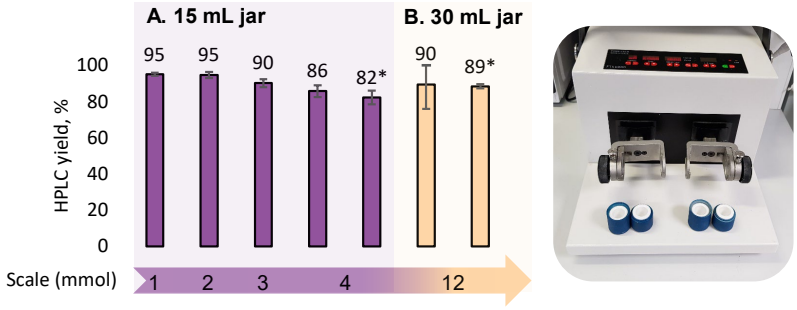

*Figure 27. Scale-up reactions in shaker mill using 15 mL (A, purple) and 30 mL (B, yellow) milling jars. HPLC yields were determined via multiple sampling (n = 3) of the reaction mixture, containing TPM as internal standard. General reaction conditions: 60 min of milling and 24 h aging at 60 °C. *– milling duration 5 min.*

As the shaker mill was operating at its maximum milling frequency of 30 Hz, the total mechanical energy input could only be increased by prolonging the milling time beyond 1 h. However, based on a previous study with mixHC[8], showing that the polycondensation reaction of D-biotin and cyclohexa-1,2-diylurea monomer can be relatively rapid (<30 min), we reduced the milling time. This was tested by conducting a reaction at the 4 mmol scale with a 5-min milling time only, demonstrating that B[6]U was formed in 82% yield, comparable to the 86% yield obtained with 1 h of milling. Thus, only a relatively short initial milling period is required to initiate the reaction, which then occurs under the static conditions of aging.

Notable changes in the reaction mixture rheology were also observed at larger scales. While the 1-mmol-scale reactions formed free-flowing solid particles after milling, upscaled reactions produced a highly adhesive paste, which coated the surfaces of the milling jars and balls, hindering removal from the milling vessel. After aging, the reaction mixture solidified into a tough mass, which was difficult to break apart with a spatula (Figure 28).

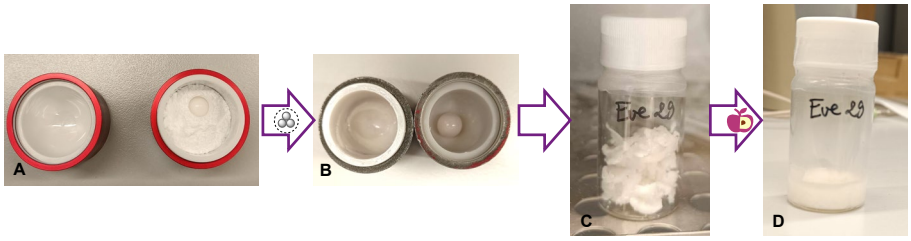

Figure 28. Photos of shaker mill upscaled reaction steps: A – starting materials in the jar, B – reaction mixture after milling, C – reaction mixture transferred to a glass vial and D – reaction mixture after aging.

The 15 mL jars were switched to larger 30 mL ones to enhance the yield of B[6]U (Figure 27B). Simultaneously, the reaction scale was tripled to 12 mmol and B[6]U was obtained with nearly 90% HPLC yield. Even though the average yield was high, substantial variation occurred in the HPLC results; data analysis according to the standard procedure resulted in values from 78% to 105% for samples collected from different sections of the milling jar. This variation was attributed to the inhomogeneity of the reaction mixture, probably due to insufficient mixing of the reagents and internal standard, resulting in erroneous determination of yields. This inhomogeneity issue was not seen at lower scales, highlighting the importance of sufficient milling. As shown in Publication II, the inhomogeneity of the reaction mixture increases the error, this is further confirmed in this study.[171] This further highlights the importance of reliable analysis when determining yields in mechanochemical reactions.

The inhomogeneity hypothesis was checked by mixing reactants manually with a spatula in a glass vial (4 mmol scale) without applying any advanced mechanical treatment. This was followed by 24 h of aging at 60 °C. Surprisingly, the reaction produced B[6]U with an average HPLC yield of 91%. However, the reaction mixture composition showed higher variation (HPLC yields from 75% to 100%, resulting in a high standard deviation of 14%) compared to the same scale shaker mill experiment, where the standard deviation was below 4%. To improve homogeneity, reactants were also grinded with a mortar and pestle for 5 min. This produced a more homogeneous reaction mixture (standard deviation below 1.6%) but resulted in a lower average HPLC yield of 34%. The incomplete conversion was attributed to the loss of volatile HBr in an open reaction vessel during grinding. These findings suggest that mechanical energy promotes effective homogenisation, enabling uniform distribution of aqueous HBr as a catalyst and templating agent, while also expediting the polycondensation reaction.

3.2.3 Scaling up in planetary mill

Further scaling up in the shaker mill was restricted by the jar volume, where the maximum reaction scale was approximately 3 g. Thus, we aimed to transfer the mechanochemical protocol to an in-house ND2L planetary mill (Torrey Hills Technologies), supplied with larger 100- and 500-mL ZrO_2-coated milling jars (Figure 29).

The initial experiments were conducted in a 100 mL jar using 10 g of D-biotin (41 mmol) with 80 × 6 mm ZrO_2 milling balls. The planetary mill was set to its maximum spinning rate (575 rpm for the milling jar and 285 rpm for the planetary disk), while maintaining the same reaction conditions as in the shaker mill. This resulted in an average HPLC yield of 83% with a relatively high standard deviation of 11%, implying to insufficient mixing.

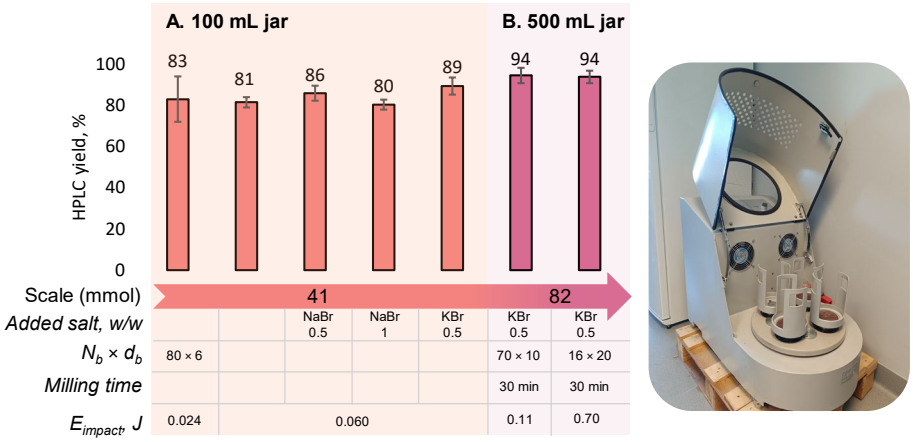

Figure 29. Scale-up reactions using 100 mL (A, orange) and 500 mL (B, pink) milling jars. HPLC yields were determined via multiple sampling (n = 3–5) of the reaction mixture, which contained TPM as internal standard. General reaction conditions: 60 min of milling (if not stated otherwise) and 24 h aging at 60 °C, 30 × 10 mm balls, no salt as additive. Acronyms used: N_b – number of balls, d_b – diameter of balls, added salt w/w – loading of salt (g) per 1 g of D-biotin.

The adhesive nature of the reaction mixture posed a major challenge here, as it caused the milling balls to stick together, hindering proper mixing. Moreover, the dense paste formed during milling could not be easily transferred to another vessel, hence the aging step was conducted directly in the same sealed milling jar (Figure 30).

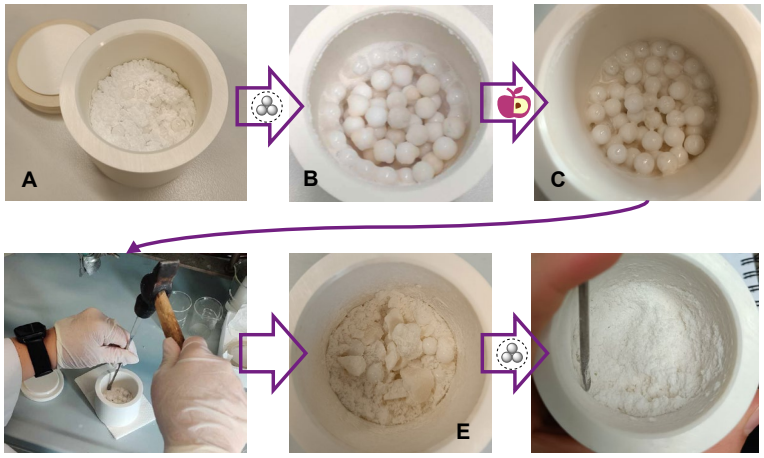

Figure 30. Photos of planetary mill upscaled reaction steps: A – starting materials in the jar, B – reaction mixture after milling, C – reaction mixture after aging, D – cracking the solid reaction mixture with a hammer and spatula, E – reaction mixture cracked into pieces and F – pulverised reaction mixture.

Using heavier 30 × 10 mm milling balls improved the homogeneity (standard deviation 2.5%), although the average HPLC remained unchanged. To modify the reaction mixture rheology, a solid grinding additive (NaBr) was introduced, which can also act as a templating agent and promote B[6]U formation during the aging step. In previous work, Pittelkow reported that the binding affinities of NaBr and KBr towards B[6]U are very

similar (K_a = 540 and K_a = 490 M^{-1}, respectively) in heavy water, with a modest preference for the sodium salt.[60] The addition of NaBr (0.5 g per 1 g of D-biotin, w/w) transformed the rheology of the reaction mixture from paste to rock-solid mass and slightly increased the HPLC yield to 86%. Nevertheless, it did not prevent aggregation into a single compact mass stuck to the milling jar and balls, as initially hoped. Increasing the NaBr loading from 0.5 to 1 w/w led to a decrease in the HPLC yield to 80%, likely due to dilution of active template and catalyst. Replacing NaBr with KBr had a positive effect, slightly increasing the HPLC yield to 89%. This finding is consistent with previous results emphasising the importance of counter-ion pairing in mechanochemistry.[172] This can be explained by the weaker crystal lattice energy of KBr compared to NaBr (672 vs 736 kJ·mol^{-1}, respectively),[173] which facilitates the easier release of bromide ions as a template into the reaction media. Regardless of these efforts, the results remained consistently below the 90–95% HPLC yields achieved in the shaker mill experiments.

Transitioning between different mechanochemical equipment can be challenging and often leads to variations in yields, as several instrument-specific parameters (jar volumes and dimensions, size and weight of milling balls, filling degree) strongly influence the outcomes.[95] The key challenge is comprehending which of these parameters are critical for reproducibility and identifying pivotal factors for consistent results. For better understanding and navigation through the selection of important parameters, we calculated and assessed the total cumulative energy input (E_{total}) and impact energies (E_{impact}) in our experiments (Table 4) using the kinematic model developed by Lungerich and co-workers.[136]

Table 4. Energy values calculated with Ball Mill online Calculator.[136]

instrument	jar volume, mL	d_b, mm	N_b	f or ω_p, Hz or rpm	time, min	E_{impact}, J	E_{total}, kJ
FTS-1000	15	10	1	30 Hz	60	0.059	64
FTS-1000	15	10	1	30 Hz	5	0.059	5.3
FTS-1000	30	10	1	30 Hz	60	0.059	64
FTS-1000	30	10	1	30 Hz	5	0.059	5.3
ND2L	100	6	80	285	60	0.024	123
ND2L	100	10	30	285	60	0.060	110
ND2L	500	10	70	285	30	0.11	228
ND2L	500	20	16	285	30	0.70	319

Despite the total energy input (E_{total}) being consistently higher in planetary mill experiments (Table 4), it did correlate with the yields in our case. However, the impact energies appeared to be more informative, as the values from the planetary mill using 6-mm (E_{impact} = 0.024 J) and 10mm (E_{impact} = 0.060 J) balls were lower or similar to those in the shaker mill (E_{impact} = 0.059 J for the 15- and 30-mL jars). We hypothesised that the lower yields obtained in these reactions could be explained by low impact energies. Using Lungerich group's Ball Mill Calculator, we found that using 500 mL jars with 10- and 20-mm milling balls would significantly increase the impact energies to 0.11 and 0.70 J, respectively.

Implementing these conditions resulted in a clear improvement, increasing the HPLC yields to 94% while scaling up to 20 g (82 mmol) of D-biotin (Figure 29B). Based on these results, it was observed that even though this model is simply kinematic and does not

consider the system's chemical reactivity and rheology, it can provide important direction in selecting crucial parameters when transitioning between different milling devices. As discussed in the literature overview, reactions occurring under aging conditions depend on E_{impact}, and the initial milling is only necessary to promote mixing and reduce the particle size and amorphisation.[128] However, the reaction does not require constant ball impacts to be sustained, and the total energy input is not critical. This also explains why the impact energy, rather than the total energy, was important in the mechanosynthesis of B[6]U.

Considering the rapid polycondensation observed in the shaker mill and very high cumulative total energy input in the planetary mill, we predicted that the milling time could be reduced to 30 min. This proved sufficient, and this modification was incorporated into the final experimental protocol. The milling time could likely be further reduced, as the total energy input was shown to be non-critical; however, this was not investigated in this work. Under optimised conditions – 82 mmol of D-biotin, 0.3 equiv. 48% aq. HBr, 0.5 KBr (w/w), 30 min milling (at 575 rpm for the milling jar and 285 rpm for the planetary disk) and 24 h of aging at 60 °C – the B[6]U product was isolated as an off-white powder in 92% yield (19.3 g) with 91% purity, as determined by qNMR analysis after aqueous work-up, filtration and drying. The work-up procedure was not optimised and was adapted from the previously reported method.[6] In the solution-based approach, after reaction completion, the reaction is quenched with water and filtered. The HCl from B[6]U is removed by dissolving the B[6]U-HCl complex in aq. NaOH, followed by precipitation with conc. H_2SO_4 and filtration. After washing with water and drying, pure B[6]U was obtained. In our approach, the pulverised material is washed with distilled water, filtered and dried. The obtained solid was dissolved with 10% aq. NaOH. This was followed by acidification with H_2SO_4; the formed white precipitate was filtered, washed with water and dried in air.

3.2.4 Stereoselectivity and green chemistry metrics

Theoretically, nine possible regioisomers of B[6]U could form, as the biotin monomer is asymmetric and the urea's nitrogen atoms are not equivalent (Figure 31). In solution state synthesis, it was reported that only one regioisomer is selectively obtained.[60]

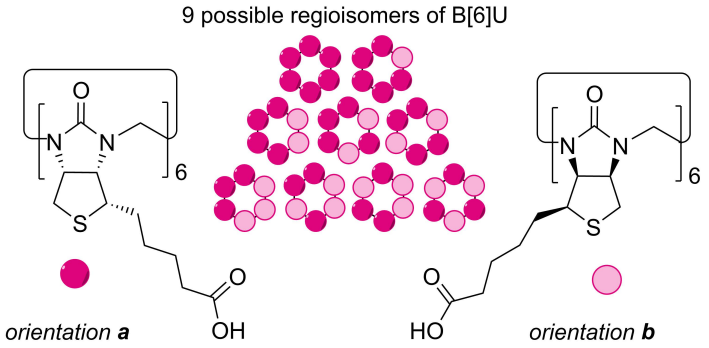

Figure 31. Possible regioisomers of B[6]U.

Additional comprehensive HPLC-MS and NMR analysis helped better understand the product impurities obtained in the developed mechanosynthesis (Figure 32). B[6]U obtained either from solution or via a mechanochemical approach contained minor amounts of regioisomeric B[6]Us and oligomers. HPLC-MS analysis, conducted by

Tatsiana Jarg, showed that the ratios of the two regioisomers were 96:4 for the solution-based synthesis and 97:3 for the mechanochemical approach (Figure 32 left). This indicates that the mechanochemical method is highly stereoselective, and DCC in the solid state closely corresponds to the solvent-based approach.

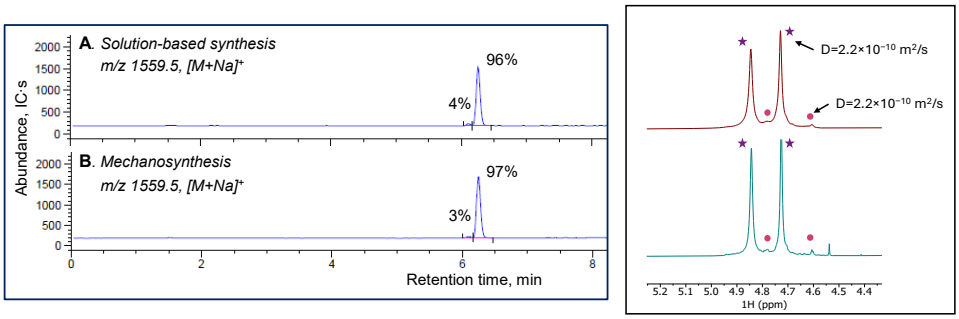

Figure 32. Left: HPLC-MS chromatograms showing the regioisomeric ratios of solution-based synthesis and mechanochemical approach. Right: ^{1}H NMR measured in DMSO-d_6 at 333K at 800 MHz. Red spectrum (top) shows B[6]U synthesised in solution and turquoise spectrum (bottom) shows B[6] synthesised via mechanochemistry. The CH_2 bridge proton signals correspond to the major and minor B[6]U regioisomers, noted as a star and circle, respectively.

Diffusion-ordered spectroscopy (DOSY) NMR experiments, conducted by Jasper Adamson, additionally confirmed the presence of two regioisomers. The major and minor isomers had the same diffusion constant (2.2×10^{-10} mm^2/s) at different chemical shifts, where the major product was at 4.843 ppm and the minor isomer at 4.606 ppm (Figure 32 right). This data is qualitative due to overlapping signals and low concentrations; however, it coincides well with the HPLC-MS results.

The CHEM21 approach was used to illustrate the advantages of the developed mechanochemical synthesis of B[6]U through green chemistry metrics (Table 5).[156] Firstly, the RME was higher for the mechanochemical reaction due to higher yields and stochiometric amounts of paraformaldehyde rather than an excess, which was used in the solution-based approach. PMI values show that the mechanochemical approach outperforms solution synthesis at the same 1 g scale, mainly due to the absence of solvent and higher yields. Especially, the reaction PMI showed roughly a 60-fold reduction (from 123 to 2). Additionally, the mechanochemical protocol reduced the work-up PMI from 728 to 306, although the original isolation and purification method remained unchanged. This is because no dilution with water was required to precipitate the product.[60] Moreover, scaling up to 20 g improved the yield due to enhanced overall efficiency and reduction of material losses in the purification; the work-up PMI was thus further reduced to 85, as a smaller amount of solvents was used in the work-up stage. Likewise, due to the reduced PMI, the TCR metric decreased tenfold for the mechanochemical synthesis compared with the solution-based method. Finally, no significant heat release or pressure increase was observed in the large-scale reactions, showing that no major safety or thermal risks were present.

Table 5. Green chemistry metrics comparison of solution-based method with the developed mechanochemical procedures.

	Solution (1 g scale)	**Shaker mill** (1 g scale)	**Planetary mill** (20 g scale)
Isolated yield[a]	45% (0.5 g)	75% (0.8 g)	92% (19.3 g)
RME	29	58	78
PMI total	851	308	87
PMI reaction	123	2	2
PMI work-up	728	306	85
Purity by qNMR	95%	82%	91%
Regioisomeric ratio	96:4		97:3
TCR	536		55

[a] Yields corrected to purity values: $Yield_{corr}$ = Yield · Purity / 100% are 43%, 62% and 84% for solution-based, shaker mill and planetary mill synthesis, respectively

4 Conclusions

This doctoral thesis has demonstrated that mechanochemical solid-state synthesis is a powerful approach to producing complex hemicucurbituril cavitands, overcoming the limitations of traditional solution-based protocols. By leveraging dynamic covalent chemistry in a bulk solvent-free environment, this work highlighted the highly efficient synthesis of chimeric mono-biotinylated hemicucurbit[8]uril (mixHC[8]) and the scalable mechanosynthesis of biotin[6]uril (B[6]U).

The primary aims of this thesis were to develop mechanochemical methods for hemicucurbituril derivatives. The key outcomes of this research are as follows:

- From a theoretical library comprising approximately 50,000 possible intermediates, mechanochemical covalent self-assembly enabled mixHC[8] product formation beyond the expected statistical distribution. Through profound systematic optimisation, the developed mechanochemical protocol afforded mixHC[8] in 38% HPLC yield using an HPF_6/KPF_6 combination as the acid and template source, with a total reaction time of 4 h. A multistep purification procedure was established to isolate pure chimeric mixHC[8]. The potential application of mixHC[8] was demonstrated through its immobilisation on 3-aminopropyl silica gel, producing a functional material capable of selective perchlorate removal.
- A contribution was made to the development of a reliable HPLC-UV method, using an internal standard, to accurately monitor yields in heterogeneous mechanochemical reaction mixtures.
- B[6]U was synthesised mechanochemically on a decagram scale, affording up to 19.3 g (92% isolated yield) of high-purity (>90%) product. This was enabled by a systematic evaluation of templating systems, which identified 48% aq. HBr as the most effective catalyst and template. The process was subsequently scaled up 82-fold, from a shaker mill to a planetary ball mill. Overall, these developments reduced the reaction process mass intensity by 60-fold and mineral acid consumption by nearly 190-fold.

Collectively, these findings demonstrate that the integration of mechanochemical synthesis with well-defined chemical templation provides an efficient, scalable, and more sustainable platform synthesising advanced functional macrocycles.

References

[1] Magna, G.; Šakarašvili, M.; Stefanelli, M.; Giancane, G.; Bettini, S.; Valli, L.; Ustrnul, L.; Borovkov, V.; Aav, R.; Monti, D.; Di Natale, C.; Paolesse, R. *ACS Appl. Mater. Interfaces* **2023**, *15* (25), 30674–30683.

[2] Anfar, Z.; Kuppan, B.; Scalabre, A.; Nag, R.; Pouget, E.; Nlate, S.; Magna, G.; Di Filippo, I.; Monti, D.; Naitana, M. L.; Stefanelli, M.; Nikonovich, T.; Borovkov, V.; Aav, R.; Paolesse, R.; Oda, R. *J. Phys. Chem. B* **2024**, *128* (6), 1550–1556.

[3] Sokolov, J.; Šindelář, V. *Chem. – Eur. J.* **2018**, *24* (58), 15482–15485.

[4] Shalima, T.; Mishra, K. A.; Kaabel, S.; Ustrnul, L.; Bartkova, S.; Tõnsuaadu, K.; Heinmaa, I.; Aav, R. *Front. Chem.* **2021**, *9:786746*.

[5] Suut-Tuule, E.; Jarg, T.; Tikker, P.; Lootus, K.-M.; Martõnova, J.; Reitalu, R.; Ustrnul, L.; Ward, J. S.; Rjabovs, V.; Shubin, K.; Nallaparaju, J. V.; Vendelin, M.; Preis, S.; Öeren, M.; Rissanen, K.; Kananovich, D.; Aav, R. *Cell Rep. Phys. Sci.* **2024**, *5* (9), 102161.

[6] Lisbjerg, M.; Valkenier, H.; Jessen, B. M.; Al-Kerdi, H.; Davis, A. P.; Pittelkow, M. *J. Am. Chem. Soc.* **2015**, *137* (15), 4948–4951.

[7] Valkenier, H.; Akrawi, O.; Jurček, P.; Sleziaková, K.; Lízal, T.; Bartik, K.; Šindelář, V. *Chem* **2019**, *5* (2), 429–444.

[8] Lang, C.; Mohite, A.; Deng, X.; Yang, F.; Dong, Z.; Xu, J.; Liu, J.; Keinan, E.; Reany, O. *Chem. Commun.* **2017**, *53* (54), 7557–7560.

[9] Pascu, M.; Ruggi, A.; Scopelliti, R.; Severin, K. *Chem. Commun.* **2012**, *49* (1), 45–47.

[10] Shy, H.; Mackin, P.; Orvieto, A. S.; Gharbharan, D.; Peterson, G. R.; Bampos, N.; Hamilton, T. D. *Faraday Discuss.* **2014**, *170*, 59–69.

[11] Dorniak, A.; Haas, M.; Brüggemann, O.; Teasdale, I.; Schöfberger, W. *J. Porphyr. Phthalocyanines* **2022**, *26* (01), 84–89.

[12] Langerreiter, D.; Kostiainen, M. A.; Kaabel, S.; Anaya-Plaza, E. *Angew. Chem. Int. Ed.* **2022**, *61* (42), e202209033.

[13] Su, Q.; Hamilton, T. D. *Beilstein J. Org. Chem.* **2019**, *15* (1), 1149–1153.

[14] Santra, S.; Kopchuk, D. S.; Kovalev, I. S.; Zyryanov, G. V.; Majee, A.; Charushin, V. N.; Chupakhin, O. N. *Green Chem.* **2016**, *18* (2), 423–426.

[15] Xi, H.-T.; Zhao, T.; Sun, X.-Q.; Miao, C.-B.; Zong, T.; Meng, Q. *RSC Adv.* **2013**, *3* (3), 691–694.

[16] Gujjarappa, R.; Khurana, R.; Fridman, N.; Keinan, E.; Reany, O. *Cell Rep. Phys. Sci.* **2024**, *5* (6), 102011.

[17] Kaabel, S.; Stein, R. S.; Fomitšenko, M.; Järving, I.; Friščić, T.; Aav, R. *Angew. Chem. Int. Ed.* **2019**, *58* (19), 6230–6234.

[18] Lehn, J.-M. *Angew. Chem. Int. Ed. Engl.* **1988**, *27* (1), 89–112.

[19] Cram, D. J.; Cram, J. M. *Science* **1974**, *183* (4127), 803–809.

[20] Yawer, M. A.; Havel, V.; Sindelar, V. *Angew. Chem. Int. Ed.* **2015**, *54* (1), 276–279.

[21] Andersen, N. N.; Eriksen, K.; Lisbjerg, M.; Ottesen, M. E.; Milhøj, B. O.; Sauer, S. P. A.; Pittelkow, M. *J. Org. Chem.* **2019**, *84* (5), 2577–2584.

[22] Reany, O.; Romero-Ruiz, M.; Khurana, R.; Mondal, P.; Keinan, E.; Bayley, H. *Angew. Chem. Int. Ed.* **2024**, *63* (39), e202406719.

[23] Aav, R.; Shmatova, E.; Reile, I.; Borissova, M.; Topić, F.; Rissanen, K. *Org. Lett.* **2013**, *15* (14), 3786–3789.

[24] Pedersen, C. J. *J. Am. Chem. Soc.* **1967**, *89* (26), 7017–7036.

[25] Lehn, J. M. *Acc. Chem. Res.* **1978**, *11* (2), 49–57.
[26] Cram, D. J. *Angew. Chem. Int. Ed. Engl.* **1988**, *27* (8), 1009–1020.
[27] *Nobel Prize in Chemistry 1987*. NobelPrize.org. https://www.nobelprize.org/prizes/chemistry/1987/press-release/ (accessed 2025-12-03).
[28] Dietrich-Buchecker, C. O.; Sauvage, J. P.; Kern, J. M. *J. Am. Chem. Soc.* **1984**, *106* (10), 3043–3045.
[29] Ortholand, J.-Y.; Slawin, A. M. Z.; Spencer, N.; Stoddart, J. F.; Williams, D. J. *Angew. Chem. Int. Ed. Engl.* **1989**, *28* (10), 1394–1395.
[30] Koumura, N.; Zijlstra, R. W. J.; van Delden, R. A.; Harada, N.; Feringa, B. L. *Nature* **1999**, *401* (6749), 152–155.
[31] *Nobel Prize in Chemistry 2016*. NobelPrize.org. https://www.nobelprize.org/prizes/chemistry/2016/popular-information/ (accessed 2025-12-03).
[32] *Nobel Prize in Chemistry 2025*. NobelPrize.org. https://www.nobelprize.org/prizes/chemistry/2025/popular-information/ (accessed 2025-12-03).
[33] Fathieh, F.; Kalmutzki, M. J.; Kapustin, E. A.; Waller, P. J.; Yang, J.; Yaghi, O. M. *Sci. Adv.* **2018**, *4* (6), eaat3198.
[34] Chen, Z.; Li, P.; Anderson, R.; Wang, X.; Zhang, X.; Robison, L.; Redfern, L. R.; Moribe, S.; Islamoglu, T.; Gómez-Gualdrón, D. A.; Yildirim, T.; Stoddart, J. F.; Farha, O. K. *Science* **2020**, *368* (6488), 297–303.
[35] Chen, C.; Feng, N.; Guo, Q.; Li, Z.; Li, X.; Ding, J.; Wang, L.; Wan, H.; Guan, G. *J. Colloid Interface Sci.* **2018**, *521*, 91–101.
[36] Kaushal, S.; Kaur, G.; Kaur, J.; Singh, P. P. *Mater. Adv.* **2021**, *2* (22), 7308–7335.
[37] Sini, K.; Bourgeois, D.; Idouhar, M.; Carboni, M.; Meyer, D. *Mater. Lett.* **2019**, *250*, 92–95.
[38] Pichon, A.; Lazuen-Garay, A.; James, S. L. *CrystEngComm* **2006**, *8* (3), 211–214.
[39] Chen, D.; Zhao, J.; Zhang, P.; Dai, S. *Polyhedron* **2019**, *162*, 59–64.
[40] Andersen, N. N.; Lisbjerg, M.; Eriksen, K.; Pittelkow, M. *Isr. J. Chem.* **2018**, *58* (3–4), 435–448.
[41] Masson, E.; Ling, X.; Joseph, R.; Kyeremeh-Mensah, L.; Lu, X. *RSC Adv.* **2012**, *2* (4), 1213–1247.
[42] Miyahara, Y.; Goto, K.; Oka, M.; Inazu, T. *Angew. Chem. Int. Ed.* **2004**, *43* (38), 5019–5022.
[43] Buschmann, H.-J.; Cleve, E.; Schollmeyer, E. *Inorg. Chem. Commun.* **2005**, *8* (1), 125–127.
[44] Jin, X.-Y.; Zhao, J.-L.; Wang, F.; Cong, H.; Tao, Z. *J. Organomet. Chem.* **2017**, *846*, 1–5.
[45] Cong, H.; Yamato, T.; Feng, X.; Tao, Z. *J. Mol. Catal. Chem.* **2012**, *365*, 181–185.
[46] Cong, H.; Yamato, T.; Tao, Z. *J. Mol. Catal. Chem.* **2013**, *379*, 287–293.
[47] Cong, H.; Yamato, T.; Tao, Z. *New J. Chem.* **2013**, *37* (11), 3778–3783.
[48] Cucolea, E. I.; Buschmann, H.-J.; Mutihac, L. *Supramol. Chem.* **2016**, *28* (9–10), 727–732.
[49] Svec, J.; Necas, M.; Sindelar, V. *Angew. Chem. Int. Ed.* **2010**, *49* (13), 2378–2381.
[50] Havel, V.; Svec, J.; Wimmerova, M.; Dusek, M.; Pojarova, M.; Sindelar, V. *Org. Lett.* **2011**, *13* (15), 4000–4003.

[51] Yawer, M. A.; Sleziakova, K.; Pavlovec, L.; Sindelar, V. *Eur. J. Org. Chem.* **2018**, *2018* (1), 41–47.
[52] Havel, V.; Babiak, M.; Sindelar, V. *Chem. – Eur. J.* **2017**, *23* (37), 8963–8968.
[53] Fiala, T.; Sleziakova, K.; Marsalek, K.; Salvadori, K.; Sindelar, V. *J. Org. Chem.* **2018**, *83* (4), 1903–1912.
[54] Rivollier, J.; Thuéry, P.; Heck, M.-P. *Org. Lett.* **2013**, *15* (3), 480–483.
[55] Lizal, T.; Sindelar, V. *Isr. J. Chem.* **2018**, *58* (3–4), 326–333.
[56] Havel, V.; Yawer, M. A.; Sindelar, V. *Chem. Commun.* **2015**, *51* (22), 4666–4669.
[57] Šlampová, A.; Šindelář, V.; Kubáň, P. *Anal. Chim. Acta* **2017**, *950*, 49–56.
[58] Singh, M.; Solel, E.; Keinan, E.; Reany, O. *Chem. – Eur. J.* **2015**, *21* (2), 536–540.
[59] Singh, M.; Solel, E.; Keinan, E.; Reany, O. *Chem. – Eur. J.* **2016**, *22* (26), 8848–8854.
[60] Lisbjerg, M.; Jessen, B. M.; Rasmussen, B.; Nielsen, B. E.; Madsen, A. Ø.; Pittelkow, M. *Chem. Sci.* **2014**, *5* (7), 2647–2650.
[61] Dalidovich, T.; Mishra, K. A.; Shalima, T.; Kudrjašova, M.; Kananovich, D. G.; Aav, R. *ACS Sustain. Chem. Eng.* **2020**, *8* (41), 15703–15715.
[62] Li, Y.; Li, L.; Zhu, Y.; Meng, X.; Wu, A. *Cryst. Growth Des.* **2009**, *9* (10), 4255–4257.
[63] Prigorchenko, E.; Öeren, M.; Kaabel, S.; Fomitšenko, M.; Reile, I.; Järving, I.; Tamm, T.; Topić, F.; Rissanen, K.; Aav, R. *Chem. Commun.* **2015**, *51* (54), 10921–10924.
[64] Kaabel, S.; Adamson, J.; Topić, F.; Kiesilä, A.; Kalenius, E.; Öeren, M.; Reimund, M.; Prigorchenko, E.; Lõokene, A.; Reich, H. J.; Rissanen, K.; Aav, R. *Chem. Sci.* **2017**, *8* (3), 2184–2190.
[65] Mishra, K. A.; Adamson, J.; Öeren, M.; Kaabel, S.; Fomitšenko, M.; Aav, R. *Chem. Commun.* **2020**, *56* (93), 14645–14648.
[66] Prigorchenko, E.; Kaabel, S.; Narva, T.; Baškir, A.; Fomitšenko, M.; Adamson, J.; Järving, I.; Rissanen, K.; Tamm, T.; Aav, R. *Chem. Commun.* **2019**, *55* (63), 9307–9310.
[67] Ustrnul, L.; Burankova, T.; Öeren, M.; Juhhimenko, K.; Ilmarinen, J.; Siilak, K.; Mishra, K. A.; Aav, R. *Front. Chem.* **2021**, *9:701028*.
[68] Ustrnul, L.; Kaabel, S.; Burankova, T.; Martõnova, J.; Adamson, J.; Konrad, N.; Burk, P.; Borovkov, V.; Aav, R. *Chem. Commun.* **2019**, *55* (96), 14434–14437.
[69] Šakarašvili, M.; Truong, K.-N.; Ustrnul, L.; Konrad, N.; Siilak, K.; Burankova, T.; Kuroda, R.; Senge, M. O.; Borovkov, V.; Ward, J. S.; Rissanen, K.; Aav, R. *Inorg. Chem.* **2025**, *64* (48), 23773–23785.
[70] Rowan, S. J.; Cantrill, S. J.; Cousins, G. R. L.; Sanders, J. K. M.; Stoddart, J. F. *Angew. Chem. Int. Ed.* **2002**, *41* (6), 898–952.
[71] Belowich, M. E.; Stoddart, J. F. *Chem. Soc. Rev.* **2012**, *41* (6), 2003–2024.
[72] Corbett, P. T.; Leclaire, J.; Vial, L.; West, K. R.; Wietor, J.-L.; Sanders, J. K. M.; Otto, S. *Chem. Rev.* **2006**, *106* (9), 3652–3711.
[73] Jin, Y.; Yu, C.; Denman, R. J.; Zhang, W. *Chem. Soc. Rev.* **2013**, *42* (16), 6634–6654.
[74] Schiff, H. *Justus Liebigs Ann. Chem.* **1864**, *131* (1), 118–119.
[75] Su, X.; Aprahamian, I. *Chem. Soc. Rev.* **2014**, *43* (6), 1963–1981.
[76] Godin, G.; Levrand, B.; Trachsel, A.; Lehn, J.-M.; Herrmann, A. *Chem. Commun.* **2010**, *46* (18), 3125–3127.
[77] Hwa Jo, H.; Edupuganti, R.; You, L.; Dalby, K. N.; Anslyn, E. V. *Chem. Sci.* **2015**, *6* (1), 158–164.
[78] Kaabel, S.; Aav, R. *Isr. J. Chem.* **2018**, *58* (3–4), 296–313.
[79] Reany, O.; Mohite, A.; Keinan, E. *Isr. J. Chem.* **2018**, *58* (3–4), 449–460.

[80] Maršálek, K.; Šindelář, V. *Org. Lett.* **2020**, *22* (4), 1633–1637.
[81] De Simone, N. A.; Chvojka, M.; Lapešová, J.; Martínez-Crespo, L.; Slávik, P.; Sokolov, J.; Butler, S. J.; Valkenier, H.; Šindelář, V. *J. Org. Chem.* **2022**, *87* (15), 9829–9838.
[82] Del Mauro, A.; Lapešová, J.; Rando, C.; Šindelář, V. *Org. Lett.* **2024**, *26* (1), 106–109.
[83] Parvari, G.; Annamalai, S.; Borovoi, I.; Chechik, H.; Botoshansky, M.; Pappo, D.; Keinan, E. *Chem. Commun.* **2014**, *50* (19), 2494–2497.
[84] Lízal, T.; Šindelář, V. *Beilstein J. Org. Chem.* **2019**, *15* (1), 1268–1274.
[85] Zeng, Q.; Long, Q.; Lu, J.; Wang, L.; You, Y.; Yuan, X.; Zhang, Q.; Ge, Q.; Cong, H.; Liu, M. *Beilstein J. Org. Chem.* **2021**, *17*, 2840–2847.
[86] Wang, L.; Han, J.; Pan, R.; Yuan, X.; You, Y.; Cen, X.; Zhang, Q.; Ge, Q.; Cong, H.; Liu, M. *Tetrahedron Lett.* **2022**, *101*, 153918.
[87] Sliwa, W.; Deska, M. *Arkivoc* **2011**, *2011* (1), 496–551.
[88] Sameni, S.; Lejeune, M.; Jeunesse, C.; Matt, D.; Welter, R. *Dalton Trans.* **2009**, 7912–7923.
[89] Nicoli, F.; Baroncini, M.; Silvi, S.; Groppi, J.; Credi, A. *Org. Chem. Front.* **2021**, *8* (19), 5531–5549.
[90] Zhao, N.; Lloyd, G. O.; Scherman, O. A. *Chem. Commun.* **2012**, *48* (25), 3070–3072.
[91] International Union of Pure and Applied Chemistry (IUPAC). *IUPAC - Mechanochemical reaction (MT07141)*. https://goldbook.iupac.org/terms/view/MT07141 (accessed 2025-10-15).
[92] Takacs, L. *Chem. Soc. Rev.* **2013**, *42* (18), 7649–7659.
[93] Tan, D.; García, F. *Chem. Soc. Rev.* **2019**, *48* (8), 2274–2292.
[94] Stolar, T.; Alić, J.; Casali, L.; Gugin, N.; Baláž, M.; Michalchuk, A. A. L.; Emmerling, F. *Chem* **2026**, *12* (2), 102880.
[95] Howard, J. L.; Cao, Q.; Browne, D. L. *Chem. Sci.* **2018**, *9* (12), 3080–3094.
[96] Burmeister, C. F.; Kwade, A. *Chem. Soc. Rev.* **2013**, *42* (18), 7660–7667.
[97] Geib, R.; Colacino, E.; Gremaud, L. *ChemSusChem* **2024**, *17* (12), e202301921.
[98] Crawford, D. E.; Miskimmin, C. K. G.; Albadarin, A. B.; Walker, G.; James, S. L. *Green Chem.* **2017**, *19* (6), 1507–1518.
[99] Medina, C.; Daurio, D.; Nagapudi, K.; Alvarez-Nunez, F. *J. Pharm. Sci.* **2010**, *99* (4), 1693–1696.
[100] Crawford, D.; Casaban, J.; Haydon, R.; Giri, N.; McNally, T.; James, S. L. *Chem. Sci.* **2015**, *6* (3), 1645–1649.
[101] Reynes, J. F.; Isoni, V.; García, F. *Angew. Chem. Int. Ed.* **2023**, *62* (44), e202300819.
[102] Do, J.-L.; Friščić, T. *ACS Cent. Sci.* **2017**, *3* (1), 13–19.
[103] Do, J.-L.; Friščić, T. *Synlett* **2017**, *28*, 2066–2092.
[104] Margetić, D.; Štrukil, V. Practical Considerations in Mechanochemical Organic Synthesis. In *Mechanochemical Organic Synthesis*; Elsevier, 2016; pp 1–54.
[105] Halasz, I.; Kimber, S. A. J.; Beldon, P. J.; Belenguer, A. M.; Adams, F.; Honkimäki, V.; Nightingale, R. C.; Dinnebier, R. E.; Friščić, T. *Nat. Protoc.* **2013**, *8* (9), 1718–1729.
[106] Štefanić, G.; Krehula, S.; Štefanić, I. *Dalton Trans.* **2015**, *44* (43), 18870–18881.
[107] Štefanić, G.; Krehula, S.; Štefanić, I. *Chem. Commun.* **2013**, *49* (81), 9245–9247.
[108] Haley, R. A.; Mack, J.; Guan, H. *Inorg. Chem. Front.* **2017**, *4* (1), 52–55.
[109] Hwang, S.; Grätz, S.; Borchardt, L. *Chem. Commun.* **2022**, *58* (11), 1661–1671.
[110] Pickhardt, W.; Grätz, S.; Borchardt, L. *Chem. – Eur. J.* **2020**, *26* (57), 12903–12911.

[111] Fulmer, D. A.; Shearouse, W. C.; Medonza, S. T.; Mack, J. *Green Chem.* **2009**, *11* (11), 1821–1825.
[112] Vogt, C. G.; Grätz, S.; Lukin, S.; Halasz, I.; Etter, M.; Evans, J. D.; Borchardt, L. *Angew. Chem. Int. Ed.* **2019**, *58* (52), 18942–18947.
[113] Takacs, L.; McHenry, J. S. *J. Mater. Sci.* **2006**, *41* (16), 5246–5249.
[114] Andersen, J.; Mack, J. *Angew. Chem. Int. Ed.* **2018**, *57* (40), 13062–13065.
[115] Cindro, N.; Tireli, M.; Karadeniz, B.; Mrla, T.; Užarević, K. *ACS Sustain. Chem. Eng.* **2019**, *7* (19), 16301–16309.
[116] Kumar, N.; Biswas, K. *Rev. Sci. Instrum.* **2015**, *86* (8), 083903.
[117] Friščić, T.; Childs, S. L.; Rizvi, S. A. A.; Jones, W. *CrystEngComm* **2009**, *11* (3), 418–426.
[118] Fang, Y.; Yu, J. *Adv. Synth. Catal.* **2026**, *368* (7), e70372.
[119] Shan, N.; Toda, F.; Jones, W. *Chem. Commun.* **2002**, No. 20, 2372–2373.
[120] Do, J.-L.; Mottillo, C.; Tan, D.; Štrukil, V.; Friščić, T. *J. Am. Chem. Soc.* **2015**, *137* (7), 2476–2479.
[121] Hutchings, B. P.; Crawford, D. E.; Gao, L.; Hu, P.; James, S. L. *Angew. Chem. Int. Ed.* **2017**, *56* (48), 15252–15256.
[122] Chatterjee, T.; Saha, D.; Ranu, B. C. *Tetrahedron Lett.* **2012**, *53* (32), 4142–4144.
[123] Suut-Tuule, E.; Schults, E.; Jarg, T.; Adamson, J.; Kananovich, D.; Aav, R. *ChemSusChem* **2025**, *18* (9), e202402354.
[124] Huskić, I.; Lennox, C. B.; Friščić, T. *Green Chem.* **2020**, *22* (18), 5881–5901.
[125] Friščić, T.; Mottillo, C.; Titi, H. M. *Angew. Chem. Int. Ed.* **2020**, *59* (3), 1018–1029.
[126] Braga, D.; Giaffreda, S. L.; Grepioni, F.; Chierotti, M. R.; Gobetto, R.; Palladino, G.; Polito, M. *CrystEngComm* **2007**, *9* (10), 879–881.
[127] Cinčić, D.; Brekalo, I.; Kaitner, B. *Chem. Commun.* **2012**, *48* (95), 11683–11685.
[128] Templ, J.; Borchardt, L. *Angew. Chem. Int. Ed.* **2026**, *65* (8), e23191.
[129] Toda, F.; Akai, H. *J. Org. Chem.* **1990**, *55* (11), 3446–3447.
[130] Tanaka, K.; Kishigami, S.; Toda, F. *J. Org. Chem.* **1991**, *56* (13), 4333–4334.
[131] Nakajima, M.; Hashimoto, S.; Noji, M.; Koga, K. *Chem. Pharm. Bull. (Tokyo)* **1998**, *46* (11), 1814–1815.
[132] Dong, L.; Li, L.; Chen, H.; Cao, Y.; Lei, H. *Adv. Sci.* **2025**, *12* (24), 2403949.
[133] Nwoye, E.; Floyd, K.; Batteas, J.; Felts, J. *RSC Mechanochemistry* **2025**, *2* (6), 911–922.
[134] Aydonat, S.; Hergesell, A. H.; Seitzinger, C. L.; Lennarz, R.; Chang, G.; Sievers, C.; Meisner, J.; Vollmer, I.; Göstl, R. *Polym. J.* **2024**, *56* (4), 249–268.
[135] Dheyab, M. A.; Abdullah, W.; Abdulwahab, S.; Alsarayreh, S. M.; Tarawneh, M. H.; Alsardi, M. M.; Alanazi, M. A.; Aziz, A. A. *RSC Mechanochemistry* **2026**, *3* (2), 161–190.
[136] Jafter, O. F.; Lee, S.; Park, J.; Cabanetos, C.; Lungerich, D. *Angew. Chem. Int. Ed.* **2024**, *63* (48), e202409731.
[137] Vugrin, L.; Carta, M.; Lukin, S.; Meštrović, E.; Delogu, F.; Halasz, I. *Faraday Discuss.* **2023**, *241*, 217–229.
[138] Rappen, M. F.; Mäder, J.; Schwemin, T.; Grätz, S.; Borchardt, L. *RSC Mechanochemistry* **2026**, *3* (3), 357–362.
[139] Bawadkji, O.; Haag, R. *RSC Mechanochemistry* **2024**, *1* (5), 536–543.
[140] Czitrom, V. *Am. Stat.* **1999**, *53* (2), 126–131.
[141] Gallego, A.; Lavayssiere, M.; Bantreil, X.; Pétry, N.; Pinaud, J.; Giani, O.; Lamaty, F. *RSC Mechanochemistry* **2026**, *3* (2), 254–264.

[142] Braconi, E.; Godineau, E. *ACS Sustain. Chem. Eng.* **2023**, *11* (28), 10545–10554.
[143] Anastas, P. T.; Warner, J. C. *Green Chemistry: Theory and Practice*; Oxford University Press, 2000.
[144] Ardila-Fierro, K. J.; Hernández, J. G. *ChemSusChem* **2021**, *14* (10), 2145–2162.
[145] Casagrande, A.; Niidu, A.; Aav, R.; Kananovich, D.; Colacino, E. Green Chemistry Tools in Mechanochemistry. In *Encyclopedia of Green Chemistry*; Elsevier, 2025; pp 550–571.
[146] Duvauchelle, V.; Meffre, P.; Benfodda, Z. *Environ. Chem. Lett.* **2023**, *21* (1), 597–621.
[147] Henderson, R. K.; Jiménez-González, C.; Constable, D. J. C.; Alston, S. R.; Inglis, G. G. A.; Fisher, G.; Sherwood, J.; Binks, S. P.; Curzons, A. D. *Green Chem.* **2011**, *13* (4), 854–862.
[148] Trost, B. *Science* **1991**, *254* (5037), 1471–1477.
[149] Fantozzi, N.; Volle, J.-N.; Porcheddu, A.; Virieux, D.; García, F.; Colacino, E. *Chem. Soc. Rev.* **2023**, *52* (19), 6680–6714.
[150] Thorne, M. F.; Gómez, M. L. R.; Bumstead, A. M.; Li, S.; Bennett, T. D. *Green Chem.* **2020**, *22* (8), 2505–2512.
[151] Sabatini, M. T.; Boulton, L. T.; Sneddon, H. F.; Sheppard, T. D. *Nat. Catal.* **2019**, *2* (1), 10–17.
[152] Métro, T.-X.; Bonnamour, J.; Reidon, T.; Sarpoulet, J.; Martinez, J.; Lamaty, F. *Chem. Commun.* **2012**, *48* (96), 11781–11783.
[153] Schneider, F.; Szuppa, T.; Stolle, A.; Ondruschka, B.; Hopf, H. *Green Chem.* **2009**, *11* (11), 1894–1899.
[154] Han, G.-F.; Li, F.; Chen, Z.-W.; Coppex, C.; Kim, S.-J.; Noh, H.-J.; Fu, Z.; Lu, Y.; Singh, C. V.; Siahrostami, S.; Jiang, Q.; Baek, J.-B. *Nat. Nanotechnol.* **2021**, *16* (3), 325–330.
[155] Reichle, S.; Felderhoff, M.; Schüth, F. *Angew. Chem. Int. Ed.* **2021**, *60* (50), 26385–26389.
[156] McElroy, C. R.; Constantinou, A.; Jones, L. C.; Summerton, L.; Clark, J. H. *Green Chem.* **2015**, *17* (5), 3111–3121.
[157] Sharma, P.; Vetter, C.; Ponnusamy, E.; Colacino, E. *ACS Sustain. Chem. Eng.* **2022**, *10* (16), 5110–5116.
[158] Onken, U.; Koettgen, A.; Scheidat, H.; Schueepp, P.; Gallou, F. *CHIMIA* **2019**, *73* (9), 730–736.
[159] Takahashi, R.; Hu, A.; Gao, P.; Gao, Y.; Pang, Y.; Seo, T.; Jiang, J.; Maeda, S.; Takaya, H.; Kubota, K.; Ito, H. *Nat. Commun.* **2021**, *12* (1), 6691.
[160] Varma Nallaparaju, J.; Nikonovich, T.; Jarg, T.; Merzhyievskyi, D.; Aav, R.; Kananovich, D. G. *Angew. Chem. Int. Ed.* **2023**, *62* (39), e202305775.
[161] Wang, G.-W.; Komatsu, K.; Murata, Y.; Shiro, M. *Nature* **1997**, *387* (6633), 583–586.
[162] Kwon, T.; Song, B.; Nam, K. W.; Stoddart, J. F. *J. Am. Chem. Soc.* **2022**, *144* (28), 12595–12601.
[163] Belenguer, A. M.; Lampronti, G. I.; De Mitri, N.; Driver, M.; Hunter, C. A.; Sanders, J. K. M. *J. Am. Chem. Soc.* **2018**, *140* (49), 17051–17059.
[164] Myers, R. H.; Montgomery, D. C.; Anderson-Cook, C. M. *Response Surface Methodology: Process and Product Optimization Using Designed Experiments (2016)*; John Wiley & Sons.
[165] *Design-Expert software*. https://www.statease.com/software/design-expert/.

[166] Sigel, H.; Scheller, K. H. *J. Inorg. Biochem.* **1982**, *16* (4), 297–310.
[167] Aoki, K.; Saenger, W. *J. Inorg. Biochem.* **1983**, *19* (3), 269–273.
[168] Altaf, M.; Stoeckli-Evans, H. *Acta Crystallogr. C* **2013**, *69* (2), 127–137.
[169] Dalidovich, T.; Nallaparaju, J. V.; Shalima, T.; Aav, R.; Kananovich, D. G. *ChemSusChem* **2022**, *15* (3), e202102286.
[170] Nallaparaju, J. V.; Satsi, R.; Merzhyievskyi, D.; Jarg, T.; Aav, R.; Kananovich, D. G. *Angew. Chem. Int. Ed.* **2024**, *63* (20), e202319449.
[171] Jarg, T.; Tamm, J.; Suut-Tuule, E.; Lootus, K.-M.; Kananovich, D.; Aav, R. *RSC Mechanochemistry* **2025**, *2* (4), 507–515.
[172] Andersen, J.; Mack, J. *Green Chem.* **2018**, *20* (7), 1435–1443.
[173] Huheey, J. E.; Keiter, E. A.; Keiter, R. L. *Inorganic Chemistry: Principles of Structure and Reactivity*; HarperCollins College Publishers, 1993.

Acknowledgements

This work was conducted in the Department of Chemistry and Biotechnology of the School of Science at Tallinn University of Technology, Estonia. The work was supported by the Estonian Research Council (grants PRG399 and PRG2169), Ministry of Education and Research through Centre of Excellence in Circular Economy for Strategic Mineral and Carbon Resources SOURCES (01.01.2024–31.12.2030, TK228).

I am forever grateful to my supervisor, Prof. Riina Aav, who welcomed me to her group during my bachelor's studies and introduced me to mechanochemistry from the very beginning. I am extremely thankful for her guidance and unwavering support throughout my studies. Her endless enthusiasm and encouragement have been a constant source of motivation in my work. I am equally thankful for my co-supervisor, Dr. Dzmitry Kananovich, who has been an inspiration through his brilliant mind, endless bright ideas and genuine passion for science. Their presence, expertise, and dedication have profoundly motivated me to become a better researcher.

I am deeply grateful to all my co-authors and collaborators. Science is rarely a solitary endeavour, and my research and progress are the result of many fruitful collaborations. Thank you for your contributions to the articles and to my research, without your knowledge this would not have been possible.

I would like to thank the past and present members of the Supramolecular group, including Mari-Liis, Nele, Eve, Riin, Ngan, Suman, Marko, Liisa, Rauno, Elena, Marina, Tatsiana, Ece, Jevgenija, Ander, Kristjan, Ketren-Marlein, Mario, Jagadeesh, Tatsiana N., Kamini, for the inspiring group seminars, fruitful discussions and memorable trips. I am also grateful to all the colleagues from 4th floor, especially Dr. Kristin Erkman, for her support and readiness to always help me with various matters. I am thankful for Dr. Kadri Kriis for reviewing my thesis and providing valuable feedback.

I would like to extend a special thank you to Eve. It was a pleasure to supervise you during your studies and witness your growth into an exceptional young scientist. Thank you for being such an amazing, curious, and hard-working student, it made our collaboration both successful and enjoyable. Tanya, thank you for being such an important part of my research. It was an absolute pleasure to work with you, and I learned a great deal from you during this time. I hold dear our friendship, and I will not forget our trip to Italy, thank you for showing me Rome for the first time. A special thank you goes to Nele. Our mutual motivational (and sometimes ranting) sessions helped to get through this stressful time of thesis writing. Thank you for all the shared laughs along the way! Ladies from 331 office – Tanya, Eve, Ženja and Ketren thank you for all the great times we shared.

Last but not least, my deepest gratitude goes to my husband, Johannes-Gristofer. You have always been there for me, no matter how difficult times have been. You have supported me and helped me get through challenging moments, whether by bringing me coffee and snacks when needed or by simply listening to me rant. Thank you for being you.

Abstract

Mechanochemical approach to biotin-containing hemicucurbiturils

This thesis describes the advancement of mechanochemical solid-state synthesis as an approach to the selective and scalable production of functional hemicucurbituril derivatives. Hemicucurbiturils are renowned for their ability to act as “host” molecules in “host-guest” complexes by interacting with smaller molecules and anions via non-covalent interactions, such as C–H···anion hydrogen bonds. These properties make hemicucurbiturils attractive for various applications; for example, they have been exploited in anion sensors from a mixture of anions and used as a transmembrane carriers. The literature overview describes synthetic strategies for hemicucurbiturils, different hemicucurbituril derivatives, their properties and applications. This is followed by a brief overview of mechanochemistry, including which instruments can be used to conduct reactions in the solid state. Different parameters affecting solid-state reactions and the advantages of mechanochemistry are discussed.

The results and discussion section is based on three articles. The first part focuses on the selective synthesis of chimeric mono-biotinylated hemicucurbit[8]uril (mixHC[8]) from a multi-component mixture of D-biotin, cyclohexaneurea and paraformaldehyde with an acid catalyst and template. Assembling such a chimeric macrocycle is challenging due to the complexity of the dynamic covalent library, which theoretically contains approximately 50,000 potential linear and cyclic intermediates. Through the design of experiment approach, by varying multiple experimental parameters simultaneously, it was identified that mixHC[8] formation is sensitive to the acid loading, while the other major product, cyclohexanohemicucurbit[8]uril (cycHC[8]), depended on the monomer ratio. Further investigation revealed that suitable templating is the primary driver for mixHC[8] amplification in the solid state. While perchlorate was an effective template, the use of hexafluorophosphate provided superior selectivity when used in combination with the same anion potassium salt, reaching 38% HPLC yield for mixHC[8]. A multistep purification procedure was developed to isolate mixHC[8] with high purity.

The second article focused on developing a reliable analytical method for monitoring heterogeneous complex solid-state reaction mixtures. The use of an internal standard (triphenylmethane), introduced prior to milling, was necessary to produce credible results.

The final article describes the development of a scalable high-yielding mechanosynthesis of biotin[6]uril. Conventional solution-based synthesis of B[6]U delivers moderate yields, is labour-intensive and produces a lot of waste. The investigation of the solid-state synthesis of B[6]U began by establishing the best template and aging duration for the synthesis. It was observed that when using only 0.3 eq. of 48% HBr as a catalyst and template, B[6]U was obtained in 96% yield after 60 min of milling and aging at 60 °C for 24 hours. The procedure was successfully scaled up 82-fold by transferring from a shaker mill to a larger planetary ball mill. Potassium bromide was introduced as a solid grinding auxiliary to manage the rheological transition from a free-flowing solid reaction mixture to a highly adhesive paste. The milling parameters were adjusted to enhance the impact energy of the reaction using Lungerich’s kinematic model as a guide, resulting in the production of 19.3 g of B[6] (92% isolated yield). This achievement marks the first mechanochemical preparation of a macrocycle in decagram

quantities. The developed mechanochemical procedure decreased the reaction time twofold, the reaction process mass intensity 60-fold, and the consumption of mineral acid 190-fold.

This research demonstrates that the synergy of mechanical energy and precise control of chemical parameters enables the synthesis of complex biotinylated macrocycles, providing a sustainable route to the selective synthesis of macrocyclic host molecules.

Lühikokkuvõte

Biotiini sisaldavate hemikukurbituriilide mehhanokeemiline süntees

Käesolev doktoritöö kirjeldab mehhanokeemilise tahkefaasi sünteesi arendamist funktsionaalsete hemikukurbituriili derivaatide selektiivseks ja skaleeritavaks valmistamiseks. Hemikukurbituriilid on tuntud oma võime poolest toimida „võõrustaja“ molekulidena „võõrustaja-külaline“ kompleksides, interakteerudes väiksemate molekulide ja anioonidega mittekovalentsete interaktsioonide kaudu, näiteks C–H···anioon vesiniksidemete abil. Need omadused muudavad hemikukurbituriilid atraktiivseks erinevates rakendustes, näiteks on neid kasutatud sensoritena anioonide segude analüüsimiseks ning transmembraansete kandjatena. Kirjanduse ülevaates käsitletakse hemikukurbituriilide sünteesi lähenemisviise ja erinevate hemikukurbituriili derivaatide omadusi ja rakendusi. Sellele järgneb lühike ülevaade mehhanokeemiast ning instrumentidest, mida kasutatakse tahkefaasi reaktsioonide läbiviimiseks. Samuti arutletakse tahkefaasi reaktsioone mõjutavate parameetrite ja mehhanokeemia eeliste üle.

Tulemuste ja arutelu osa põhineb kolmel artiklil. Esimene osa keskendub mono-biotinüleeritud hemikukurbit[8]uriili (mixHC[8]) selektiivsele sünteesile D-biotiini, tsükloheksaanuurea ja paraformaldehüüdi multikomponentsest segust happe katalüsaatori ja malli juuresolekul. Sellise kiraalse makrotsükli sünteesimine on keeruline suure dünaamilise kovalentse raamatukogu moodustumise tõttu, kuna see sisaldab teoreetiliselt ligikaudu 50 000 võimalikku lineaarset ja tsüklilist vaheühendit. Kasutades eksperimentide planeerimise (DoE) lähenemist ning varieerides samaaegselt mitmeid eksperimentaalseid parameetreid, leiti, et mixHC[8] moodustumine on tundlik happe koguse suhtes, samas kui teine peamine produkt, tsükloheksanohemikukurbit[8]uriil (cycHC[8]), sõltus monomeeride suhtest. Edasised katsed näitasid, et sobiv mall on peamine tegur, mis mõjutab mixHC[8] amplifikatsiooni tahkes olekus. Kuigi perkloraat osutus efektiivseks malliks, andis heksafluorofosfaadi kasutamine kombinatsioonis sama aniooni kaaliumisoolaga parema selektiivsuse, saades mixHC[8] 38% HPLC saagisega. Puhta ja kõrge puhtusastmega mixHC[8] eraldamiseks töötati välja mitme-etapiline isoleerimise protseduur.

Teine artikkel keskendus usaldusväärse analüütilise meetodi arendamisele heterogeensete ja keerukate tahkefaasi reaktsioonisegude jälgimiseks. Kinnitati, et usaldusväärsete tulemuste saamiseks oli vajalik sisestandardi (trifenüülmetaan) lisamine enne jahvatamist.

Viimane artikkel kirjeldab biotiin[6]uriili (B[6]U) skaleeritava ja kõrge saagisega mehhanosünteesi arendamist. B[6]U tavapärane lahuses läbiviidav süntees annab mõõdukaid saagiseid, on töömahukas ning tekitab suures koguses jäätmeid. B[6]U tahkefaasi sünteesi uurimine algas sobivaima malli ja laagerdumise aja määramisest. Leiti, et ainult 0,3 ekvivalendi 48% HBr-i kasutamine katalüsaatori ja mallina võimaldas saada pärast 60 minutit jahvatamist ja 24 tundi laagerdamist 60 °C juures B[6]U 96% HPLC saagisega. Mehhanokeemiline süntees skaleeriti edukalt üles 82 korda, viies reaktsioon vibratsioonilisest kuulveskist suuremasse planetaarkuulveskisse. Reaktsioonisegu reoloogilise muutuse kontrollimiseks vabalt voolavast tahkest reaktsioonisegust tugevalt adhesiivseks pastaks lisati tahket kaaliumbromiidi. Tuginedes Lungerichi kineetilisele mudelile, kohandati jahvatusparameetreid, et suurendada reaktsiooni löögienergiat,

mille tulemusena saadi 19,3 g B[6]U-d (92% isoleeritud saagis). See on esimene näide makrotsükli mehhanokeemilisest sünteesist dekagramm skaalas. Väljatöötatud mehhanokeemiline protseduur vähendas reaktsiooniaega kaks korda, protsessi massiintensiivsust 60 korda ja mineraalhappe kasutust 190 korda.

Käesolev uurimistöö näitab, et mehhaanilise energia ja keemiliste parameetrite täpse kontrolli sünergia võimaldab keerukate biotinüleeritud makrotsüklite sünteesi, pakkudes jätkusuutlikku lähenemist makrotsükliliste võõrustaja molekulide selektiivseks valmistamiseks.

Appendix 1

Publication I

E. Suut-Tuule[‡], T. Jarg[‡], P. Tikker, K.-M. Lootus, J. Martõnova, R. Reitalu, L. Ustrnul, J. S. Ward, V. Rjabovs, K. Shubin, J. V. Nallaparaju, M. Vendelin, S. Preis, M. Öeren, K. Rissanen, D. Kananovich, R. Aav. Mechanochemically Driven Covalent Self-Assembly of a Chiral Mono-Biotinylated Hemicucurbit[8]uril. *Cell Reports Physical Science*, **2024**, 5, 102161.

Cell Reports
Physical Science

CellPress
OPEN ACCESS

Article

Mechanochemically driven covalent self-assembly of a chiral mono-biotinylated hemicucurbit[8]uril

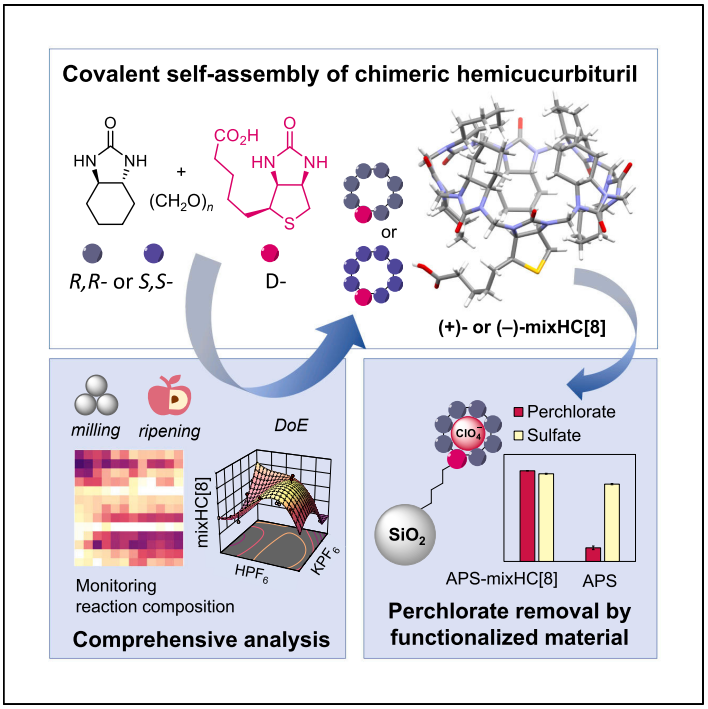

Suut-Tuule and Jarg et al. demonstrate that mechanochemistry enhances reactivity and significantly improves selectivity in the solid-state synthesis of mono-biotinylated hemicucurbit[8]urils. The application of the chimeric macrocycle is showcased by its immobilization on silica and subsequent use as a selective solid-phase extraction material for perchlorate removal.

Elina Suut-Tuule, Tatsiana Jarg, Priit Tikker, ..., Kari Rissanen, Dzmitry Kananovich, Riina Aav

riina.aav@taltech.ee

Highlights

Dynamic covalent chemistry in solid state delivers chimeric hemicucurbit[8]urils

Two major products are amplified from ca. 50,000 possible compounds

Mechanochemistry and anionic templation drive covalent self-assembly

Silica modified by biotinylated macrocycle is suitable for perchlorate capture

Suut-Tuule et al., Cell Reports Physical Science 5, 102161
September 18, 2024
https://doi.org/10.1016/j.xcrp.2024.102161

Cell Reports
Physical Science

CellPress
OPEN ACCESS

Article

Mechanochemically driven covalent self-assembly of a chiral mono-biotinylated hemicucurbit[8]uril

Elina Suut-Tuule,[1,8] Tatsiana Jarg,[1,8] Priit Tikker,[2] Ketren-Marlein Lootus,[1] Jevgenija Martõnova,[1] Rauno Reitalu,[1] Lukas Ustrnul,[1] Jas S. Ward,[3] Vitalijs Rjabovs,[4,5] Kirill Shubin,[6] Jagadeesh V. Nallaparaju,[1] Marko Vendelin,[7] Sergei Preis,[2] Mario Öeren,[1] Kari Rissanen,[3] Dzmitry Kananovich,[1] and Riina Aav[1,9,10,*]

SUMMARY

Solution-based synthesis of complex molecules with high efficiency leverages supramolecular control over covalent bond formation. Herein, we present the mechanosynthesis of chiral mono-biotinylated hemicucurbit[8]urils (mixHC[8]s) via the condensation of D-biotin, (*R,R*)- or (*S,S*)-cyclohexa-1,2-diylurea, and paraformaldehyde. The selectivity of self-assembly is enhanced through mechanochemistry and by fostering non-covalent interactions, achieved by eliminating solvents and conducting the reaction in the solid state. Rigorous analysis of intermediates reveals key processes and chemical parameters influencing dynamic covalent chemistry. The library of ca. 50,000 theoretically predicted intermediates and products leads to covalent self-assembly of chiral hemicucurbiturils. Mechanochemically prepared diastereomeric (−)- and (+)-mixHC[8]s are suitable for anion binding and derivatization. Immobilization of the macrocycles on aminated silica produces a functional material capable of selective capture of anions, as demonstrated by efficient perchlorate removal from a spiked mineral matrix.

INTRODUCTION

The spontaneous organization of molecular species relies on non-covalent interactions, resulting in intricate aggregates. Such supramolecular self-assembly can facilitate the formation of covalent bonds leading to complex molecules and may be exceptionally responsive to minor changes in the reaction conditions, resulting in the amplification of particular products.[1] In the case of increased molecular crowding, the dynamics of an interaction between species is accelerated compared to a dilute environment, which has been demonstrated for strongly hydrogen-bonded base pairs of nucleic acids.[2] Furthermore, in the solid state at extreme concentrations, unobstructed by solvent, the number of non-covalent interactions between counterparts increases, enabling the formation of products that are less favored in solution.[3,4] Mechanochemical activation enhances chemical reactivity and provides a solvent-free sustainable approach in chemical syntheses.[5–7]

Single-bridged cucurbituril-type molecular containers, hemicucurbit[*n*]urils (HC[*n*]s) are renowned for their anion-binding properties and typically assembled from urea monomers in a one-pot reaction with dynamic covalent chemistry (DCC).[8–10] Although the size of the macrocycle can be controlled by anion templation,[8,11–15] HC[*n*]s prevalently consist of six units.[12,16,17] Up to date, 8-membered HC[*n*]s have been synthesized exclusively from chiral C_2-symmetric cyclohexa-1,2-diylurea (CU)

[1]Tallinn University of Technology, Department of Chemistry and Biotechnology, 12618 Tallinn, Estonia

[2]Tallinn University of Technology, Department of Materials and Environmental Technology, 19086 Tallinn, Estonia

[3]University of Jyvaskyla, Department of Chemistry, 40014 Jyväskylä, Finland

[4]National Institute of Chemical Physics and Biophysics, 12618 Tallinn, Estonia

[5]Institute of Chemistry and Chemical Technology, Riga Technical University, 1048 Riga, Latvia

[6]Latvian Institute of Organic Synthesis, 1006 Riga, Latvia

[7]Tallinn University of Technology, Department of Cybernetics, 12618 Tallinn, Estonia

[8]These authors contributed equally

[9]X (formerly Twitter): @RiinaAav

[10]Lead contact

*Correspondence: riina.aav@taltech.ee

https://doi.org/10.1016/j.xcrp.2024.102161

monomers, and the corresponding (*R*,*R*)- and (*S*,*S*)-cyclohexanohemicucurbit[8]urils (cycHC[8]s) can be assembled both in solution[18] and the solid state.[17] Their larger cavity expands the range of applications, and the insertion of another functional monomer, such as D-biotin, into the cycHC[8] scaffold can further enhance receptor versatility. Biotin is a naturally occurring and commercially available compound with a carboxylic group suitable for derivatization. Furthermore, it has previously been used in the synthesis of chiral macrocycles.[13] So far, the reported chimeric HC[*n*]s assembled from non-equivalent urea monomers have been limited to 6-membered hybrid HC[*n*]s prepared in solution via multi-step approaches[19,20] and mono-functionalized bambus[6]urils obtained in a one-pot reaction.[21–23] The difficulties in the single-step formation of non-uniformly composed macrocycles arise from a plethora of possible linear and cyclic intermediates. Consequently, arranging a chaotic mixture into a well-organized molecule presents considerable challenges, and the number of combinations increases with the number of monomeric units.

Mechanochemistry has been utilized in the synthesis of several macrocycles,[17,24–30] inducing covalent assembly of uniformly structured monomers. As mechanosynthesis enables overcoming the solubility barriers and promotes reactions between compounds with drastic polarity differences, its potential can be exploited even further. To the best of our knowledge, there have been no reports describing covalent self-assembly of macrocycles from mixtures of various monomers in the solid state. The formation of chiral chimeric HC[*n*]s via DCC in the solid state could pave the way to novel synthetic approaches, unlocking access to versatile applications.

The present work describes a mechanochemically activated solid-state condensation of (*R*,*R*)- or (*S*,*S*)-CU, D-biotin ((*S*,*S*,*R*)-B), and paraformaldehyde and their selective covalent self-assembly into the enantiopure mono-biotinylated HC[8]s (−)-((*S*,*S*,*R*)(*R*,*R*)$_7$)-mixHC[8] or (+)-((*S*,*S*,*R*)(*S*,*S*)$_7$)-mixHC[8], along with homomeric cycHC[8]s. The challenges of assembling a chimeric mono-functionalized 8-membered macrocycle are related to the number of possible combinations of monomeric units and their chemical reactivity. Fine-tuning of the reaction conditions enabled amplification of the two major products, chimeric mixHC[8] and homomeric cycHC[8], among 498 potential 8-membered HC[*n*]s[31] (Figure 1; theoretical number of linear cyclic oligomers in the supplemental experimental procedures; Data S1).

The covalent assembly process is essentially solvent free and has a very low process mass intensity (PMI; the mass of all used reagents per formed product[32]). The most significant chemical and technical factors affecting macrocyclization were identified with response surface methodology (RSM) and thorough analysis of intermediates by high-performance liquid chromatography-mass spectrometry (HPLC-MS) provided mechanistic insight into this complex process. The affinity of mixHC[8] for selected anions and the subtle differences in the binding properties of the two chimeric diastereomers were determined by isothermal titration calorimetry (ITC) and characterized by single-crystal X-ray crystallography (SC-XRD) and modeling studies. Furthermore, a practical example of the selective anion capture by silica-immobilized mixHC[8] was demonstrated in the efficient removal of perchlorate from a spiked mineral matrix.

RESULTS AND DISCUSSION

Covalent assembly of hemicucurbiturils in the solid state

The first attempts to synthesize mono-functionalized mixHC[8] in solution according to the protocol developed for cycHC[8][18] were promising. The condensation of

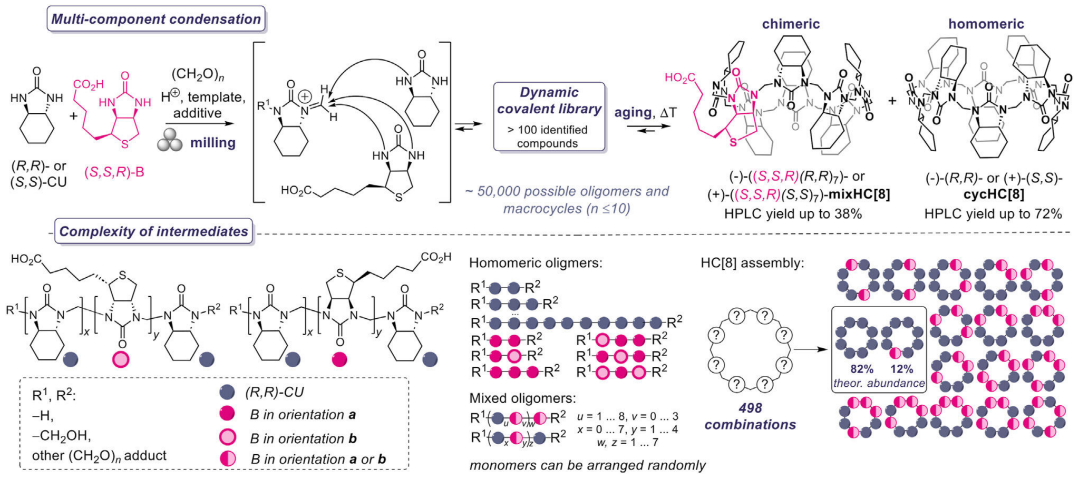

Figure 1. Synthetic scheme and complexity of intermediates during formation of the HC[8]s studied in this work

Multi-component condensation of (*S,S,R*)-biotin (B) and (*R,R*)- or (*S,S*)-cyclohexa-1,2-diylurea (CU) to homomeric cycHC[8]s and chimeric mixHC[8]s. The complexity of the intermediates in the DCL is expressed via possible numbers of oligomers, HC[8]s, and the abundance of major HC[8]s resulting from the 1:7 (B:CU) ratio of starting materials (theoretical number of linear cyclic oligomers in the supplemental experimental procedures; Data S1). The best reaction conditions afford 38% and 34% yields of mixHC[8] and cycHC[8], respectively: 1 equiv B, 7 equiv CU, 8 equiv $(CH_2O)_n$ in the presence of 2 equiv HPF_6 and 1 equiv KPF_6, milled at 30 Hz for 60 min and aged at 60°C for 3 h. (Table S15). The highest yield (72%) of cycHC[8] was observed under the following conditions: 1 equiv B, 15 equiv CU, 16 equiv $(CH_2O)_n$ in the presence of 3 equiv $HClO_4$, milled at 30 Hz for 60 min and aged at 45°C for 24 h (Table S2).

biotin and CU taken in stoichiometric 1:7 molar ratio with paraformaldehyde, mediated by trifluoroacetic acid in acetonitrile, produced mixHC[8] and cycHC[8] in 9% and 38% yields, respectively (see synthesis in solution in the supplemental experimental procedures; Data S1). The ratio of the macrocycles did not reflect the statistical distribution based on the starting monomer ratio, which implied a strong influence of the chemical parameters. In solution-based synthesis, compatibility between the solvent and reagents governs the fast diffusion and mixing of starting materials, intermediates, and products, as well as their reactivity. Poor solubility can obstruct reactions, especially in DCC, due to suppressed exchange between reactants. We envisioned that mixHC[8]s may be assembled with higher efficiency in the solid state, where solubility is not critical, non-covalent interactions are not obstructed by the solvent, and templation is enhanced due to a high concentration of reactants.[3] According to the previous study,[17] covalent self-assembly in the solid state required just a minute amount of a liquid additive[33–35] to facilitate proton transfer and delivery of the anionic template, as well as to promote conformational flexibility. The complexity of the dynamic covalent library (DCL) drastically increases in multicomponent reactions; for instance, the incorporation of non-C_2 symmetric (*R,S*)-CU units resulted in higher stereochemical diversity and the formation of several diastereomeric HC[*n*]s (i.e., *cis*-cycHC[6] and inverted-*cis*-cycHC[6]).[36] Similarly, condensation of chiral CU and non-C_2 symmetric biotin into linear and cyclic oligomers can be realized via various combinations, considering the possibility of different orientations of the biotin unit (Figure 1). For instance, all forms with a length of 2 to 10 monomers result in ca. 50,000 cyclic and linear oligomers. However, the number of possible products can be decreased by templation. Variation of position, orientation, and number of B and CU monomers leads to 498 potential 8-membered macrocycles[31] (Figure 1; theoretical number of linear cyclic oligomers in the

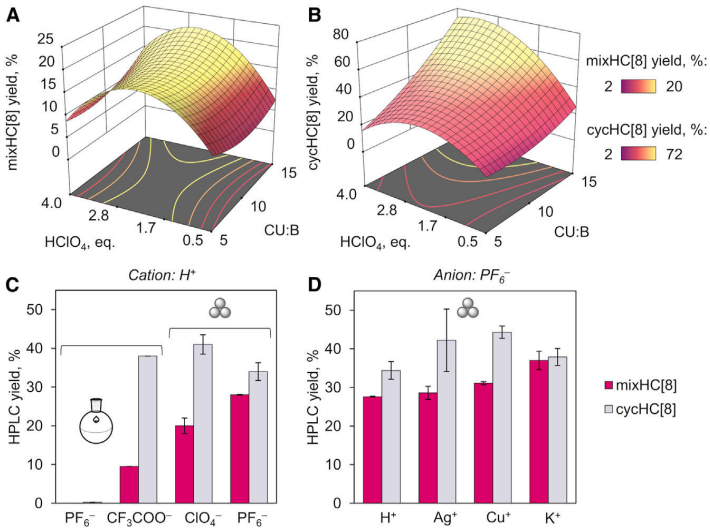

Figure 2. 3D response surfaces and bar charts expressing the formation of HC[8]s

(A and B) 3D response surfaces displaying the influence of the ratio of monomers and loading of aq. $HClO_4$ on the HPLC yields of (A) mixHC[8] and (B) cycHC[8].

(C and D) Bar charts comparing the effect of the acid anions (CF_3COO^-, ClO_4^-, and PF_6^-) in solution and the solid state (C) and hexafluorophosphate salt cations (Ag^+, Cu^+, K^+) in the solid state (D) on the yields of cycHC[8] (gray) and mixHC[8] (magenta). Error bars on HPLC yields express standard deviation between reproduced reactions (n= 2–8). For more details, see Table S7.

supplemental experimental procedures; Data S1). Full conversion of the 1:7 ratio of B and CU into HC[8]s is expected to direct 498 combinations to 12% and 82% of mixHC[8] and cycHC[8], respectively (Figure 1; Table S1).

The fact that solution-phase synthesis did not result in a statistical ratio of more favored HC[8]s encouraged us to study if the selectivity of mono-biotinylated mixHC[8] formation can be increased via tuning the conditions of the mechanosynthesis. To investigate the effect of multiple reaction parameters on the assembly of 8-membered macrocycles, we utilized RSM for experimental design and screening of reaction conditions.[37] The HPLC yields of mixHC[8] and cycHC[8] obtained after the aging step were plotted as 3D response surfaces, highlighting the conditions favorable for the assembly of mixHC[8] compared to cycHC[8] (Figures 2A, 2B, S3, and S4; Tables S2–S6). The ratio of monomers, loading of aqueous mineral acid ($HClO_4$), milling duration, and aging temperature, which affect macrocyclization,[8] were simultaneously explored.

The formation of mixHC[8] and cycHC[8] proved to be sensitive to the monomer ratio and acid loading (Figures 2A and 2B). Variations of the monomer ratios within the range of 1:5 to 1:15 did not significantly affect the yield of chimeric mixHC[8] (Figure 2A; Table S2); however, using an excess of CU clearly resulted in the enhanced generation of cycHC[8] (Figure 2B; Table S2). The quantity of $HClO_4$ appeared to be the vital parameter affecting the formation of mixHC[8]. The highest yields of mixHC[8] were attained within the specific range of $HClO_4$ loadings of 1.2–3.0 equiv (Figure 2A), while cycHC[8] was less dependent on the quantity of acid catalyst. This observation highlights the difference in formation of mixHC[8] and cycHC[8] in

response to varied reaction conditions. The impacts of milling time and aging temperature appeared to be less significant, and the optimal temperature for ripening mixHC[8] was found to range from 40°C to 65°C. RSM helped to reach a 20% yield of mixHC[8] under standard conditions—3 equiv of template, 1 h ball milling followed by 24 h aging at 60°C—selected for further optimization studies.

It was hypothesized that an alternative template could amplify the formation of the target macrocycle. The binding studies for the cycHC[8] receptor revealed the following ranking of anion affinity: SbF_6^- > PF_6^- > ReO_4^- > ClO_4^-.[11] The use of hexafluoroantimonate (SbF_6^-) as a template did not seem practical since $HSbF_6$ mainly exists as the HF/SbF_5 superacid system.[38,39] Hexafluorophosphate (PF_6^-), on the other hand, serves as an efficient template for the synthesis of homomeric cycHC[8] in solution.[18] Due to its advantageous templating potential, HPF_6 was chosen as an alternative reagent to mediate the solid-state synthesis of mixHC[8]. In addition, it is safer to handle than perchlorates, which are known for their undesirable oxidative, flammable, and explosive hazards.[40,41] Interestingly, the use of HPF_6 resulted in decreased formation of homomeric cycHC[8], contrary to an improved yield (28%) of mixHC[8] (Figure 2C; Table S7). Since the mixHC[8] assembly was highly sensitive to the quantity of acid (Figure 2A), we tested three hexafluorophosphate salts ($AgPF_6$, $[Cu(CH_3CN)_4]PF_6$, and KPF_6) as additives to partially substitute the acid while keeping the amount of template anion constant (Figure 2D; Table S7). Additionally, we anticipated that the Ag^+ and Cu^+ cations could serve as potential promoters for the generation of mixHC[8] due to their affinity for biotin.[42–44] As depicted in Figure 2D, the Ag^+ and Cu^+ salts had a negligible effect on the formation of mixHC[8] while improving the yield of homomeric cycHC[8] compared to the reaction with HPF_6. The latter points at the effective decrease in the concentration of antagonistic[45] CU-rich mixed oligomers, which reassembled and provided CU to cyclize into cycHC[8]. The best result was achieved with KPF_6, which afforded the highest yield of mixHC[8] (37%) with the accompanying formation of cycHC[8] (38%) (Figure 2D). Further variation of HPF_6/KPF_6 equivalence by RSM, however, did not improve the formation of mixHC[8] (Tables S8–S12; Figure S8). It was additionally confirmed that the stoichiometric ratio of the starting monomers provided the best mixHC[8] yield (Table S13). Once the key chemical parameters had been identified, the durations of ball milling and aging at moderately elevated temperatures were optimized, leading to the best 38% yield of mixHC[8] in a 4 h total reaction time (Tables S14 and S15; for conditions, see the Figure 1 caption).

The changes in the content of intermediates and products were analyzed by HRMS. Altogether, over 100 reaction species were identified in the crude reaction mixtures during different stages of covalent assembly and mapped based on MS signal intensities (Figures 3A and S9–S13; Tables S16 and S29; MatchMass tool[46]). The results display the dynamic changes in the composition of the reaction mixture during milling and aging. Biotin was found to be incorporated into different linear oligomers $(CU)_x(B)_y$ (x = 1 … 8, y = 1 … 4), as well as into a number of mono-, di-, tri-, and tetra-biotinylated mixHC[n]s (n = 6 … 8). Homomeric CU oligomers dominate at the initial phase of the polycondensation reaction (milling time: 5 min) and are kinetically favored products. Consequently, the milling time must be sufficient (60 min; Tables S14 and S15) to enable the accumulation of the slowly generated mixed biotin-containing chains. The content of the mixed oligomers (n = 6–8), which are essential for mixHC[n] formation, significantly increased after 45–60 min milling. This difference in the contents of the short- and long-milled mixtures emphasizes the dynamic shuffling of the monomers, which resulted in an increased random distribution of biotin upon prolonged milling. The low content of macrocycles in DCL

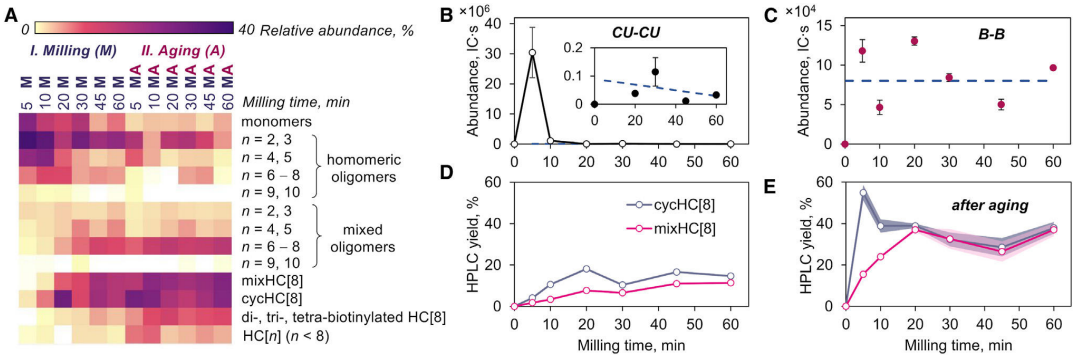

Figure 3. Dynamic covalent library composition and changes in the content of dimers and HC[8]s during mechanosynthesis

DCL composition summarized in a heatmap (A) based on MS abundance of the detected species (Tables S29 and S16; Figure S10); content of homomeric dimers CU-CU (B) and B-B (C) and HPLC yields of macrocycles (D and E) during milling and after aging. The content of the dimers is reported as the MS abundance for triplicate measurements ($n = 3$) ± standard deviation, and the linear fit is expressed as dashed lines. The yields of macrocycles are presented as mean values obtained in a series of replicated experiments ($2 \leq n \leq 4$) with confidence intervals. More details are provided in Figures S11–S15 and Table S19.

directly after milling can be attributed to the unfavorable complexation with the template,[11,17] most likely due to increased entropy during mechanical agitation. The macrocyclic products predominantly ripened at the aging stage, at which point the mixed and homomeric oligomers underwent additional, although less intense, crossover unit exchange. Moreover, crossover between monomers from macrocycles was observed under similar conditions using cycHC[*n*]s and biotin as the starting materials for mixHC[8] synthesis (Table S17), which confirms the dynamic character of the covalent self-assembly.

Further understanding of the dynamic processes and interconversion of intermediates occurring at the milling stage was obtained by tracking the fate of selected short oligomers (Figures 3B and 3C; Table S18). The changes in the content of characteristic dimers and trimers prior to and after the aging stage were determined by HPLC-MS analyses. The collected data confirmed that coupling between the CU monomers is kinetically preferred and occurs at the initial phase of the polycondensation reaction. Thus, the quantity of the CU-CU dimer drastically increased after 5 min of milling and subsequently underwent rapid decay (Figure 3B). Such fast dynamics and decay were absent for the biotin units, reflecting a major difference in the condensation between biotin and CU. In contrast to CU, the condensation of the biotin units to the respective dimer, B-B, reached its maximum at the beginning of the reaction and probably acts as a transient intermediate (Figures 3B and 3C). Similar behavior was observed for the respective trimers (Table S18). The yields of the macrocycles generated at the milling stage did not exceed 20% but greatly increased during aging (Figures 3D and 3E). Notably, the macrocyclic content in the aged mixtures is significantly affected by milling duration, when monomer shuffling occurs. Thus, aging of the short-milled (5 min) reaction mixture, which contained mainly homomeric CU oligomers, resulted in the ripening of cycHC[8] as the dominant product (55% yield), along with a minor quantity of mixHC[8] (16% yield). However, fast reversible C–N bond formation and cleavage during milling caused rapid dynamic changes in the oligomeric profile with a random distribution of the biotin units. Upon prolonged milling (60 min; Tables S14 and S15), the yield of mixHC[8] notably increased from 16% to 37%, with a concurrent decrease in the yield of cycHC[8] to 38%, resulting

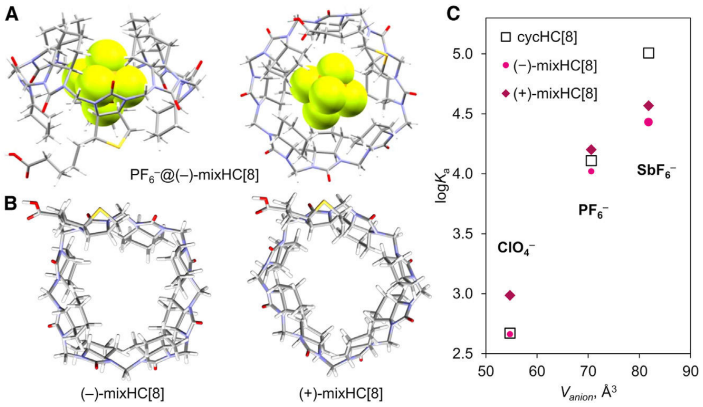

Figure 4. Structures of mixHC[8]s and data on anion binding

PF_6^-@(−)-mixHC[8] inclusion complex from SC-XRD (A) (CCDC: 2251913). DFT low-energy structures of (−)- and (+)-mixHC[8] diastereomers (B) (see the computational study in the supplemental experimental procedures; Data S2). Correlation between anion volumes (V_{anion}) and association constants ($\log K_a$) was determined by ITC for complexes with (TBA)ClO_4, (TBA)PF_6 (TBA = tetrabutylammonium), and $NaSbF_6$ salts in methanol using one-to-one binding model (C) (Table S6.1).

in a 1:1 product ratio. Finally, a close examination of the aging duration (Table S15) revealed that the maximum content of mixHC[8] was achieved in 3 h, when the templated self-assembly process was essentially complete.

The developed mechanochemical procedure significantly surpassed mixHC[8] synthesis in solution, yielding superior selectivity and conversion rates (Table S30). Solution-state processes are affected by diffusion, with diffusion constants varying for monomers, aggregates, and oligomeric intermediates due to size differences. In mechanochemistry, reaction rates do not directly depend on the molecular size of the intermediates but rather on the number of molecular collisions.[47] In addition to the chemical advantages, solvent-free synthesis produces less waste (PMI = 4) compared to the reaction in solution (PMI = 306) and is more sustainable based on the respective green metrics (Table S30).[32]

Diastereoisomeric (−)- and (+)-mixHC[8]s were synthesized via condensation of either (*R*,*R*)-CU or (*S*,*S*)-CU with (*S*,*S*,*R*)-B, isolated in 16% and 11% yields with high purity (88% and 90%, respectively), and characterized by nuclear magnetic resonance (NMR) and infrared spectroscopy (Figures S16–S32).

Anion binding properties

The encapsulation of suitably sized anionic guests by HC[*n*]s is likely governed by electrostatic and orbital interactions.[48] In addition, the anions form weak interactions with C-H groups of HC[*n*]s pointing inside the cavity.[49] Efficient anion recognition has been reported for bambusurils,[22,50–53] heterobambusurils,[54] biotinurils,[55,56] and cycHC[*n*]s.[11] We were fortunate to obtain single crystals of the PF_6^- inclusion complex with (−)-mixHC[8] (Figures 4A and S33–S39; Tables S19 and S20). A DFT modeling study of the mixHC[8] diastereomers (Figure S40; Tables S21–S24; Data S2) revealed clear differences in their conformations (Figure 4B; Data S2). The cavity, which is mainly surrounded by CU units, is mostly

distorted by the biotin position. Therefore, its influence on the anion binding properties was evaluated via comparison of the three HC[8] hosts.

Encapsulation of the selected anions by the mixHC[8]s was studied by ITC (Figures 4C and S51–S54; Table S25); the data for cycHC[8] were available from a previous work.[11] Complexation between the mono-biotinylated macrocycles and chaotropic anions (ClO_4^-, PF_6^-, and SbF_6^-) in methanol and a methanol-water mixture (1:1) occurred as an exothermic enthalpy-driven process. The association constants for PF_6^- were greater than that of ClO_4^- in both media, which explains the better templating properties of PF_6^-. Noticeably, the differences between the affinities of the three HC[8] derivatives are the smallest for the templating PF_6^- anion, while for ClO_4^- and SbF_6^-, either (+)-mixHC[8] or cycHC[8], respectively, exhibit stronger binding. The noted dissimilarities highlight distinctions in the cavities and point to the steric differences of these host compounds, which have potential in a diverse array of applications and unique guest-binding properties.

Selective capture of perchlorate by immobilized mixHC[8]

The mixHC[8] can be utilized to afford functional materials, which was showcased by the selective removal of perchlorates from contaminated soil samples. Perchlorate is a persistent pollutant that adversely affects human health by interfering with thyroid hormone production and occurs in soil, ground water, and food.[40,41] The accumulation of perchlorate in fertilizers, soil, and irrigation water leads to increased plant uptake and subsequent food-chain transfer.[57,58] This pollutant has been found in various environmental matrices and typically originates from human activities.

The carboxylate side chain of mixHC[8] enabled its facile covalent immobilization on the surface of 3-aminopropyl silica gel (APS; Figure 5A).[59] The resulting solid perchlorate-extracting material (mixHC[8]-APS) contained ca. 12% (w/w) of mixHC[8], based on infrared spectroscopic analysis (Figures 5B and S55). Once covalently attached to APS, the macrocycle remains in the solid phase even in the solvents where it is commonly soluble (i.e., dichloromethane, methanol) and can, therefore, be applied in solid-phase extraction. To prove the removal of perchlorate in the presence of other minerals, a regolith simulant[60] was employed as the matrix of the known composition and spiked with $(TBA)ClO_4$, imitating contamination with perchlorate (1% w/w). The obtained model mixture contained cations (Ca^{2+}, Mg^{2+}, Fe^{2+}, Fe^{3+}), oxides, and kosmotropic anions (SO_4^{2-}, CO_3^{2-}) but was essentially free of the organic matter (Table S26). According to ion chromatography analysis (Tables S27 and S28; Figures S56–S59), the methanolic extract of the contaminated matrix contained primarily perchlorate and sulfate, the latter arising from the $MgSO_4$ component (Table S26). Treatment of the methanolic extract with solid mixHC[8]-APS resulted in the complete removal of ClO_4^-, in contrast to non-modified APS, which adsorbed ca. 15% ClO_4^- (Figures 5C and S59; Table S28).

The extraction of sulfate occurred with similar efficiency (ca. 85%–97%) using both APS and mixHC[8]-APS materials, demonstrating that mixHC[8] is not the main contributor responsible for the capture of SO_4^{2-}. The absence of mixHC[8] affinity toward sulfate was additionally confirmed by an ITC experiment (Table S25; Figures S47 and S54).

The captured perchlorate was easily removed by washing mixHC[8]-APS material with water, taking advantage of the weaker binding in the aqueous medium, which demonstrates the potential for the material's reusability.[61]

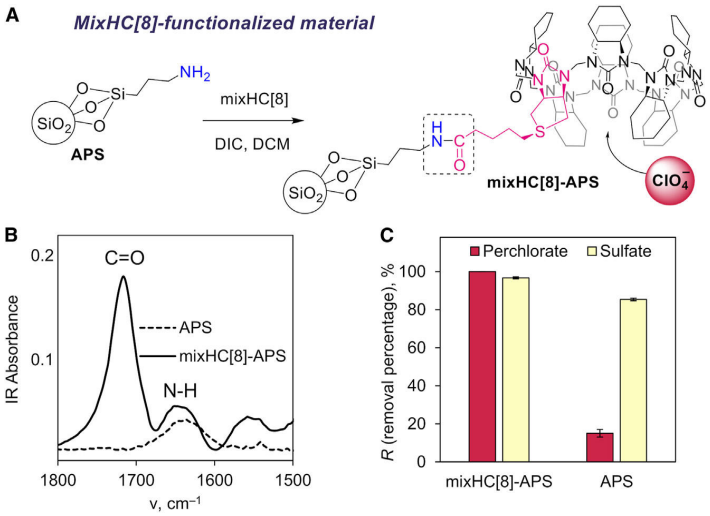

Figure 5. Derivatization of aminated silica by mixHC[8] and perchlorate removal efficiency of the obtained material

Immobilization of mixHC[8] on APS (A), DIC – *N,N′*-diisopropylcarbodiimide, and DCM (dichloromethane); characterization of material by infrared (IR) (B) and perchlorate removal from spiked mineral matrix using mixHC[8]-APS and non-modified APS, determined by ion chromatography (C). The error bars represent the standard deviation between the parallel experiments ($n \geq 2$) (isothermal calorimetric titration and immobilization of mixHC[8] on APS in the supplemental experimental procedures).

In conclusion, an efficient mechanochemical protocol for the synthesis of enantiopure mono-biotinylated HC[8]s was developed. The process involves two stages: (1) the mechanochemically assisted and acid-catalyzed polycondensation of D-biotin, (*R,R*)- or (*S,S*)-CU, and formaldehyde and (2) the aging step, in which the template-driven covalent self-assembly of oligomers into macrocycles takes place. Screening experiments uncovered the key process and chemical parameters affecting the assembly: the ratio of the monomers, the loading of the acid catalyst, and the nature of the templating anion. The present study offers insight into the complex mixture of oligomeric intermediates, including their interconversion and self-organization processes en route to the macrocyclic products. HPLC-MS analysis of short oligomers revealed differences in condensation kinetics of paraformaldehyde with biotin and CU into homomeric dimers and trimers under mechanochemical agitation. The faster condensation of CU led to amplification of the homomeric cycHC[8] during the aging of shortly agitated reaction mixtures. On the contrary, upon prolonged ball milling, which ensures sufficient shuffling of monomers, higher efficiency in the formation of the chimeric mixHC[8] in 38% yield was achieved. The mechanochemically driven solid-state approach allowed for the fine-tuning of the composition of the rich DCL and directing covalent self-assembly processes beyond statistical distribution. Diastereomeric (−)- and (+)-mixHC[8]s were isolated and their structures characterized by DFT, NMR, and SC-XRD methods. Furthermore, the comparison of their affinities toward chaotropic anions pointed at specific binding differences, which makes the chimeric family of HC[8] appealing for host-guest chemistry. The biotin carboxylate group of the mixHC[8] enabled its facile covalent immobilization on aminated silica. The functional material obtained was employed in the selective capture of anions, as

demonstrated by the complete removal of perchlorate from an extract of a mineral model mixture. Further applications of these chiral chimeric hemicucurbiturils are currently being studied.

EXPERIMENTAL PROCEDURES

Resource availability

Lead contact

Further information and requests for resources should be directed to and will be fulfilled by the lead contact, Riina Aav (riina.aav@taltech.ee).

Materials availability

All materials generated in this study are available from the lead contact without restrictions for research purposes.

Data and code availability

All data supporting this study's findings are included in the article and its supplemental information and are also available from the authors upon request. Crystallographic data for the structures reported in this paper have been deposited at the Cambridge Crystallographic Data Center under CCDC: 2251913. Copies of these data can be obtained free of charge via www.ccdc.cam.ac.uk/data_request/cif.

SUPPLEMENTAL INFORMATION

Supplemental information can be found online at https://doi.org/10.1016/j.xcrp.2024.102161.

ACKNOWLEDGMENTS

The authors would like to thank Jasper Adamson and Indrek Reile for input on the NMR analysis. The research by R.A., L.U., D.K., J.S.W., and K.R. was funded by the European Union's H2020- FETOPEN grant 828779 (INITIO). E.S.-T., T.J., K.-M.L., J.V.N., J.M., R.R., and M.O. were financed by Estonian Research Council grants PRG399 and PRG2169. R.A. was funded by the Ministry of Education and Research through Centre of Excellence in Circular Economy for Strategic Mineral and Carbon Resources (01.01.2024–31.12.2030, TK228). The authors also acknowledge COST Action CA18112 "Mechanochemistry for Sustainable Industry" for supporting research in mechanochemistry.

AUTHOR CONTRIBUTIONS

All authors contributed to the manuscript's preparation and have provided their approval for the final version of the manuscript. The authors' specific contributions are as follows: E.S.-T. was the main contributor for the development of the synthesis and mixHC[8] characterization and participated in binding studies; T.J. was the main contributor of the chemical analysis, binding, immobilization, and perchlorate removal studies; P.T. and S.P. contributed to perchlorate removal; K.-M.L., K.S., and J.V.N. contributed to the synthesis; J.M., J.S.W., and K.R. contributed to SC-XRD analysis; R.R. and M.Ö. contributed to computational studies; L.U. contributed to the script for MS data analysis and binding studies; M.V. contributed to the assessment of combinatorics; V.R. contributed to NMR analysis; D.K. contributed to conceptualization of the synthesis, perchlorate removal, and assessment of green metrics; and R.A. contributed to conceptualization of the overall research, data analysis, writing, and supervision.

DECLARATION OF INTERESTS

This research has been filed for patent application EP23181344.5 and PCT/IB2024/056236. Authors: R.A., E.S.-T., T.J., Tatsiana Nikonovich, D.K., and L.U. Title: "Method of preparation of chimeric HC[n]s, derivatives, and uses thereof," priority date: June 26, 2023.

Received: May 22, 2024
Revised: July 15, 2024
Accepted: July 29, 2024
Published: August 20, 2024

REFERENCES

1. Schnitzer, T., Preuss, M.D., van Basten, J., Schoenmakers, S.M.C., Spiering, A.J.H., Vantomme, G., and Meijer, E.W. (2022). How subtle changes can make a difference: Reproducibility in complex supramolecular systems. Angew. Chem. *61*, e202206738. https://doi.org/10.1002/ange.202206738.

2. Yamaoki, Y., Nagata, T., Kondo, K., Sakamoto, T., Takami, S., and Katahira, M. (2022). Shedding light on the base-pair opening dynamics of nucleic acids in living human cells. Nat. Commun. *13*, 7143. https://doi.org/10.1038/s41467-022-34822-4.

3. Kwon, T.W., Song, B., Nam, K.W., and Stoddart, J.F. (2022). Mechanochemical enhancement of the structural stability of pseudorotaxane intermediates in the synthesis of rotaxanes. J. Am. Chem. Soc. *144*, 12595–12601. https://doi.org/10.1021/jacs.2c00515.

4. Dračínský, M., Hurtado, C.S., Masson, E., and Kaleta, J. (2021). Stuffed pumpkins: Mechanochemical synthesis of host–guest complexes with cucurbit[7]uril. Chem. Commun. *57*, 2132–2135. https://doi.org/10.1039/D1CC00240F.

5. Friščić, T., Mottillo, C., and Titi, H.M. (2020). Mechanochemistry for synthesis. Angew. Chem. *132*, 1030–1041. https://doi.org/10.1002/ange.201906755.

6. Cuccu, F., De Luca, L., Delogu, F., Colacino, E., Solin, N., Mocci, R., and Porcheddu, A. (2022). Mechanochemistry: New tools to navigate the uncharted territory of "impossible" reactions. ChemSusChem *15*, e202200362. https://doi.org/10.1002/cssc.202200362.

7. Reynes, J.F., Isoni, V., and García, F. (2023). Tinkering with mechanochemical tools for scale-up. Angew. Chem., Int. Ed. Engl. *62*, e202300819. https://doi.org/10.1002/anie.202300819.

8. Kaabel, S., and Aav, R. (2018). Templating effects in the dynamic chemistry of cucurbiturils and hemicucurbiturils. Isr. J. Chem. *58*, 296–313. https://doi.org/10.1002/ijch.201700106.

9. Lehn, J.-M. (1999). Dynamic combinatorial chemistry and virtual combinatorial libraries. Chem. Eur J. *5*, 2455–2463. https://doi.org/10.1002/(SICI)1521-3765(19990903)5:9<2455::AID-CHEM2455>3.0.CO;2-H.

10. Corbett, P.T., Leclaire, J., Vial, L., West, K.R., Wietor, J.-L., Sanders, J.K.M., and Otto, S. (2006). Dynamic combinatorial chemistry. Chem. Rev. *106*, 3652–3711. https://doi.org/10.1021/cr020452p.

11. Kaabel, S., Adamson, J., Topić, F., Kiesilä, A., Kalenius, E., Öeren, M., Reimund, M., Prigorchenko, E., Lõokene, A., Reich, H.J., et al. (2017). Chiral hemicucurbit[8]uril as an anion receptor: Selectivity to size, shape and charge distribution. Chem. Sci. *8*, 2184–2190. https://doi.org/10.1039/C6SC05058A.

12. Andersen, N.N., Lisbjerg, M., Eriksen, K., and Pittelkow, M. (2018). Hemicucurbit[n]urils and their derivatives – Synthesis and applications. Isr. J. Chem. *58*, 435–448. https://doi.org/10.1002/ijch.201700129.

13. Lisbjerg, M., Jessen, B.M., Rasmussen, B., Nielsen, B.E., Madsen, A.Ø., and Pittelkow, M. (2014). Discovery of a cyclic 6 + 6 hexamer of D-biotin and formaldehyde. Chem. Sci. *5*, 2647–2650. https://doi.org/10.1039/C4SC00990H.

14. Havel, V., Yawer, M.A., and Sindelar, V. (2015). Real-time analysis of multiple anion mixtures in aqueous media using a single receptor. Chem. Commun. *51*, 4666–4669. https://doi.org/10.1039/C4CC10108A.

15. Yawer, M.A., Havel, V., and Sindelar, V. (2015). A bambusuril macrocycle that binds anions in water with high affinity and selectivity. Angew. Chem., Int. Ed. Engl. *54*, 276–279. https://doi.org/10.1002/anie.201409895.

16. Lizal, T., and Sindelar, V. (2018). Bambusuril anion receptors. Isr. J. Chem. *58*, 326–333. https://doi.org/10.1002/ijch.201700111.

17. Kaabel, S., Stein, R.S., Fomitšenko, M., Järving, I., Friščić, T., and Aav, R. (2019). Size-control by anion templating in mechanochemical synthesis of hemicucurbiturils in the solid state. Angew. Chem., Int. Ed. Engl. *58*, 6230–6234. https://doi.org/10.1002/anie.201813431.

18. Prigorchenko, E., Öeren, M., Kaabel, S., Fomitšenko, M., Reile, I., Järving, I., Tamm, T., Topić, F., Rissanen, K., and Aav, R. (2015). Template-controlled synthesis of chiral cyclohexylhemicucurbit[8]uril. Chem. Commun. *51*, 10921–10924. https://doi.org/10.1039/C5CC04101E.

19. Zeng, Q., Long, Q., Lu, J., Wang, L., You, Y., Yuan, X., Zhang, Q., Ge, Q., Cong, H., and Liu, M. (2021). Synthesis of a novel aminobenzene-containing hemicucurbituril and its fluorescence spectral properties with ions. Beilstein J. Org. Chem. *17*, 2840–2847. https://doi.org/10.3762/bjoc.17.195.

20. Wang, L., Han, J., Pan, R., Yuan, X., You, Y., Cen, X., Zhang, Q., Ge, Q., Cong, H., and Liu, M. (2022). Synthesis of hybrid thiohemicucurbiturils. Tetrahedron Lett. *101*, 153918. https://doi.org/10.1016/j.tetlet.2022.153918.

21. Maršálek, K., and Šindelář, V. (2020). Monofunctionalized bambus[6]urils and their conjugates with crown ethers for liquid–liquid extraction of inorganic salts. Org. Lett. *22*, 1633–1637. https://doi.org/10.1021/acs.orglett.0c00216.

22. De Simone, N.A., Chvojka, M., Lapešová, J., Martínez-Crespo, L., Slávik, P., Sokolov, J., Butler, S.J., Valkenier, H., and Šindelář, V. (2022). Monofunctionalized fluorinated bambusurils and their conjugates for anion transport and extraction. J. Org. Chem. *87*, 9829–9838. https://doi.org/10.1021/acs.joc.2c00870.

23. Del Mauro, A., Lapešová, J., Rando, C., and Šindelář, V. (2024). Merging bambus[6]uril and biotin[6]uril into an enantiomerically pure monofunctionalized hybrid macrocycle. Org. Lett. *26*, 106–109. https://doi.org/10.1021/acs.orglett.3c03715.

24. Langerreiter, D., Kostiainen, M.A., Kaabel, S., and Anaya-Plaza, E. (2022). A greener route to blue: Solid-state synthesis of phthalocyanines. Angew. Chem., Int. Ed. Engl. *61*, e202209033. https://doi.org/10.1002/anie.202209033.

25. Pascu, M., Ruggi, A., Scopelliti, R., and Severin, K. (2013). Synthesis of borasiloxane-based macrocycles by multicomponent condensation reactions in solution or in a ball mill. Chem. Commun. *49*, 45–47. https://doi.org/10.1039/C2CC37538A.

26. Sim, Y., Shi, Y.X., Ganguly, R., Li, Y., and García, F. (2017). Mechanochemical synthesis of phosphazane-based frameworks. Chem. Eur J. *23*, 11279–11285. https://doi.org/10.1002/chem.201701619.

27. Xi, H.-T., Zhao, T., Sun, X.-Q., Miao, C.-B., Zong, T., and Meng, Q. (2013). Rapid and efficient solvent-free synthesis of cyclophanes based on bipyridinium under mechanical ball milling. RSC Adv. *3*, 691–694. https://doi.org/10.1039/C2RA22802E.

28. Kunde, T., Pausch, T., Guńka, P.A., Krzyżanowski, M., Kasprzak, A., and Schmidt,

B.M. (2022). Fast, solvent-free synthesis of ferrocene-containing organic cages via dynamic covalent chemistry in the solid state. Chem. Sci. *13*, 2877–2883. https://doi.org/10.1039/D1SC06372C.

29. Shy, H., Mackin, P., Orvieto, A.S., Gharbharan, D., Peterson, G.R., Bampos, N., and Hamilton, T.D. (2014). The two-step mechanochemical synthesis of porphyrins. Faraday Discuss *170*, 59–69. https://doi.org/10.1039/C3FD00140G.

30. Su, Q., and Hamilton, T.D. (2019). Extending mechanochemical porphyrin synthesis to bulkier aromatics: Tetramesitylporphyrin. Beilstein J. Org. Chem. *15*, 1149–1153. https://doi.org/10.3762/bjoc.15.111.

31. MathWorld–A Wolfram Web Resource. Weisstein, E. W. Necklace. https://mathworld.wolfram.com/Necklace.html.

32. McElroy, C.R., Constantinou, A., Jones, L.C., Summerton, L., and Clark, J.H. (2015). Towards a holistic approach to metrics for the 21st century pharmaceutical industry. Green Chem. *17*, 3111–3121. https://doi.org/10.1039/C5GC00340G.

33. Friščić, T., Childs, S.L., Rizvi, S.A.A., and Jones, W. (2009). The role of solvent in mechanochemical and sonochemical cocrystal formation: A solubility-based approach for predicting cocrystallisation outcome. CrystEngComm *11*, 418–426. https://doi.org/10.1039/B815174A.

34. Do, J.-L., and Friščić, T. (2017). Chemistry 2.0: Developing a new, solvent-free system of chemical synthesis based on mechanochemistry. Synlett *28*, 2066–2092. https://doi.org/10.1055/s-0036-1590854.

35. Belenguer, A.M., Lampronti, G.I., De Mitri, N., Driver, M., Hunter, C.A., and Sanders, J.K.M. (2018). Understanding the influence of surface solvation and structure on polymorph stability: A combined mechanochemical and theoretical approach. J. Am. Chem. Soc. *140*, 17051–17059. https://doi.org/10.1021/jacs.8b08549.

36. Prigorchenko, E., Kaabel, S., Narva, T., Baškir, A., Fomitšenko, M., Adamson, J., Järving, I., Rissanen, K., Tamm, T., and Aav, R. (2019). Formation and trapping of the thermodynamically unfavoured inverted-hemicucurbit[6]uril. Chem. Commun. *55*, 9307–9310. https://doi.org/10.1039/C9CC04990H.

37. Myers, R.H., Montgomery, D.C., and Anderson-Cook, C.M. (2016). Response Surface Methodology: Process and Product Optimization Using Designed Experiments (John Wiley & Sons).

38. Czapla, M., and Skurski, P. (2015). Strength of the Lewis–Brønsted superacids containing In, Sn, and Sb and the electron binding energies of their corresponding superhalogen anions. J. Phys. Chem. A *119*, 12868–12875. https://doi.org/10.1021/acs.jpca.5b10205.

39. Bour, C., Guillot, R., and Gandon, V. (2015). First evidence for the existence of hexafluoroantimonic(V) acid. Chem. Eur J. *21*, 6066–6069. https://doi.org/10.1002/chem.201500334.

40. Urbansky, E.T. (2002). Perchlorate as an environmental contaminant. Environ. Sci. Pollut. Res. Int. *9*, 187–192. https://doi.org/10.1007/BF02987487.

41. Kumarathilaka, P., Oze, C., Indraratne, S.P., and Vithanage, M. (2016). Perchlorate as an emerging contaminant in soil, water and food. Chemosphere *150*, 667–677. https://doi.org/10.1016/j.chemosphere.2016.01.109.

42. Sigel, H., and Scheller, K.H. (1982). Metal ion complexes of D-biotin in solution. Stability of the stereoselective thioether coordination. J. Inorg. Biochem. *16*, 297–310. https://doi.org/10.1016/S0162-0134(00)80266-4.

43. Aoki, K., and Saenger, W. (1983). Interactions of biotin with metal ions. X-ray crystal structure of the polymeric biotin-silver(i) nitrate complex: metal bonding to thioether and ureido carbonyl groups. J. Inorg. Biochem. *19*, 269–273. https://doi.org/10.1016/0162-0134(83)85031-4.

44. Altaf, M., and Stoeckli-Evans, H. (2013). Chiral one- and two-dimensional silver(I)–biotin coordination polymers. Acta Crystallogr. C *69*, 127–137. https://doi.org/10.1107/S0108270113000322.

45. Lehn, J.-M. (2013). Perspectives in chemistry—steps towards complex matter. Angew. Chem., Int. Ed. Engl. *52*, 2836–2850. https://doi.org/10.1002/anie.201208397.

46. Ustrnul, L., Jarg, T., Jantson, M., Osadchuk, I., Anton, L., and Aav, R. (2024). MatchMass: A web-based tool for efficient mass spectrometry data analysis. Preprint at ChemRxiv. https://doi.org/10.26434/chemrxiv-2024-9j8n7.

47. Ma, X., Yuan, W., Bell, S.E.J., and James, S.L. (2014). Better understanding of mechanochemical reactions: Raman monitoring reveals surprisingly simple 'pseudo-fluid' model for a ball milling reaction. Chem. Commun. *50*, 1585–1587. https://doi.org/10.1039/C3CC47898J.

48. Ortolan, A.O., Madureira, L., Rodríguez-Kessler, P.L., Maturana, R.G., Olea Ulloa, C., Caramori, G.F., Parreira, R.L., and Muñoz-Castro, A. (2023). The nature of the central halide encapsulation in bambusuril hosts (BU[6]). Structural and interaction energy insights in BU[6]·X− (X = Cl, Br, I) from relativistic DFT calculations. Inorg. Chim. Acta. *555*, 121596. https://doi.org/10.1016/j.ica.2023.121596.

49. Öeren, M., Shmatova, E., Tamm, T., and Aav, R. (2014). Computational and ion mobility MS study of (All-S)-Cyclohexylhemicucurbit[6]uril structure and complexes. Phys. Chem. Chem. Phys. *16*, 19198–19205. https://doi.org/10.1039/C4CP02202E.

50. Jašíková, L., Rodrigues, M., Lapešová, J., Lízal, T., Šindelář, V., and Roithová, J. (2019). Bambusurils as a mechanistic tool for probing anion effects. Faraday Discuss *220*, 58–70. https://doi.org/10.1039/C9FD00038K.

51. Sokolov, J., Štefek, A., and Šindelář, V. (2020). Functionalized chiral bambusurils: Synthesis and host-guest interactions with chiral carboxylates. ChemPlusChem *85*, 1307–1314. https://doi.org/10.1002/cplu.202000261.

52. Itterheimová, P., Bobacka, J., Šindelář, V., and Lubal, P. (2022). Perchlorate solid-contact ion-selective electrode based on dodecabenzylbambus[6]uril. Chemosensors *10*, 115. https://doi.org/10.3390/chemosensors10030115.

53. Rando, C., Vázquez, J., Sokolov, J., Kokan, Z., Nečas, M., and Šindelář, V. (2022). Highly efficient and selective recognition of dicyanoaurate(I) by a bambusuril macrocycle in water. Angew. Chem., Int. Ed. Engl. *61*, e202210184. https://doi.org/10.1002/anie.202210184.

54. Reany, O., Mohite, A., and Keinan, E. (2018). Hetero-bambusurils. Isr. J. Chem. *58*, 449–460. https://doi.org/10.1002/ijch.201700138.

55. Lisbjerg, M., Nielsen, B.E., Milhøj, B.O., Sauer, S.P.A., and Pittelkow, M. (2015). Anion binding by biotin[6]uril in water. Org. Biomol. Chem. *13*, 369–373. https://doi.org/10.1039/C4OB02211D.

56. Andersen, N.N., Eriksen, K., Lisbjerg, M., Ottesen, M.E., Milhøj, B.O., Sauer, S.P.A., and Pittelkow, M. (2019). Entropy/enthalpy compensation in anion binding: Biotin[6]uril and biotin-l-sulfoxide[6]uril reveal strong solvent dependency. J. Org. Chem. *84*, 2577–2584. https://doi.org/10.1021/acs.joc.8b02797.

57. Calderón, R., Palma, P., Arancibia-Miranda, N., Kim, U.-J., Silva-Moreno, E., and Kannan, K. (2022). Occurrence, distribution and dynamics of perchlorate in soil, water, fertilizers, vegetables and fruits and associated human exposure in Chile. Environ. Geochem. Health *44*, 527–535. https://doi.org/10.1007/s10653-020-00680-6.

58. Chen, Y., Zhu, Z., Wu, X., Zhang, D., Tong, J., Lin, Y., Yin, L., Li, X., Zheng, Q., and Lu, S. (2022). A nationwide investigation of perchlorate levels in staple foods from China: Implications for human exposure and risk assessment. J. Hazard Mater. *439*, 129629. https://doi.org/10.1016/j.jhazmat.2022.129629.

59. Tabakci, M. (2008). Immobilization of calix[6]arene bearing carboxylic acid and amide groups on aminopropyl silica gel and its sorption properties for Cr(VI). J. Inclusion Phenom. Macrocycl. Chem. *61*, 53–60. https://doi.org/10.1007/s10847-007-9392-2.

60. Cannon, K.M., Britt, D.T., Smith, T.M., Fritsche, R.F., and Batcheldor, D. (2019). Mars global simulant MGS-1: A rocknest-based open standard for basaltic Martian regolith simulants. Icarus *317*, 470–478. https://doi.org/10.1016/j.icarus.2018.08.019.

61. Shalima, T., Mishra, K.A., Kaabel, S., Ustrnul, L., Bartkova, S., Tõnsuaadu, K., Heinmaa, I., and Aav, R. (2021). Cyclohexanohemicucurbit[8]uril inclusion complexes with heterocycles and selective extraction of sulfur compounds from water. Front. Chem. *9*, 786746. https://doi.org/10.3389/fchem.2021.786746.

Appendix 2

Publication II

T. Jarg, J. Tamm, E. Suut-Tuule, K.-M. Lootus, D. Kananovich, R. Aav. How reliable is internal standard method in monitoring mechanochemical synthesis? A case study of triphenylmethane in HPLC-UV-MS analysis of hemicucurbit[n]urils. *RSC Mechanochemistry,* **2025**, 2, 507-515.

Volume 2
Number 4
July 2025
Pages 491–618

RSC Mechanochemistry

rsc.li/RSCMechanochem

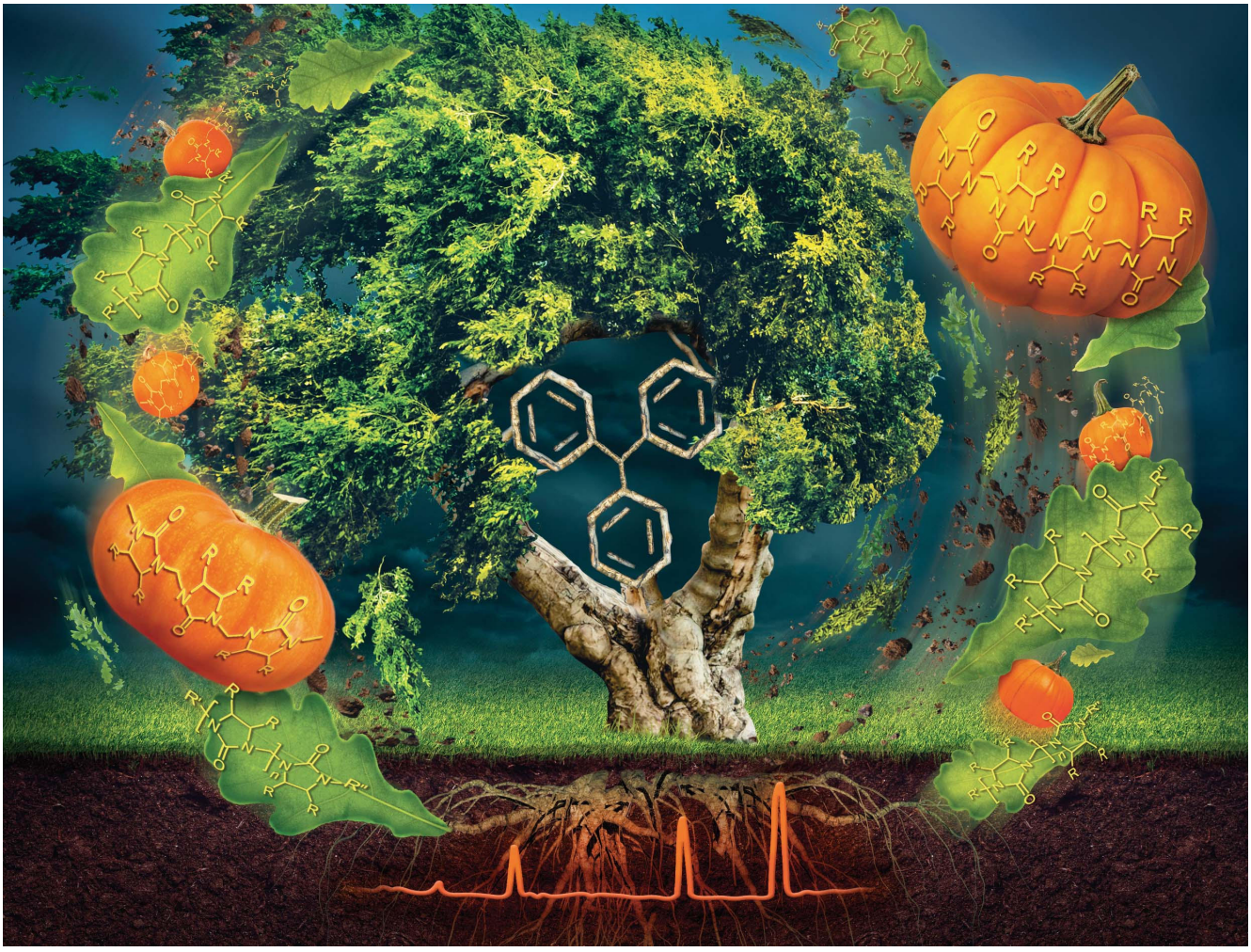

ISSN 2976-8683

ROYAL SOCIETY OF CHEMISTRY

PAPER

Riina Aav *et al.*

How reliable is internal standard method in monitoring mechanochemical synthesis? A case study of triphenylmethane in HPLC-UV-MS analysis of hemicucurbit[*n*]urils

RSC Mechanochemistry

ROYAL SOCIETY OF CHEMISTRY

PAPER

View Article Online
View Journal | View Issue

Cite this: *RSC Mechanochem.*, 2025, **2**, 507

How reliable is internal standard method in monitoring mechanochemical synthesis? A case study of triphenylmethane in HPLC-UV-MS analysis of hemicucurbit[*n*]urils†

Tatsiana Jarg, Jevgenija Tamm, Elina Suut-Tuule, Ketren-Marlein Lootus, Dzmitry Kananovich and Riina Aav *

Quantitative analysis of crude reaction mixtures is essential for the development of new synthetic methodologies and conducting mechanistic studies. While internal standard method is widely used for determining reaction yields in homogeneous solvent-based organic synthesis, its application in mechanochemical synthesis, which often involves heterogeneous mixtures, has not been properly validated. This study showcases applicability of triphenylmethane (TPM) as a solid internal standard in liquid-assisted, multi-component synthesis of homomeric cycHC[8] and mono-biotinylated mixHC[8] eight-membered cyclohexanohemicucurbit[*n*]urils. A fast and reliable HPLC-UV-MS analytical procedure was developed to determine yields by analyzing crude reaction mixtures, as a prerequisite of applying design-of-experiments optimisation approach. The influence of various parameters, including TPM concentration, reactant mixture weight, milling time, and the type and amount of liquid-assisted grinding additive, on the validity of the analysis was systematically studied. The results indicate that the primary challenge to trustworthy analysis arises from the non-uniform distribution of components. However, this issue can be detected with proper sampling and mitigated by optimising parameters to ensure uniform distribution of the internal standard throughout the reaction mixture. The results could be valuable for ensuring the credibility of *ex situ* and *in situ* analytical methods used to track the progress of mechanochemical reactions through single-point measurements.

Received 20th December 2024
Accepted 6th April 2025

DOI: 10.1039/d4mr00145a

rsc.li/RSCMechanochem

Introduction

Mechanochemical organic synthesis is gaining attention as a greener and more environmentally benign alternative to traditional synthesis in organic solvents.[1–3] Additionally, it enhances the reactivity of solids, leading to faster, higher-yielding, and more selective chemical reactions.[4,5] These benefits have led to the emergence and rapid growth of new advanced synthetic methods that rely on mechanochemical activation,[6,7] as well as a significant increase in their applications, including the synthesis of complex molecules such as pharmaceuticals,[8–13] functional materials,[14–17] supramolecules[18,19] and macrocyclic cavitands.[20–31] The development, optimisation, kinetic tracking, and mechanistic studies of mechanochemical reactions require a robust, widely accessible, and convenient analytical method for the rapid and reliable determination of product yields in the crude reaction mixtures. This is especially important when applying the design-of-experiments approach for rational screening and optimisation,[32] which is also a prerequisite for automation in future.[33]

Mechanochemical reactions can be conveniently monitored *in situ*[34,35] by powder X-ray diffraction (PXRD),[36] Raman,[37] X-ray absorption[38] and solid-state nuclear magnetic resonance (NMR)[39,40] spectroscopy, which provide valuable information on reactivity and real-time kinetics without interrupting the process. Quantitative PXRD monitoring with the addition of crystalline silicon, which addresses the issue of sample amount variation within the vessel, is a rare example of using the internal standard method for *in situ* analysis of mechanochemical reactions.[41]

However, the progress of mechanochemical reactions is prevalently followed by more accessible *ex situ* monitoring methods, such as NMR,[8,10,12,20–22,26,42] Fourier-transform infrared (FTIR)[8,20,24] and UV-vis[23,25,42] spectroscopies. While the application of these techniques is straightforward for analysing reactions that produce a single major component, reactions that yield complex mixtures may require additional chromatographic separation. For instance, high-performance liquid chromatography coupled with mass spectrometry (HPLC-MS) has been used for analysis of challenging systems.[13,26–28,30,31]

Department of Chemistry and Biotechnology, Tallinn University of Technology, Akadeemia tee 15, 12618 Tallinn, Estonia. E-mail: riina.aav@taltech.ee

† Electronic supplementary information (ESI) available. See DOI: https://doi.org/10.1039/d4mr00145a

In traditional solvent-based organic synthesis, an internal standard is often employed for quantitative analysis, typically using ^{1}H NMR spectroscopy.[43,44] The selection of the internal standard must meet certain criteria: it should be non-volatile, chemically inert, and uniformly distributed within the reaction medium. While uniform distribution is easily achieved in organic solvents, it is not guaranteed under mechanochemical conditions, where inhomogeneity and fluctuating multi-phase compositions are common. The effectiveness of mass transfer in these systems depends on the nature of the compounds as well as specific factors such as milling frequency and duration, the number and size of milling balls, the presence of liquid-assisted grinding (LAG) additives, and the degree of jar filling.[5] Although the issue of potential non-uniform distribution of the internal standard can be mitigated by homogenizing the entire reaction mixture during work-up, concerns about the reliability of the internal standard method remain when single-point sampling is involved. This challenge is particularly relevant in upscaled preparations and scenarios where samples are collected from the reaction mixture at regular intervals. In such cases, the trustworthiness of the method may be compromised. Additionally, some reactants, LAG additives, and products may be volatile, potentially altering the total mass of the reaction mixture and leading to inaccurate yield calculations. To the best of our knowledge, there have been no systematic studies validating the internal standard method in mechanochemistry for this type of measurements.

Here, we present a case study demonstrating the successful use of triphenylmethane (TPM) as a solid internal standard for the reliable determination of macrocyclic product yields from crude reaction mixtures (Fig. 1) obtained through a dynamic covalent chemistry approach. Cyclohexanohemicucurbit[*n*]urils (cycHC[*n*], $n = 6$ or 8) are the first examples of hemicucurbit[*n*]uril macrocycles[45] synthesized both in solution[46,47] and mechanochemically *via* ball-milling.[26] These cavitands form in a stepwise process, first producing linear oligomers by polycondensation of urea monomers with formaldehyde, followed by cyclisation of the oligomeric chains around a suitable anionic template. Thermodynamic equilibrium is reached during the aging of the reaction mixture at elevated temperatures, which enhances templation during macrocyclisation in the solid state.[26,31] Both steps are reversible and generate a diverse array of intermediates, resulting in a dynamic covalent library (DCL).[48] The number of produced species rapidly increases when distinct urea monomers are used, such as in the assembly of mono-biotinylated cyclohexanohemicucurbit[8]uril (mixHC[8]).[31] Additionally, the acid-catalysed condensation of urea monomers with formaldehyde produces water, leading to a fluctuating liquid-to-solid ratio (η, μl mg^{-1})[49] at the milling and aging stages, and sample preparation. In the synthesis of mixHC[8], the content of water resulting from LAG additive and condensation can make up to approximately 20% of reaction mixture by weight. The varying multi-phase, multi-component composition of the reaction mixture and the risks of uncontrollable water evaporation during aging at elevated temperatures pose significant challenges for analysis. We discovered that quantitative HPLC-UV-MS is more advantageous for analysing the DCL complexity compared to PXRD, FTIR, and NMR.

During the optimisation of the synthesis, we gathered a large dataset from over 100 reaction runs, which enabled us to pinpoint the conditions under which the internal standard method yields reliable results, as well as to identify conditions that could lead to erroneous single-point measurements due to non-uniform distribution of the internal standard. The reliability of the method was evaluated through assessments of stability, linearity, limits of detection (LoD) and quantitation (LoQ), accuracy, and reproducibility.

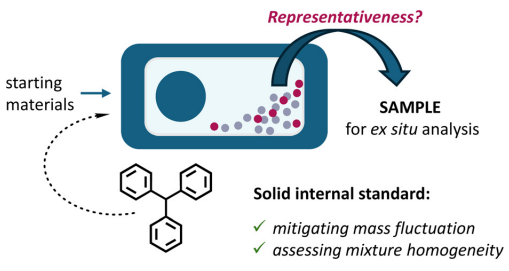

Fig. 1 Addition of a solid internal standard prior to milling to improve the representativeness of single-point samples for *ex situ* analysis, investigated in this work.

Experimental

Materials, reagents and solvents

All reagents were purchased from commercial suppliers. HPLC grade solvents (acetonitrile, isopropanol, absolute ethanol, chloroform stabilized with amylene) and LC-MS grade formic acid were procured from Thermo Fischer Scientific. The cycHC[*n*] used as the reference standards were synthesized in our laboratory according to the published procedures.[26,46,47] The purity of the macrocycles (90–98%) was determined by quantitative ^{1}H NMR.[50]

Mechanochemical synthesis of mixHC[8]

D-Biotin (46 mg, 0.19 mmol, 1 equiv.), (*R*,*R*)- or (*S*,*S*)-*N*,*N*′-cyclohexa-1,2-diylurea (183 mg, 1.30 mmol, 7 equiv.), paraformaldehyde (45 mg, 1.50 mmol, 8 equiv.) and triphenylmethane (5–15 mg, as internal standard for HPLC yield determination) were placed into a 14 mL ZrO_2 jar sleeved in aluminium and charged with two 10 mm ZrO_2 balls (*ca.* 3.5 g). The template and LAG additive consisting of aqueous acid or acid combined with the corresponding salt (0.56 mmol, 3 equiv.) was added to the mixture, which was then set to mill in a Form-Tech Scientific FTS-1000 shaker mill at 30 Hz for 1 h. Subsequently, the milling jar was sealed with parafilm and reaction mixture was aged in a VWR INCU-Line IL10 incubator at 60 °C for 24 h, and the resulting crude mixture was quenched with water and dried under air at room temperature. The sampling for HPLC-UV-MS analysis was performed after the aging step, before quenching; the amounts of starting materials

and reagents, as well as milling time and aging temperature varied during screening and optimisation experiments.[31]

PXRD

PXRD analysis was performed on Bruker D8 Advanced Diffractometer with Fe-filtered Co radiation and LynxEye detector, collecting data in the range of 2θ from 4 to 40°. The samples (*ca.* 38 mg) were mixed with absolute ethanol (2–3 drops) to form a paste, which was spread on a glass slide.

FTIR spectroscopy

The vibrational spectra were recorded on Bruker Tensor 27 FTIR spectrometer. The samples were prepared as KBr pellets (*ca.* 1.7 mg crude reaction mixture and *ca.* 125 mg KBr).

^{1}H NMR spectroscopy

^{1}H NMR spectra were acquired on 400 MHz Bruker Avance III spectrometer. The samples were prepared by dissolving *ca.* 20 mg of reaction mixture in 1 : 1 mixture of perdeuterated chloroform and methanol. All chemical shifts were reported in ppm units and referenced to tetramethylsilane (δ ^{1}H 0.00 ppm).

HPLC-UV-MS

HPLC-UV-MS analysis was carried out on Agilent 1200 Series System, comprising a G1322A degasser, low-pressure mixing G1311A quaternary pump, G1329A autosampler, G1316A thermostated column compartment, G1365B multi-wavelength detector, and a G6125B single quadrupole mass detector (mass accuracy ±0.13 Da) equipped with a multimode ion source. The chromatographic separation was performed on a Phenomenex Kinetex XB-C18 column (150 mm × 4.6 mm, 2.6 μm). Eluents A (water/0.1% formic acid) and B (acetonitrile/0.1% formic acid) were used in a 10-minute gradient from A : B 50 : 50 (v/v) to A : B 10 : 90 (v/v), followed by a 2-minute isocratic hold at A : B 10 : 90 (v/v). The composition then returned to A : B 50 : 50 (v/v) over 1 minute, with a 4-minute equilibration step. The flow rate was maintained at 0.75 mL min^{-1}. The column temperature was set at 30 °C and injection volume at 2 μL. UV-absorbance was monitored at 210 nm detection wavelength with a 4 nm bandwidth without a reference, using a standard 10 mm, 13 μL flowcell. The peaks were identified by electrospray ionisation mass spectrometry (ESI-MS) with the following spray chamber parameters: drying gas flow 5 L min^{-1}, drying gas temperature 300 °C, nebulizer pressure 60 psig, vaporizer temperature 150 °C, capillary voltage 2000 V and charging electrode voltage 2000 V. The mass spectra were acquired in positive ionisation mode within m/z 500–2000 range and fragmentor voltage 80 V.

Sample preparation

The crude reaction mixture (*ca.* 300 mg) distributed across the surface of the jar and milling balls was combined using a spatula, and random sampling was performed from different sections of the reaction vessel, providing minimum three *ca.* 1 mg probes. Each probe was dissolved in chloroform : isopropanol 1 : 1 (v/v) mixture to prepare a sample with a concentration *ca.* 1 mg mL^{-1}. The solution was then filtered through 0.2 μm PTFE membrane syringe filter to remove salt templates insoluble in organic solvents.

Calibration procedure

Stock solutions of mixHC[8], cycHC[8], cycHC[6] and TPM were prepared using Radwag MYA 11.4Y microbalances and calibrated automatic pipettes of 20–200 μL and 100–1000 μL volumes. Calibration solutions of known concentrations were prepared in three parallels by consequent dilution of three independent stock solutions, using chloroform : isopropanol 1 : 1 (v/v) mixture as the solvent. The concentration range varied from 0.9 mg mL^{-1} to LoD (see ESI† for more details).

The calibration graphs were constructed by plotting peak areas against the concentration. The obtained ten-point calibration curves for each compound were fitted using linear regression analysis, yielding linear equations ($y = kx$, with the intercept was set to 0) and corresponding R^2 values.

Determination of yields

The macrocyclic content was quantified *via* calibration graphs. The conversion of starting materials to products was determined as the ratio of urea monomers incorporated into the macrocycle (*i.e.*, the amount of macrocycle multiplied by the number of monomeric units) to the total monomer content, and expressed as the macrocycle yield. Formulae (1)–(6) were used to derive the final eqn (7) used for yield calculation:

$$\%\ \text{Yield} = \frac{n_{\text{HC}} \cdot N_{\text{mon}}}{n_{\text{st.mon}}} \times 100 \tag{1}$$

$$n_{\text{HC}} = \frac{m_{\text{RM}} \cdot \omega_{\text{HC,RM}}}{M_{\text{HC}}} \tag{2}$$

$$\omega_{\text{HC,RM}} = \omega_{\text{HC,CMA}} \cdot f = \frac{\omega_{\text{HC,CMA}} \cdot \omega_{\text{IS,RM}}}{\omega_{\text{IS,CMA}}} \tag{3}$$

$$\omega_{\text{HC,CMA}} = \omega_{\text{HC,S}} = \frac{c_{\text{HC}}}{c_{\text{S}}} = \frac{S_{\text{HC}} \cdot V_{\text{S}}}{k_{\text{HC}} \cdot m_{\text{S}}} \tag{4}$$

$$\omega_{\text{IS,CMA}} = \omega_{\text{IS,S}} = \frac{c_{\text{IS}}}{c_{\text{S}}} = \frac{S_{\text{IS}} \cdot V_{\text{S}}}{k_{\text{IS}} \cdot m_{\text{S}}} \tag{5}$$

$$\omega_{\text{IS,RM}} = \frac{m_{\text{IS}} \cdot P_{\text{IS}}}{m_{\text{RM}} \times 100} \tag{6}$$

$$\%\ \text{Yield} = \frac{S_{\text{HC}} \cdot k_{\text{IS}} \cdot m_{\text{IS}} \cdot P_{\text{IS}} \cdot N_{\text{mon}}}{S_{\text{IS}} \cdot k_{\text{HC}} \cdot M_{\text{HC}} \cdot n_{\text{st.mon}}} \tag{7}$$

where n_{HC} – the number of moles of the macrocycle, mmol; N_{mon} – number of monomeric units in the macrocycle; $n_{\text{st.mon}}$ – total number of moles of starting monomers (biotin and (*R*,*R*)-*N*,*N*′-cyclohexa-1,2-diylurea), mmol; m_{RM} – total mass of reactant mixture, including internal standard, mg; M_{HC} – molar weight of the macrocycle, g mol; $\omega_{\text{HC,RM}}$, $\omega_{\text{HC,CMA}}$ and $\omega_{\text{HC,S}}$ – theoretical mass fraction of the macrocycle relative to the reactant mixture (recalculated *via* internal standard), in the

crude mixture after aging and in the sample, respectively; $\omega_{IS,RM}$, $\omega_{IS,CMA}$ and $\omega_{IS,S}$ – mass fraction of the internal standard in the reactant mixture based on the weighed amount, in the crude mixture after aging and in the sample based on analysis; f – correction factor (the ratio of internal standard percentage in the reactant mixture to its percentage in the sample, which represents crude mixture after aging); c_S, c_{HC} and c_{IS} – concentrations of the crude mixture after aging, macrocycle and internal standard in the sample solution, respectively, mg mL; m_S – mass of the crude mixture after aging used in the sample preparation, mg; V_S – volume of the solvent mixture used in the sample preparation, mL; S_{HC} and S_{IS} – peak areas of the macrocycle and internal standard, respectively, mAU s; k_{HC} and k_{IS} – the slopes of the calibration curves for the macrocycle and internal standard, respectively, mAU s mL mg^{-1}; m_S – mass of aged crude mixture sample, mg; V_S – volume of solvent mixture used in the sample preparation, mL; m_{IS} – mass of internal standard, mg; P_{IS} – purity of internal standard, %. For more details, see ESI (Scheme S1).†

The analysis was performed in triplicate, and the HPLC yields were reported as the mean value ± standard deviation between parallel measurements.

Linearity, LoQ and LoD

Linearity was assessed based on the plots of residuals and LINEST analysis. LoQ and LoD were determined by signal-to-noise ratio (S/N) of 10 and 3, respectively.

Accuracy and reproducibility

The test solution of crude reaction mixture containing internal standard, was spiked with small additions of TPM and macrocycles. The method accuracy, which shows the closeness of the analysis result to the true value, was evaluated by recovery bias, which reflects the difference between experimentally found and theoretical concentration values (for more details, see ESI†). Method reproducibility was assessed for 2 × 9 independent samples collected from two crude reaction mixtures, based on relative standard deviation (RSD).

Results and discussion

Multi-component self-assembly of mixHC[8] in solid state leads to a particularly complex mixture containing two major products (mixHC[8] and cycHC[8]) along with numerous linear intermediates as well as other macrocyclic species[31] (Fig. 2). The crude reaction mixtures were analysed after milling and after aging by PXRD, FTIR and ^{1}H NMR methods. As reported previously,[26] PXRD technique was not applicable for *in situ* monitoring of mechanochemical synthesis of cycHC[n] due to amorphous nature of the reaction mixture and difficulties in maintaining the controlled reaction environment. *Ex situ* PXRD analysis of the starting materials used in mixHC[8] synthesis revealed some crystalline phases, nevertheless the milled crude mixture samples, as well as the aged product samples were amorphous, making this methodology not suitable for reaction monitoring (Fig. S1†). The application of other spectroscopic

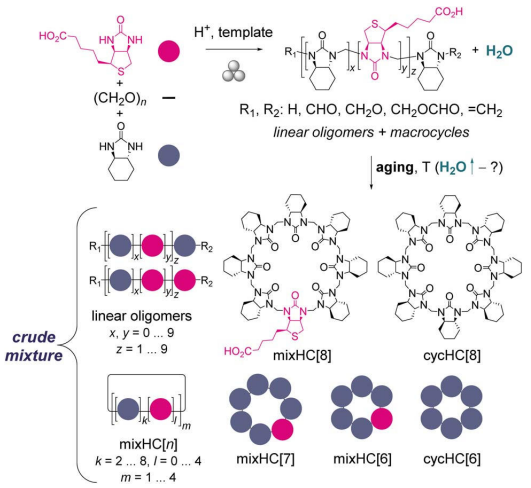

Fig. 2 General scheme of mixHC[8] synthesis in solid state, describing the composition of crude reaction mixture.

techniques, such as FTIR and UV spectroscopies, is also limited, as no significant changes appear between the vibrational spectra of starting monomers, intermediates and macrocycles (Fig. S2–S6†), and no characteristic UV bands occur upon the formation of different products.[50]

The large number of intermediates formed during the synthesis drastically complicate ^{1}H NMR spectra (Fig. S7–S11†), which undermines the application of conventional ^{1}H NMR for reliable data interpretation and quantitation. Therefore, employing a separation method, *e.g.* HPLC, appeared to be essential to ensure discrimination between the components. The individual analytes can be identified based on their retention times and using additional techniques such as MS.[26] In order to reliably determine yields, TPM was added as an inert solid internal standard to the mixture of reactants prior to milling. Importantly, the use of internal standard is advantageous since it allows to mitigate the problem of uncontrollable evaporation of water at the aging step and during subsequent manipulations with the sample.

Development of method for quantitative HPLC-UV analysis

Separation of mixHC[8] crude mixture components by HPLC-UV provided chromatograms suitable for quantification (Fig. 3A). ESI-MS analysis confirmed the formation of the two major macrocycles – mixHC[8] and cycHC[8], accompanied by minor by-products, found at trace levels under UV and MS detection: di-biotinylated mixHC[8], mixHC[7], mixHC[6], cycHC[6] (Fig. 3B, S12 and Table S1†). Generally, HPLC-UV chromatograms contained only peaks belonging to the macrocycles, as the linear oligomers have significantly lower UV-absorbance.[50]

The stability of sample solution was investigated in different solvent mixtures. The cycHC[n] macrocycles are most soluble in chlorinated solvents, such as chloroform, while biotin and biotin-containing oligomers prefer more polar solvents, such as

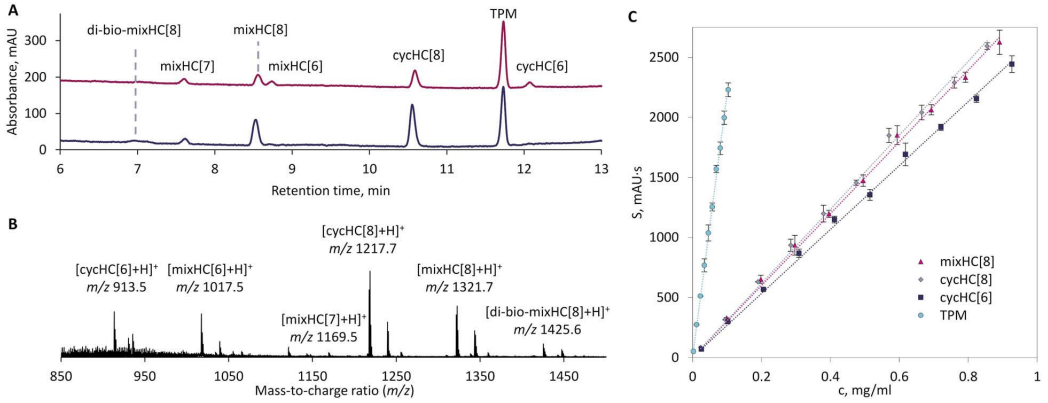

Fig. 3 (A) Representative HPLC-UV chromatograms of the crude reaction mixtures obtained in two separate experiments (detection at 210 nm); (B) (+)ESI-MS spectrum of the depicted chromatogram region used for peak identification; (C) calibration curves for determination of HPLC yields, the error bars represent standard deviation between triplicates.

methanol. Therefore, chloroform was mixed with an alcohol to ensure sample miscibility with an aqueous-based eluent. Since the mixHC[8] crude mixture contains strong mineral acid used in the synthesis ($HClO_4$ or HPF_6), the products and intermediates can still undergo dynamic interconversion in solution. Moreover, acidic medium initiates esterification[51] of biotin carboxylic group and affects sample stability. Esterification rate, however, depends on alcohol reactivity, for instance, isopropanol provides solutions stable for at least 24 h compared to methanol, where esterification occurs much faster (Table S2 and Fig. S13†).

Plotting peak areas against the corresponding concentrations of the macrocycles and internal standard confirmed linear dependency between their concentration and UV signal with correlation coefficients $R^2 > 0.995$ and random residuals throughout the range of method application (Fig. 3C, S14 and Table S3†). Previously reported quantitative HPLC-UV procedure described the UV-absorption properties of cycHC[*n*] homologues,[50] and based on the slopes of the calibration curves the new mono-biotinylated mixHC[8] exhibited a response nearly identical to that of cycHC[8]. Compared to the macrocycles, the TPM absorbance was found to be *ca.* 7 times stronger, which justifies using low amounts of internal standard. The developed HPLC-UV-MS method demonstrated sufficiently low LoQ and LoD, allowing for detection of minor macrocyclic products (*ca.* 1% w/w).

Distribution of internal standard during ball milling

TPM was selected as the internal standard due to its convenient solid form, prominent UV absorbance and chemical inertness under the reaction conditions. The latter was confirmed by ball milling of TPM and starting materials in the presence of HPF_6, resulting in (98.7 ± 0.5)% internal standard recovery upon analysis of the entire reaction mixture, which was quantitatively transferred into a 100 mL volumetric flask, dissolved in the solvent mixture and filtered (Fig. 4A and Table S4†).

However, the recovery values obtained *via* replicate triple-point sampling showed noticeable variation between different reaction runs and recovery bias values, mainly affected by the LAG additive and its nature (Fig. 4A and Table S4†). Neat grinding (NG) in the absence of acid prevented polycondensation and ensured permanent composition of solids upon mechanical mixing, resulting in (98.2 ± 0.4)% TPM recovery with low variation. The reaction with 60% aq. HPF_6

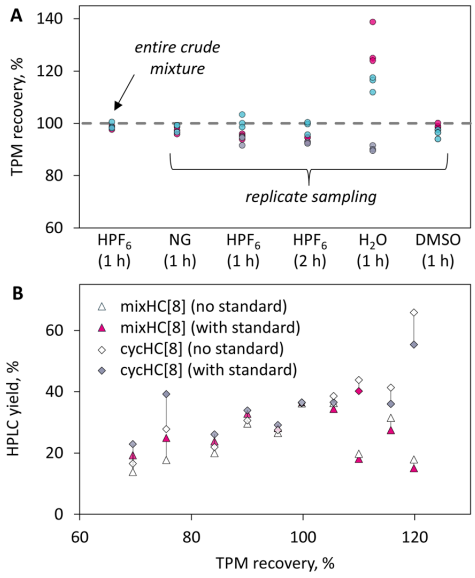

Fig. 4 (A) Recovery of the internal standard after ball milling 300 mg solids at 30 Hz under NG and LAG (60% aq. HPF_6, water or DMSO, $\eta = 0.2$ μL mg^{-1}) conditions; independent milling experiments are colour-coded, the points correspond to the replicate analyses; (B) the estimated error of yield determination using or neglecting the internal standard, indicated by filled and hollow markers, respectively.

provided (96 ± 4)% and (95 ± 3)% recoveries after 1 h and 2 h of milling, respectively, and noticeable variance between the parallels. The observed differences between reactions performed under identical conditions could point at the LAG effects on mixing efficiency. The experiment with addition of pure water instead of aqueous HPF_6 caused recovery bias up to 39% and large variation of the obtained TPM recovery values (112 ± 20)%. We hypothesised that the observed non-uniformity in the sample content could be caused by poor miscibility of hydrophobic internal standard and starting materials (except biotin) with water, that prevents proper homogenization during the milling. The latter was supported by replacing water with DMSO which can solubilize both the monomers and TPM. Indeed, DMSO as a LAG additive resulted in much better mixing and consequently smaller bias and variation of the recovery values (98 ± 2)%. In agreement with previous, the presence of aqueous acid induces protonation and higher polarity of solid surface, and therefore better mixing. However, the TPM recovery values observed during the yield determination of mixHC[8] and cycHC[8] macrocycles in the aged samples likely reflect uncontrollable water evaporation and absorption during milling, aging and sample preparation. In our study, these effects led to a change of up to 30% in the total mass of the reaction mixture (Fig. 4B). Consequently, the absence of an internal standard could produce misleading results.

The non-uniform distribution of the internal standard caused by inefficient mass transfer also results in erroneous analytical response. This prompted us to study how additional factors affect distribution of TPM in the reaction media. The explored variables included: (i) TPM loading (%, w/w), (ii) amount of LAG additive (60% aq. HPF_6, μL mg^{-1}), (iii) total mass of solid reactants and (iv) milling duration. Milling frequency (30 Hz) and number of balls (2 × 10 mm, *ca.* 3.5 g) were kept constant. Distribution of internal standard within the reaction mixtures was assessed based on relative standard deviation (RSD) of the TPM peak areas from the replicate measurements, RSD ≤ 5% was regarded as the acceptance criterion of sufficient homogeneity.

First, the data acquired from the reactions performed with variable amount of TPM (ranging from 1% to 4% w/w) showed no significant difference (RSD < 5%) in the distribution of the standard throughout the tested loading range (Fig. 5A and Table S5†). Second, the effect of the LAG agent loading was evaluated in the range of η = 0.15–1.15 μL mg^{-1} in 14 mL milling jars. As we showed before, the nature of LAG additive can cause adverse effects depending on the miscibility of LAG agent with solid components. In the case of mixHC[8] synthesis,[31] aqueous mineral acid, used as the catalyst and LAG additive, resulted in acceptably uniform distribution of the internal standard (RSD < 5%) at η < 0.5 μL mg^{-1} (Fig. 5B). However, higher η values resulted in increased inhomogeneity (RSD up to 10%, Fig. 5B and Table S6†). Third, the variable loading of the solids (range 280–390 mg) in 14 mL jar at η < 0.5 μl mg^{-1} kept distribution of the standard within the acceptable range(Fig. 5C, S15 and Table S6†). Finally, since mixing of solid reactants in mechanochemistry is time-dependent, the duration of milling was tested. Screening the milling times from 5 to 90 min resulted in uniform distribution of the internal standard in the aged mixtures (RSD < 5%, Fig. 5D and Table S7†), showing that homogeneity was achieved in rather short period of time. Overall, these results evidence that the nature of LAG agent and its loading have the most pronounced effect on the distribution of TMP among all studied parameters.

Distribution of products during ball milling

The distribution of the macrocyclic products in the crude mixtures followed the same trends observed for the internal standard (Fig. S16†), indicating that higher amount of LAG additive caused noticeable inhomogeneity. In such instances random replicate sampling from different points of the crude mixture is vital to increase reliability of the analysis. In addition, the data acquired during optimisation and screening experiments demonstrated that the distribution of the products is largely governed by the reaction outcome. Thus, ball-milling and aging performed under unfavourable conditions during optimisation in some cases resulted in poor yields, and

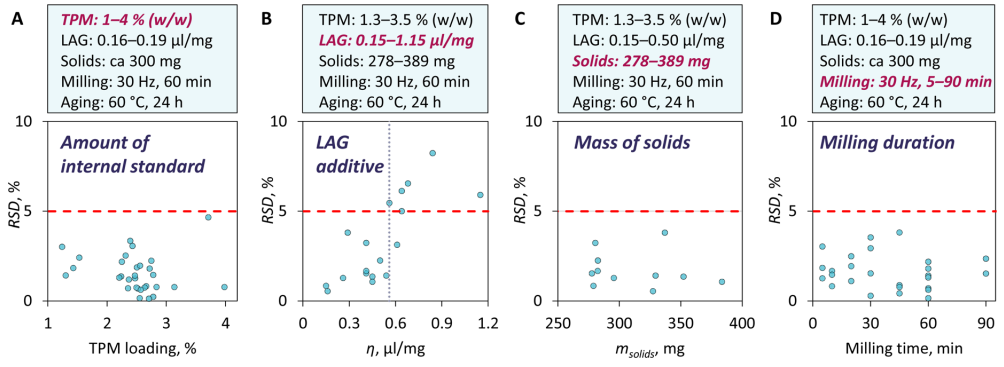

Fig. 5 Distribution of the internal standard across reaction mixture during milling depending on its concentration (A), LAG additive amount (B), mass of solid reactants (C) and milling duration (D), expressed as RSD of TPM peak areas acquired in triplicate measurements.

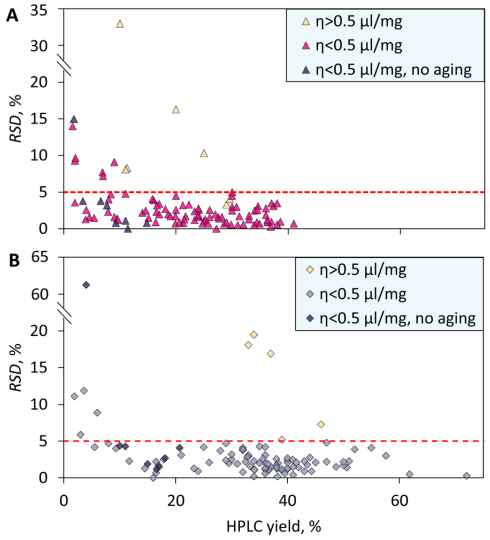

Fig. 6 Distribution of mixHC[8] (A) and cycHC[8] (B) in the crude mixtures under different reaction conditions, expressed as RSD of corresponding peak areas from replicate measurements ($n = 3$). For more details see Table S8.†

consequently higher variation of the replicate measurements (Fig. 6 and Table S8†).

The analysis of reactions carried out under optimal conditions prior to the aging step showcased the importance of the milling duration: the mixture milled for just 5 min afforded macrocycles in low yields with RSD values of 33% and 61% for mixHC[8] and cycHC[8], respectively (Fig. 6 and Table S8†). Noteworthy, the concentration of the internal standard was sufficiently uniform in all crude mixtures, with the exception of reactions with $\eta > 0.5$ μl mg^{-1} (Table S8†). These results show, that although 5 min mixing in a shaker mill was enough for the uniform distribution of the internal standard as a minor additive, it was not sufficient to homogenise other components of the mixture, which resulted in high RSD of yields across the reaction mixture. Therefore, analysing crude mixtures milled for a short period of time requires extra caution. Increasing the number of sampled probes can provide more reliable results.

Method accuracy was assessed based on spike recovery for TPM, mixHC[8] and cycHC[8] additions (Tables S9 and S10†). The bias did not exceed 2.7%, which was considered acceptable for the purpose of the current analysis.

Reproducibility studies were performed on two crude mixtures ball-milled and aged under optimal conditions *via* sampling 9 random probes from each vessel. The analysis resulted in *ca.* 1% standard deviation of the obtained yield values: (31 ± 1)% and (32 ± 1)% for mixHC[8] and cycHC[8], respectively. The RSD ($n = 9$) of the HPLC yield values satisfied the established 5% threshold (Table S11†). The variance of replicate measurements did not depend on additional mixing of the milling jar contents with a spatula prior to sampling.

Conclusions

In this study, we validated the use of TPM as an internal standard for determining yields in the mechanochemical synthesis of cyclohexanohemicucurbit[*n*]urils from a mixture of different urea monomers. This complex multicomponent reaction is characterised by the generation of numerous, interconvertible intermediates and products, the presence of an aqueous-based LAG additive poorly miscible with the starting materials, and a fluctuating liquid-to-solid ratio due to volatility of water. These factors pose significant challenges for chemical analysis, necessitating an efficient separation technique coupled with an internal standard for reliable yield determination.

To address these challenges, we developed a quantitative HPLC-UV-MS method using TPM as a solid internal standard to determine the yields of macrocyclic products from crude reaction mixtures. This method was further applied to optimise reaction conditions through a design-of-experiments approach.[31] The reliability of the method was confirmed through assessments of its linearity, accuracy, and reproducibility.

Importantly, we identified limitations in the internal standard methodology that could lead to erroneous yield values. These errors arose from the non-uniform distribution of the hydrophobic internal standard in the presence of an aqueous-based LAG agent. Our findings underscore the need to consider the miscibility of the internal standard with the LAG additive as a key selection criterion and highlight the importance of validating internal standard selection by ensuring its homogeneous distribution across the reaction mixture. In addition to reactions mediated by liquids, the solid internal standard approach may be utilized to access homogeneity of reaction mixtures performed under neat grinding conditions.

On the other hand, we found that the distribution of the internal standard was uniform (RSD < 5%) and was not significantly affected by its loading (1–4% w/w), the total mass of solids in the milling jars (280–390 mg), or the milling time (5–90 min). The macrocyclic products generally exhibited similar distribution trends to those of the internal standard, although reactions with low yields showed uneven product concentrations throughout the reaction vessel.

Given the potential for significant variability in component distribution depending on the reaction, any analytical method involving single-point measurements should be rigorously validated under mechanochemical conditions to ensure the credibility of the results. Uniform distribution across the reaction mixture should be verified through random replicate sampling, particularly for rapid reactions (<5 min) and systems with poorly miscible reactants that can lead to non-uniform reaction mixtures. Further studies on the application of the internal standard method for quantitative description of various mechanochemical processes will enhance understanding in the field.

Data availability

All experimental and characterization data and detailed experimental procedures are available in the published article and ESI.†

Author contributions

TJ: investigation, measurements, data collection, methodology, validation, analysis of results, writing – original draft; JT, EST, KML: investigation, data collection; DK: methodological advice, conceptualization, writing – review and editing; RA: supervision, methodology, conceptualization, writing – review and editing.

Conflicts of interest

The authors declare no conflicts of interest.

Acknowledgements

The research was funded by Estonian Research Council grant PRG2169, and by the Ministry of Education and Research through Centre of Excellence in Circular Economy for Strategic Mineral and Carbon Resources (01.01.2024–31.12.2030, TK228).

References

1 S. L. James, C. J. Adams, C. Bolm, D. Braga, P. Collier, T. Friščić, F. Grepioni, K. D. M. Harris, G. Hyett, W. Jones, A. Krebs, J. Mack, L. Maini, A. G. Orpen, I. P. Parkin, W. C. Shearouse, J. W. Steed and D. C. Waddell, *Chem. Soc. Rev.*, 2012, **41**, 413–447.
2 T. Friščić, C. Mottillo and H. M. Titi, *Angew. Chem., Int. Ed.*, 2020, **59**, 1018–1029.
3 R. T. O'Neill and R. Boulatov, *Nat. Rev. Chem*, 2021, **5**, 148–167.
4 G. A. Bowmaker, *Chem. Commun.*, 2013, **49**, 334–348.
5 J. L. Howard, Q. Cao and D. L. Browne, *Chem. Sci.*, 2018, **9**, 3080–3094.
6 K. Kubota, Y. Pang, A. Miura and H. Ito, *Science*, 2019, **366**, 1500–1504.
7 C. Patel, E. André-Joyaux, J. A. Leitch, X. M. de Irujo-Labalde, F. Ibba, J. Struijs, M. A. Ellwanger, R. Paton, D. L. Browne, G. Pupo, S. Aldridge, M. A. Hayward and V. Gouverneur, *Science*, 2023, **381**, 302–306.
8 D. E. Crawford, A. Porcheddu, A. S. McCalmont, F. Delogu, S. L. James and E. Colacino, *ACS Sustain. Chem. Eng.*, 2020, **8**, 12230–12238.
9 F. Puccetti, S. Lukin, K. Užarević, E. Colacino, I. Halasz, C. Bolm and J. G. Hernández, *Chem.–Eur. J.*, 2022, **28**, e202104409.
10 J. Gómez-Carpintero, C. Cabrero, J. D. Sánchez, J. F. González and J. C. Menéndez, *Green Chem. Lett. Rev.*, 2022, **15**, 638–645.
11 M. Lavayssiere and F. Lamaty, *Chem. Commun.*, 2023, **59**, 3439–3442.
12 R. Geib, E. Colacino and L. Gremaud, *ChemSusChem*, 2024, **17**, e202301921.
13 T. Nikonovich, T. Jarg, J. Martõnova, A. Kudrjašov, D. Merzhyievskyi, M. Kudrjašova, F. Gallou, R. Aav and D. Kananovich, *RSC Mechanochem.*, 2024, **1**, 189–195.
14 L. P. Jameson and S. V. Dzyuba, *Beilstein J. Org. Chem.*, 2013, **9**, 786–790.
15 M. Pérez-Venegas, T. Arbeloa, J. Bañuelos, I. López-Arbeloa, N. E. Lozoya-Pérez, B. Franco, H. M. Mora-Montes, J. L. Belmonte-Vázquez, C. I. Bautista-Hernández, E. Peña-Cabrera and E. Juaristi, *Eur. J. Org Chem.*, 2021, **2021**, 253–265.
16 T. Stolar and K. Užarević, *CrystEngComm*, 2020, **22**, 4511–4525.
17 E. M. Lloyd, J. R. Vakil, Y. Yao, N. R. Sottos and S. L. Craig, *J. Am. Chem. Soc.*, 2023, **145**, 751–768.
18 T. Friščić, *Chem. Soc. Rev.*, 2012, **41**, 3493.
19 A. Bose and P. Mal, *Beilstein J. Org. Chem.*, 2019, **15**, 881–900.
20 B. Içli, N. Christinat, J. Tönnemann, C. Schüttler, R. Scopelliti and K. Severin, *J. Am. Chem. Soc.*, 2009, **131**, 3154–3155.
21 M. Pascu, A. Ruggi, R. Scopelliti and K. Severin, *Chem. Commun.*, 2013, **49**, 45–47.
22 H.-T. Xi, T. Zhao, X.-Q. Sun, C.-B. Miao, T. Zong and Q. Meng, *RSC Adv.*, 2013, **3**, 691–694.
23 H. Shy, P. Mackin, A. S. Orvieto, D. Gharbharan, G. R. Peterson, N. Bampos and T. D. Hamilton, *Faraday Discuss.*, 2014, **170**, 59–69.
24 Y. Yang, F. Bu, J. Liu, I. Shakir and Y. Xu, *Chem. Commun.*, 2017, **53**, 7481–7484.
25 Q. Su and T. D. Hamilton, *Beilstein J. Org. Chem.*, 2019, **15**, 1149–1153.
26 S. Kaabel, R. S. Stein, M. Fomitšenko, I. Järving, T. Friščić and R. Aav, *Angew. Chem., Int. Ed.*, 2019, **58**, 6230–6234.
27 E. Oliva, D. Mathiron, S. Rigaud, E. Monflier, E. Sevin, H. Bricout, S. Tilloy, F. Gosselet, L. Fenart, V. Bonnet, S. Pilard and F. Djedaini-Pilard, *Biomolecules*, 2020, **10**, 339.
28 T. Dalidovich, K. A. Mishra, T. Shalima, M. Kudrjašova, D. G. Kananovich and R. Aav, *ACS Sustain. Chem. Eng.*, 2020, **8**, 15703–15715.
29 D. Langerreiter, M. A. Kostiainen, S. Kaabel and E. Anaya-Plaza, *Angew. Chem., Int. Ed.*, 2022, **61**, e202209033.
30 R. Gujjarappa, R. Khurana, N. Fridman, E. Keinan and O. Reany, *Cell Rep. Phys. Sci.*, 2024, 102011.
31 E. Suut-Tuule, T. Jarg, P. Tikker, K.-M. Lootus, J. Martõnova, R. Reitalu, L. Ustrnul, J. S. Ward, V. Rjabovs, K. Shubin, J. V. Nallaparaju, M. Vendelin, S. Preis, M. Öeren, K. Rissanen, D. Kananovich and R. Aav, *Cell Rep. Phys. Sci.*, 2024, 102161.
32 C. J. Taylor, A. Pomberger, K. C. Felton, R. Grainger, M. Barecka, T. W. Chamberlain, R. A. Bourne, C. N. Johnson and A. A. Lapkin, *Chem. Rev.*, 2023, **123**, 3089–3126.
33 A. Slattery, Z. Wen, P. Tenblad, J. Sanjosé-Orduna, D. Pintossi, T. den Hartog and T. Noël, *Science*, 2024, **383**, eadj1817.
34 S. Lukin, L. S. Germann, T. Friščić and I. Halasz, *Acc. Chem. Res.*, 2022, **55**, 1262–1277.
35 A. A. L. Michalchuk and F. Emmerling, *Angew. Chem., Int. Ed.*, 2022, **61**, e202117270.
36 I. Halasz, S. A. J. Kimber, P. J. Beldon, A. M. Belenguer, F. Adams, V. Honkimäki, R. C. Nightingale,

R. E. Dinnebier and T. Friščić, *Nat. Protoc.*, 2013, **8**, 1718–1729.
37 D. Gracin, V. Štrukil, T. Friščić, I. Halasz and K. Užarević, *Angew. Chem., Int. Ed.*, 2014, **53**, 6193–6197.
38 P. F. M. de Oliveira, A. A. L. Michalchuk, A. G. Buzanich, R. Bienert, R. M. Torresi, P. H. C. Camargo and F. Emmerling, *Chem. Commun.*, 2020, **56**, 10329–10332.
39 J. G. Schiffmann, F. Emmerling, I. C. B. Martins and L. Van Wüllen, *Solid State Nucl. Magn. Reson.*, 2020, **109**, 101687.
40 E. Bartalucci, C. Schumacher, L. Hendrickx, F. Puccetti, I. d'Anciães Almeida Silva, R. Dervişoğlu, R. Puttreddy, C. Bolm and T. Wiegand, *Chem.–Eur. J.*, 2023, **29**, e202203466.
41 I. Halasz, T. Friščić, S. A. J. Kimber, K. Užarević, A. Puškarić, C. Mottillo, P. Julien, V. Štrukil, V. Honkimäki and R. E. Dinnebier, *Faraday Discuss.*, 2014, **170**, 203–221.
42 D. Langerreiter, M. A. Kostiainen, S. Kaabel and E. Anaya-Plaza, *Angew. Chem., Int. Ed.*, 2022, **61**, e20220903.
43 S. Mahajan and I. P. Singh, *Magn. Reson. Chem.*, 2013, **51**, 76–81.
44 R. Muhamadejev, R. Melngaile, P. Paegle, I. Zibarte, M. Petrova, K. Jaudzems and J. Veliks, *J. Org. Chem.*, 2021, **86**, 3890–3896.
45 N. N. Andersen, M. Lisbjerg, K. Eriksen and M. Pittelkow, *Isr. J. Chem.*, 2018, **58**, 435–448.
46 R. Aav, E. Shmatova, I. Reile, M. Borissova and F. Topić, *Org. Lett.*, 2013, **15**, 3786–3789.
47 E. Prigorchenko, M. Öeren, S. Kaabel, M. Fomitšenko, I. Reile, I. Järving, T. Tamm, F. Topić, K. Rissanen and R. Aav, *Chem. Commun.*, 2015, **51**, 10921–10924.
48 S. Kaabel and R. Aav, *Isr. J. Chem.*, 2018, **58**, 296–313.
49 T. Friščić, S. L. Childs, S. A. A. Rizvi and W. Jones, *CrystEngComm*, 2009, **11**, 418–426.
50 M. Fomitšenko, A. Peterson, I. Reile, H. Cong, S. Kaabel, E. Prigorchenko, I. Järving and R. Aav, *New J. Chem.*, 2017, **41**, 2490–2497.
51 M. Lisbjerg, H. Valkenier, B. M. Jessen, H. Al-Kerdi, A. P. Davis and M. Pittelkow, *J. Am. Chem. Soc.*, 2015, **137**, 4948–4951.

Appendix 3

Publication III

E. Suut-Tuule, E. Schults, T. Jarg, J. Adamson, D. Kananovich, R. Aav. Scalable mechanochemical synthesis of biotin[6]uril. *ChemSusChem*, **2025**, e202402354.

.

ChemSusChem

Research Article
doi.org/10.1002/cssc.202402354

Chemistry Europe
European Chemical Societies Publishing

www.chemsuschem.org

Scalable Mechanochemical Synthesis of Biotin[6]uril

Elina Suut-Tuule,[a] Eve Schults,[a] Tatsiana Jarg,[a] Jasper Adamson,[b, c] Dzmitry Kananovich,[a] and Riina Aav*[a]

Biotin[6]uril, a chiral, water-soluble and anion binding macrocycle, is formed via dynamic covalent chemistry. In this study, we present a scalable and high-yielding synthesis of biotin[6]uril via a mechanochemical solid-state approach. The optimized protocol involves mechanical grinding of solid D-biotin with paraformaldehyde in the presence of 0.3 equivalents of 48% aqueous HBr, which functions as a catalyst, template, and liquid grinding additive. This mechanochemical process is carried out in a shaker or planetary mill, followed by aging at an elevated temperature to produce biotin[6]uril with an HPLC yield of up to 96%. The condensation and macrocyclization reaction was successfully scaled up 82-fold, producing nearly 20 g of biotin[6]uril with a high 92% isolated yield and 91% purity. Compared to conventional solution-based method, this mechanochemical approach offers several advantages, including significantly higher yields, shorter reaction times, enhanced scalability, simpler operational requirements, and substantially lower process mass intensity.

Introduction

Biotin[6]uril (B[6]U, Scheme 1) is a chiral macrocyclic cavitand from the cucurbituril family, first reported a decade ago by Pittelkow and co-workers.[1–4] The macrocycle consists of six D-biotin (vitamin B7) units linked through methylene bridges, forming a water-soluble receptor with a hydrophobic cavity (86–102 Å^3), which can slightly adapt its size while binding inorganic anions.[2] This property is characteristic of the hemicucurbit[*n*]uril family (HC[*n*], where $n=4$–12), which in general exhibits high affinity for electron-rich guests.[5–7] Bambus[6]urils, belonging to the same family of compounds, currently hold record in binding of anions like perchlorate and iodate with affinity close to $\log K_a=8$ in aqueous media.[8,9] Enantiopure cyclohexanohemicucurbit[8]uril (cycHC[8]), a cyclohexano-derivative of HC, can encapsulate beside anions also electron-rich heterocycles with up to $K_a=66\ M^{-1}$ affinity.[10] Moreover, cycHC[*n*] ($n=6$, 8) can bind electrophilic guests like metalloporphyrins outside the cavity through coordination to a urea carbonyl with total $\log K_{total}$ close to 9.[11] Supramolecular properties allow HCs to function as anion receptors,[4,12,13] transmembrane anion carriers,[3,14] components of supramolecular architectures suitable for chirality recognition,[15,16] and in environmental science applications, such as sensing and removing pollutants.[10,17] Biotin[6]uril with six carboxylate units in the side chain provides a convenient opportunity for tuning the properties of the parent macrocycle through derivatization, for instance esterification[3] or amide coupling.[18]

Like all HCs, bambus[*n*]urils, hetero-bambusurils and cycHC[*n*], B[6]U is prepared via a thermodynamically driven, anion-templated polycondensation reaction of urea monomers (D-biotin) with paraformaldehyde, catalyzed by a strong Brønsted acid.[1] The polycondensation occurs upon heating an aqueous acid solution, producing a dynamic covalent library of linear and cyclic oligomers. The counter anion of a strong Brønsted acid catalyst (typically, a mineral acid) serves as a template in the amplification of a single macrocyclic product formed during template-assisted self-organization. Although the macrocycle is formed in a single preparative step, the solvent-based protocol for B[6]U delivers moderate yields of 40–60%, is labor-intensive and generates hazardous waste, primarily due to the use of significant amount of strong mineral acids, making scale-up more challenging. For instance, the preparation of the B[6]U·HCl complex yields 48% after 2 days of heating at 60 °C in 7 M aqueous HCl, requiring 50 mL of strong acid to produce 0.5 g of material. The highest yield of 63% (135 mg) for B[6]U was obtained by heating in 3.5 M aqueous H_2SO_4 with 5 M NaBr as the templating agent.[1]

Currently, mechanochemical methods in organic synthesis are recognized as a greener and more sustainable alternative to traditional solvent-based methods.[19–28] Their advantages stem from drastically reduced solvent use and high reaction rates achieved at ambient temperatures, resulting in high conversions and yields in shorter reaction times. There is a limited number of macrocycles, that have been synthesized via ball milling[17,29–37] and the scale of these reactions remained below two grams of synthesized products. We have demonstrated the benefits of dynamic covalent chemistry via mechanochemistry in the preparation of cycHC[*n*]s ($n=6$, 8),[37] which proceeded in nearly quantitative yields and outperformed solvent-based

[a] Department of Chemistry and Biotechnology, Tallinn University of Technology, Tallinn, Estonia
[b] National Institute of Chemical Physics and Biophysics, Tallinn, Estonia
[c] Virumaa College School of Engineering, Tallinn University of Technology, Kohtla-Järve, Estonia

Correspondence: Riina Aav, Department of Chemistry and Biotechnology, Tallinn University of Technology, Akadeemia tee 15, Tallinn 12618, Estonia. Email: riina.aav@taltech.ee

Supporting Information for this article is available on the WWW under https://doi.org/10.1002/cssc.202402354

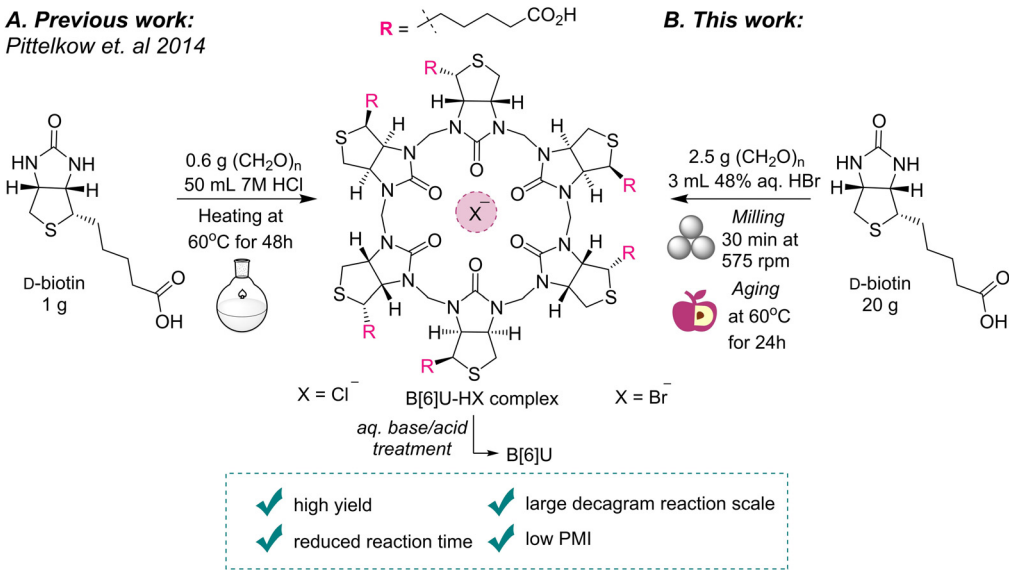

Scheme 1. (A) Synthesis of biotin[6]uril via a solvent-based approach (previous work)[1] and (B) via a mechanochemical method (this work).

methods.[38,39] This protocol also reduces environmental impact by avoiding organic solvents and lowering mineral acid consumption by a hundred times. This work was followed by mechanochemical synthesis of *thio*-analogs of cycHC[8] and unsubstituted *thio*-HC[6].[36] Recently, we further adapted this approach for the selective preparation of mono-biotinylated HC[8] from a mixture of two distinct urea monomers.[17]

Given our interest in developing new chiral supramolecular receptors, we sought an efficient protocol for synthesizing B[6]U in multigram quantities and focused on adapting the mechanochemical method for its preparation. Herein, we report a practical approach for the synthesis of B[6]U under solvent-free conditions using a shaker mill, followed by successful scale-up in a planetary mill, producing decagram quantities with HPLC yields up to 94%. In addition to higher yields and greater convenience, the mechanochemical method surpasses the solution-based approach in terms of environmental footprint, as demonstrated by green chemistry metrics.

Results and Discussion

Analogously to previous works,[17,36,37] the solid-state synthesis of B[6]U involved two steps: (i) generation of a dynamic covalent library of oligomers, achieved through a mechanochemical acid-catalyzed polycondensation of D-biotin monomer with paraformaldehyde in a shaker mill; and (ii) aging at 60 °C to promote template-assisted covalent self-assembly, yielding the macrocyclic product. Screening reactions were conducted on a 1 mmol scale (based on D-biotin) by milling the reactants in 15 mL ZrO_2-coated grinding jars for 1 h at 30 Hz using a single ZrO_2 milling ball. After milling, the solid reaction mixture was transferred to a capped glass vial and aged at 60 °C for several hours, followed by sampling of the solid reaction mixture repeated *n* times ($n = 2–3$) for HPLC analysis (see section 2 in the Supporting Information). HPLC yields were calculated based on calibration plots for B[6]U and triphenylmethane (TPM) as internal standard. Careful sampling and analysis helped to follow inhomogeneity of reaction mixtures, which is caused either by insufficient mixing of reagents or incomplete progress of condensation reaction.

During the optimization experiments, primary focus was on finding the best templating agent and the optimal aging duration, as the two key factors influencing the yield of the macrocycle. The milling duration was kept constant (1 h) and was selected to ensure the completion of the condensation reaction between paraformaldehyde and biotin, and homogenous distribution of templating agent.[17,37]

The selection of the anionic template is crucial, as it drives the self-assembly process and stabilizes the forming macrocycle. Anions with higher binding affinity typically serve as superior templates.[17,40] In the solution-based synthesis of B[6]U, chloride and bromide anions have been shown to be effective templates.[1] Under mechanochemical conditions (Figure 1A, Table S3), using 38% aq. HCl (0.5 equiv.) resulted in a 64% HPLC yield of B[6]U after 24 h aging, higher than the 48% achieved with the solution-based method. However, the best results in mechanochemical synthesis were obtained using 48% aq. HBr (91% HPLC yield), and reducing the amount of HBr to 0.3 equiv. further increased the yield to 95%. This result is consistent with the much higher binding constant of bromide ($K_a = 540\ M^{-1}$) compared to chloride ($K_a = 59\ M^{-1}$).[1] Interestingly, the influence of the template (Br^- vs Cl^-) on product yield is more pronounced in solid-state synthesis (>91% vs 64%)

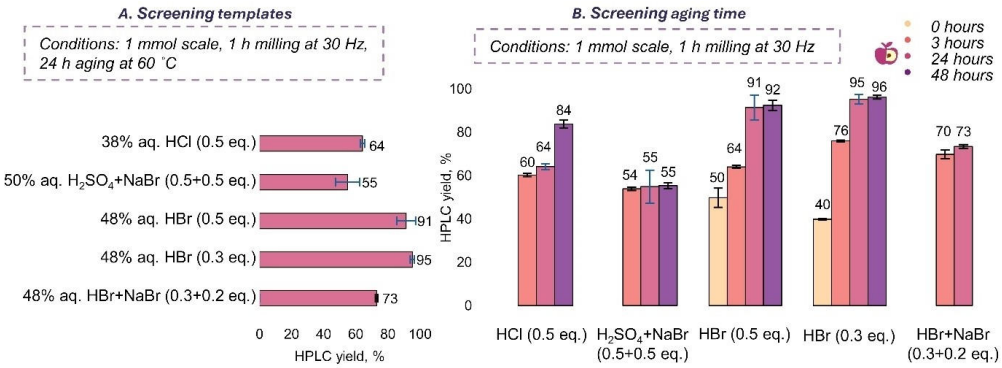

Figure 1. Screening different templates (**A**) and aging duration (**B**). General conditions: reaction scale 1 mmol of D-biotin, 60 min of milling at 30 Hz; A: aging at 60 °C for 24 h; B: aging at 60 °C for different durations. HPLC yields were determined by sampling the reaction mixture, containing triphenylmethane (TPM) as internal standard, *n* times ($n = 2–3$). Blue error bars express total error including within- and between-reaction variance, black error bars express standard deviation of replicate measurements. For details see sections 2.1–2.2 in Supporting Information.

than in the solution phase (63% vs 48%),[1] likely due to increased interaction with the templating anion in the concentrated reaction media, which is less obstructed by solvent molecules.[17,41] On the other hand, the combination of 50% aq. H_2SO_4 (0.5 equiv.) with NaBr (0.5 equiv.) produced only a 55% yield of B[6]U, and the combination of 48% aq. HBr with solid NaBr additive was similarly ineffective. It is important to add, that mechanochemical transformations under liquid-assisted grinding (LAG) conditions might be also very sensitive to changes in the amount and properties of LAG additive.[42,43] In B[6]U synthesis, the LAG additive was water from aqueous acid solutions and η value remained between 0.13–0.21 $\mu L \bullet mg^{-1}$. This variation is relatively small compared to the significant change in the templating media caused by the addition of NaBr salt and the sulfate anion, as the presence of either appears to hinder the self-assembly of B[6]U under these conditions.

To optimize aging time, different aging durations across all five selected templating agents were evaluated (Figure 1B, Table S4). Shortening the aging time from 24 h to 3 h consistently resulted in lower yields (54–76%), showing that insufficient aging leads to incomplete product formation. Increasing the aging time to 48 h generally improved yields, with HCl delivering a prominent increase from 64% to 84%. However, with the optimal template (0.3 equiv. HBr), the yield remained similar to the 24-hour aging time, indicating that the self-organization process for HBr template is faster, which coincides with higher affinity of B[6]U toward bromide.[1] Overall, 24 h of aging proved to be optimal for the HBr template, and aging was found to be essential for macrocycle formation. Without this step, milling alone resulted in a significant drop in HPLC yield to 40% leaving majority of reaction content in the form of linear oligomers with various lengths, which represent statistical mixture of dynamic covalent library members. These findings align with our previous work,[17,37] confirming that an additional aging stage is essential for optimal amplification of the templated macrocycle, helping to reduce the need for extensive purification from linear oligomers.

In summary, the most efficient conditions for B[6]U synthesis were identified as using 0.3 equiv. of 48% aq. HBr with 1 h of milling and 24 h of aging at 60 °C, yielding up to 95% B[6]U.

The next goal of our study was to scale up the developed process while maintaining high yields, with the ultimate aim of achieving multigram-scale synthesis of B[6]U. Upscaling mechanochemical reactions is often a challenging task, warranting a dedicated study separate from the development of the new method. To date, limited examples of large-scale organic mechanosynthesis processes (greater than 100 mmol) have been reported in the literature, most of which utilize continuous synthesis via twin-screw extrusion.[44–48] Moreover, according to our knowledge there are no upscaled mechanochemical methods for synthesis of macrocycles.[17,29–37]

We began upscaling in a shaker mill using the same 15 mL ZrO_2-coated grinding jars as in the experiments described above, while increasing jar loading and maintaining previously identified optimal conditions (Figure 2A, Table S5). Increasing the scale from 1 to 4 mmol resulted in a gradual decrease in HPLC yield, down to 84%. This trend is common and was also observed in our previous upscaling reactions in the same shaker mill,[49–51] as the same amount of mechanical energy is distributed across a larger quantity of reactants.

Since the instrument was already operating at its maximum milling frequency (30 Hz), the input of mechanical energy could only be increased by extending the milling duration beyond 1 h. However, based on previous work on condensation of paraformaldehyde with a mixture of cyclohexa-1,2-diylurea and D-biotin,[17] we assumed that conversion into linear oligomers is relatively fast, making the longer milling time unnecessary. Indeed, on the 4 mmol scale, we confirmed that milling for just 5 min produced B[6]U with an 82% yield after aging, virtually the same as the 84% yield obtained with 1 h of milling.

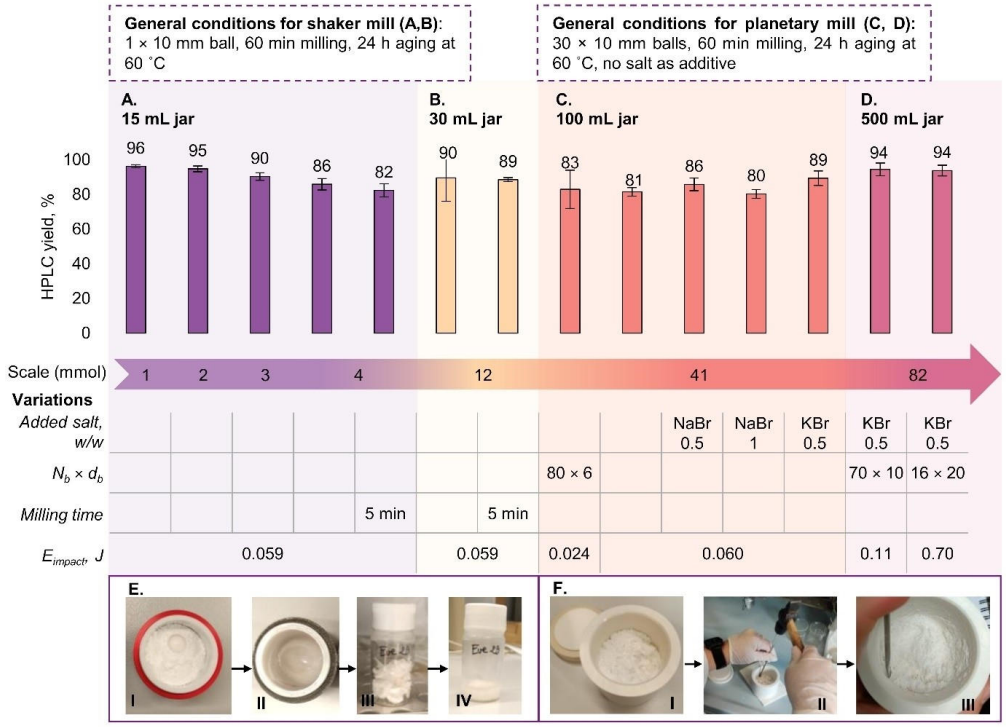

Figure 2. Scale-up reactions using 15 mL (**A**), 30 mL (**B**), 100 mL (**C**) and 500 mL (**D**) ZrO_2-milling jars. HPLC yields were determined via multiple sampling ($n = 3$–5) of the reaction mixture, which contained TPM as internal standard. The error bars show the standard deviation of replicate measurements. Used acronyms: N_b – number of balls, d_b – diameter of ball, added salt, w/w – loading of bromide salt (g) per 1 g of D-biotin. **E**: Photos of shaker mill experiments: (I) starting materials in a 30 mL milling jar; (II) reaction mixture after milling; (III) reaction mixture transferred in a sealed vial before aging; and (IV) aged reaction mixture; **F**: Photos of planetary mill experiments: (I) starting materials in a 100 mL milling jar; (II) milled and aged reaction mixture is cracked lose with a spatula and a hammer; (III) powdered reaction mixture.

Changes in the rheology of the reaction mixture at the larger scale were also observed. While the 1 mmol reactions produced readily flowing solid particles after milling, upscaled experiments resulted in a highly adhesive paste that coated the surfaces of the jars and milling balls, making it hard to remove from the milling vessel. After aging, the reaction mixture solidified into a tough chunk, that was difficult to break with a spatula (Figure 2E).

To further improve yield of B[6]U, 15 mL grinding jars were switched to larger 30 mL ones (Figure 2B, Table S5). This change resulted in nearly 90% HPLC yield in the tripled reaction scale (up to 12 mmol). Although the 12 mmol reactions showed a high average HPLC yield of 90%, there was considerable variation in the results of HPLC analysis (from 78% to 105%) of the samples collected from different sections of the reaction vessel, caused by inhomogeneity of the reaction mixture due to insufficient mixing of both the reagents and the internal standard. Such inhomogeneity problem was not observed at lower scales suggesting that sufficient milling is crucial.

To verify this hypothesis, we manually mixed the reactants (4 mmol scale) with a spatula in a glass vial, *avoiding any advanced mechanochemical treatment*, followed by 24 h of aging at 60 °C (Table S6). Surprisingly, the reaction proceeded well, yielding B[6]U with an average HPLC yield of 91%, although much higher variation in composition (from 75% to 100% HPLC yields) was found in comparison to the same scale shaker mill experiment (standard deviation $< 4\%$). To achieve a better homogeneity, we also tried grinding the reactants with a mortar and pestle for 5 min (Table S7). Homogeneous mixture was produced (standard deviation $< 1.6\%$), however this resulted in a lower average HPLC yield of 34% and incomplete conversion, likely due to the loss of volatile aqueous HBr in mortar under air. Based on these results, we suggest that the mechanical energy facilitates homogenization to enable uniform distribution of aqueous HBr as a catalyst and templating agent, while also accelerating the polycondensation reaction.

Further scaling in the shaker mill was limited by jar volume, restricting preparations to a maximum of approximately 3 g. Therefore, we sought to transfer our protocol into available in-house ND2L planetary mill (Torrey Hills Technologies), equipped with larger 100- and 500-mL ZrO_2-milling jars (Figure 2 C–D, Table S8).

The first experiments were performed in a 100-mL jar starting from 10 g of D-biotin (41 mmol), by using 80×6 mm

ZrO_2-milling balls at maximal available spinning rate (575 rpm for the milling jar and 285 rpm for a planetary disk), while keeping the reaction conditions same as in the shaker mill. This resulted in 83% average HPLC yield of B[6]U but with rather high standard deviation of 11%, indicating poor mixing. We found that the adhesive behaviour of the reaction mixture posed a significant problem in this case, as it caused the milling balls to stick together preventing proper mixing. Additionally, the dense paste formed after milling could not be transferred to another vessel, so the aging process was carried out in the same sealed milling jar. Using heavier 30×10 mm ZrO_2-milling balls resulted in a better homogeneity (standard deviation 2.5%), but did not increase the average HPLC yield. In order to change the reaction mixture rheology, we introduced a solid grinding additive (NaBr) that can also act as a templating agent promoting generation of B[6]U at the aging stage. It was known from Pittelkow's work that binding affinities of NaBr and KBr to B[6]U in heavy water are very similar ($K_a = 540\ M^{-1}$ and $K_a = 490\ M^{-1}$, respectively) with slight preference to sodium salt.[1] The grinding additive (0.5 g of NaBr per 1 g of D-biotin, w/w) changed the rheology from paste to rock-solid matter and slightly increased the HPLC yield to 86%. Although it did not prevent coalescence into a single chunk stuck to the surface of the milling jar and balls as we hoped. Further increase in the loading of NaBr from 0.5 to 1 w/w resulted in decreased HPLC yield of 80%, probably due to active template and catalyst dilution effect. However, we discovered that the addition of KBr instead of NaBr had a positive influence, slightly improving the HPLC yield up to 89%. This observation stays in line with previous results highlighting the importance of counter-ion paring in mechanochemistry.[52] It correlates with weaker crystal lattice energy of KBr compared to NaBr (672 and 736 $kJ \cdot mol^{-1}$, respectively),[53] which contributes more to the release of bromide as a template. Nevertheless, despite all the efforts, the outcomes were still consistently lower than 90–95% HPLC yields obtained in the shaker mill experiments.

Transitioning between different mechanochemical instruments is often problematic and can result in variable yields due to the influence of multiple instrument-dependent parameters, such as jar volumes and dimensions, the jar filling factor, and the size and weight of the milling balls.[25] The key challenge lies in understanding how these parameters affect reproducibility, and identifying the critical factors for consistent results. To rationally navigate through the selection of the key parameters, we calculated and analyzed the cumulative total energy feed and values of impact energies in our experiments by using the kinematic model developed by Lungerich and co-workers[54] (Figure 2, Table S9, E_{impact} values in J). Although the cumulative total energy (E_{total}) was consistently higher in the planetary mill experiments, it did not correlate directly with yields in our case. However, we observed that the impact energy values in the planetary mill with 6 mm balls ($E_{impact} = 0.024$ J) and 10 mm balls ($E_{impact} = 0.060$ J) were, respectively, lower or comparable to those in the shaker-mill ($E_{impact} = 0.059$ J, for the 15- and 30 mL jars). Using the Lungerich group's ball mill calculator,[54] we predicted that switching to 500 mL milling jars equipped with 10- and 20 mm ZrO_2 milling balls would enhance the impact energy, reaching values of 0.11 and 0.70 J, respectively. To our delight, this adjustment improved the reaction and led to an increased 94% HPLC yield, while scaling up to 82 mmol (20 g) of D-biotin. These findings demonstrate that even an approximate kinematic model, which does not account for the system's chemistry or rheology, can provide valuable guidance in selecting critical parameters when transitioning between different types of mechanochemical equipment. Given the fast reaction rate of the polycondensation observed in the shaker mill experiments and the high cumulative total energy input in the planetary mill, we surmised that the milling time could also be reduced to 30 min. This adjustment was incorporated into the final experimental protocol (see experimental part), which yielded the final product as an off-white powder in 92% isolated yield (19.3 g) and 91% purity (determined by qNMR analysis), after aqueous work-up, filtration, and drying.

The understanding of product impurities was enhanced by performing additional comprehensive HPLC-MS and NMR analyses, including ^1H, ^{13}C, HSQC, HMBC and DOSY experiments (sections 5 and 6 in Supporting Information). B[6]U obtained in either solution or solid state contained minor amounts of diastereomeric B[6]Us and linear oligomers. The ratio of the two diastereomers was determined to be 96:4 and 97:3 for solution- and mechanochemical syntheses, respectively. The latter confirmed that the mechanochemical process is highly stereoselective and dynamic covalent chemistry of mechanosynthesis closely matches that of the solvent-based approach.

To demonstrate advantages of mechanochemistry through green chemistry metrics, analysis was performed by using CHEM21 approach (Table 1, section 7 in Supporting Information).[55] First, reaction mass efficiency (RME) was better for the mechanochemical reactions due to higher yields and stoichiometric loading of paraformaldehyde over excess in the solution-based method. Comparison of process mass intensity (PMI) values shows that mechanochemical synthesis outperforms solution synthesis at the same 1 g scale, primarily due to higher yields and the absence of reaction solvents. Notably, the reaction PMI exhibited a nearly 60-fold reduction (from 123 to 2). Despite no significant changes to the original isolation and purification method was introduced, the mechanochemical

Table 1. Comparing green metrics of solution-based synthesis with the developed mechanochemical procedures.

	Solution (1 g scale)	**Shaker mill** (1 g scale)	**Planetary mill** (20 g scale)
Isolated yield[a]	45% (0.5 g)	75% (0.8 g)	92% (19.3 g)
RME	29	58	78
PMI total	851	308	87
PMI reaction	123	2	2
PMI work-up	728	306	85
Purity by qNMR	95%	82%	91%

[a] Yields corrected with the reference to purity: Yieldcorr = Yield · Purity / 100 are 43%, 62%, 84% for solution, shaker mill and planetary mill synthesis, respectively

protocol reduced the work-up PMI from 728 to 306, since dilution with water was not necessary to precipitate the product.[1] As expected, scaling up to 20 g further improved the yield by enhancing overall efficiency and reducing material losses during isolation and work-up, with a PMI reduction to 85, due to lower work-up solvent consumption. Additionally, no significant heat release or pressure increase was observed in large-scale experiments, indicating no major thermal or safety risks.

Conclusions

In conclusion, we have developed a practical method for the preparation of biotin[6]uril with a high yield by leveraging the advantages of mechanochemical solid-state synthesis. Notably, this work represents the first mechanochemical preparation of a macrocycle in decagram quantities. The optimized protocol involves mixing solid D-biotin with paraformaldehyde (1 equiv.) in the presence of a liquid templating agent, 48% aqueous HBr (0.3 equiv.), in a shaker or planetary mill, followed by aging at 60 °C for 24 h. The reaction was successfully scaled up 82-fold, enabling the synthesis of up to 19.3 g of product with high 92% isolated yield and 91% purity. Additionally, energy calculations using Lungerich's kinematic model provided valuable guidance for transitioning from a shaker to a planetary mill while maintaining the high HPLC yields. This mechanochemical approach offers significant advantages over the conventional solution-based method, including higher yields, a reduction in reaction time (from 48 to 24 h), the ability to scale up significantly, more straightforward operations, and a remarkable lower process mass intensity.

Experimental Section

Procedure for biotin[6]uril synthesis: D-Biotin (20 g, 82 mmol), paraformaldehyde (2.5 g, 82 mmol, 1 equiv.), potassium bromide (10 g, 84 mmol), and 48% aq. HBr (3 mL, 27 mmol, 0.3 equiv.) were placed into a 500 mL ZrO_2-coated milling jar, charged with 70×10 mm ZrO_2 milling balls. The mixture was set to mill for 30 min at a maximum rotation speed (milling jar angular speed $\omega_j = 575$ rpm; planetary disk angular speed $\omega_p = 285$ rpm, with a single rotation direction change after 15 min). The milling jar was sealed with parafilm and placed in an incubator for aging at 60 °C for 24 h. After aging, the reaction mixture solidified. The solid was cautiously cracked using a spatula struck with a hammer to release the stuck milling balls, and the material was then milled at a maximum rotation speed for 1–2 min. The resulting pulverized material was transferred onto a glass filter, washed with distilled water (4×100 mL) and dried. The obtained solid was dissolved in 10% aq. NaOH (250 mL) at stirring, the solution was placed in an ice bath, and conc. H_2SO_4 (15 mL) was slowly added at stirring until the pH 2–3. White solid precipitated, which was further filtered, washed with water (4×200 mL), dried in air and then under reduced pressure. Purity of B[6]U in the obtained solid (19.3 g, 92% to theoretical mass) was determined by qNMR as 91% (w/w), which corresponds to 84% yield. Determined diastereomeric puriti (97:3) and other analytical data for the obtained product are in accordance with previously reported for biotin[6]uril (See Supporting Information).

Supporting Information

Supporting information includes equipment specific parameters, experimental data, and green chemistry metrics calculations.

Acknowledgments

The authors would like to thank Peeter Loomägi and LaboBalt OÜ for their in-kind contribution of the ND2L planetary mill (Torrey Hills Technologies) and its accessories, and Jevgenija Tamm for her assistance during manuscript preparation. Authors thank Estonian Research Council grants PRG2169 and PSG400, Ministry of Education and Research through Centre of Excellence in Circular Economy for Strategic Mineral and Carbon Resources SOURCES (01.01.2024–31.12.2030, TK228) and the project „Increasing the knowledge intensity of Ida-Viru entrepreneurship" co-funded by the European Union for funding.

Conflict of Interests

The authors declare no conflict of interest.

Data Availability Statement

The data that support the findings of this study are available in the supplementary material of this article.

Keywords: mechanochemistry · ball milling · template synthesis · macrocycles · green chemistry

[1] M. Lisbjerg, B. M. Jessen, B. Rasmussen, B. E. Nielsen, A. Ø Madsen, M. Pittelkow, *Chem. Sci.* **2014**, *5*, 2647–2650.
[2] M. Lisbjerg, B. E. Nielsen, B. O. Milhøj, S. P. A. Sauer, M. Pittelkow, *Org. Biomol. Chem.* **2015**, *13*, 369–373.
[3] M. Lisbjerg, H. Valkenier, B. M. Jessen, H. Al-Kerdi, A. P. Davis, M. Pittelkow, *J. Am. Chem. Soc.* **2015**, *137*, 4948–4951.
[4] N. N. Andersen, K. Eriksen, M. Lisbjerg, M. E. Ottesen, B. O. Milhøj, S. P. A. Sauer, M. Pittelkow, *J. Org. Chem.* **2019**, *84*, 2577–2584.
[5] N. N. Andersen, M. Lisbjerg, K. Eriksen, M. Pittelkow, *Isr. J. Chem.* **2018**, *58*, 435–448.
[6] T. Lizal, V. Sindelar, *Isr. J. Chem.* **2018**, *58*, 326–333.
[7] O. Reany, A. Mohite, E. Keinan, *Isr. J. Chem.* **2018**, *58*, 449–460.
[8] T. Fiala, K. Sleziakova, K. Marsalek, K. Salvadori, V. Sindelar, *J. Org. Chem.* **2018**, *83*, 1903–1912.
[9] C. Rando, J. Vázquez, J. Sokolov, Z. Kokan, M. Nečas, V. Šindelář, *Angew. Chem. Int. Ed.* **2022**, *61*, e202210184..
[10] T. Shalima, K. A. Mishra, S. Kaabel, L. Ustrnul, S. Bartkova, K. Tõnsuaadu, I. Heinmaa, R. Aav, *Front. Chem.* **2021**, *9*.
[11] L. Ustrnul, S. Kaabel, T. Burankova, J. Martõnova, J. Adamson, N. Konrad, P. Burk, V. Borovkov, R. Aav, *Chem. Commun.* **2019**, *55*, 14434–14437.

[12] R. Khurana, F. Alami, C. A. Nijhuis, E. Keinan, J. Huskens, O. Reany, *Chem. - Eur. J.* **2024**, *30*, e202302968.
[13] O. Reany, M. Romero-Ruiz, R. Khurana, P. Mondal, E. Keinan, H. Bayley, *Angew. Chem. Int. Ed.* **2024**, *63*, e202406719.
[14] H. Valkenier, O. Akrawi, P. Jurček, K. Sleziaková, T. Lízal, K. Bartik, V. Šindelář, *Chem* **2019**, *5*, 429–444.
[15] G. Magna, M. Šakarašvili, M. Stefanelli, G. Giancane, S. Bettini, L. Valli, L. Ustrnul, V. Borovkov, R. Aav, D. Monti, C. Di Natale, R. Paolesse, *ACS Appl. Mater. Interfaces* **2023**, *15*, 30674–30683.
[16] Z. Anfar, B. Kuppan, A. Scalabre, R. Nag, E. Pouget, S. Nlate, G. Magna, I. Di Filippo, D. Monti, M. L. Naitana, M. Stefanelli, T. Nikonovich, V. Borovkov, R. Aav, R. Paolesse, R. Oda, *J. Phys. Chem. B* **2024**, *128*, 1550–1556.
[17] E. Suut-Tuule, T. Jarg, P. Tikker, K.-M. Lootus, J. Martõnova, R. Reitalu, L. Ustrnul, J. S. Ward, V. Rjabovs, K. Shubin, J. V. Nallaparaju, M. Vendelin, S. Preis, M. Öeren, K. Rissanen, D. Kananovich, R. Aav, *Cell Rep.* **2024**, *5*, 102161.
[18] T. Dalidovich, K. A. Mishra, T. Shalima, M. Kudrjašova, D. G. Kananovich, R. Aav, *ACS Sustainable Chem. Eng.* **2020**, *8*, 15703–15715.
[19] L. Konnert, A. Gauliard, F. Lamaty, J. Martinez, E. Colacino, *ACS Sustainable Chem. Eng.* **2013**, *1*, 1186–1191.
[20] O. Galant, G. Cerfeda, A. S. McCalmont, S. L. James, A. Porcheddu, F. Delogu, D. E. Crawford, E. Colacino, S. Spatari, *ACS Sustainable Chem. Eng.* **2022**, *10*, 1430–1439.
[21] J. Alić, M.-C. Schlegel, F. Emmerling, T. Stolar, *Angew. Chem. Int. Ed.* **2024**, *63*, e202414745.
[22] K. J. Ardila-Fierro, J. G. Hernández, *ChemSusChem* **2021**, *14*, 2145–2162.
[23] F. Cuccu, L. De Luca, F. Delogu, E. Colacino, N. Solin, R. Mocci, A. Porcheddu, *ChemSusChem* **2022**, *15*, e202200362.
[24] T. Friščić, C. Mottillo, H. M. Titi, *Angew. Chem.* **2020**, *132*, 1030–1041.
[25] J. L. Howard, Q. Cao, D. L. Browne, *Chem. Sci.* **2018**, *9*, 3080–3094.
[26] E. Juaristi, C. G. Avila-Ortiz, *Synthesis* **2023**, *55*, 2439–2459.
[27] J. L. Atwood, M. J. Hardie, C. L. Raston, C. A. Sandoval, *Org. Lett.* **1999**, *1*, 1523–1526.
[28] J. Antesberger, G. W. V. Cave, M. C. Ferrarelli, M. W. Heaven, C. L. Raston, J. L. Atwood, *Chem. Commun.* **2005**, 892–894.
[29] M. Pascu, A. Ruggi, R. Scopelliti, K. Severin, *Chem. Commun.* **2012**, *49*, 45–47.
[30] H. Shy, P. Mackin, A. S. Orvieto, D. Gharbharan, G. R. Peterson, N. Bampos, T. D. Hamilton, *Faraday Discuss.* **2014**, *170*, 59–69.
[31] Q. Su, T. D. Hamilton, *Beilstein J. Org. Chem.* **2019**, *15*, 1149–1153.
[32] D. Langerreiter, M. A. Kostiainen, S. Kaabel, E. Anaya-Plaza, *Angew. Chem. Int. Ed.* **2022**, *61*, e202209033.
[33] A. Dorniak, M. Haas, O. Brüggemann, I. Teasdale, W. Schöfberger, *J. Porphyrins Phthalocyanines* **2022**, *26*, 84–89.
[34] S. Santra, D. S. Kopchuk, I. S. Kovalev, G. V. Zyryanov, A. Majee, V. N. Charushin, O. N. Chupakhin, *Green Chem.* **2016**, *18*, 423–426.
[35] H.-T. Xi, T. Zhao, X.-Q. Sun, C.-B. Miao, T. Zong, Q. Meng, *RSC Adv.* **2012**, *3*, 691–694.
[36] R. Gujjarappa, R. Khurana, N. Fridman, E. Keinan, O. Reany, *Cell Rep.* **2024**, *5*, 102011.
[37] S. Kaabel, R. S. Stein, M. Fomitšenko, I. Järving, T. Friščić, R. Aav, *Angew. Chem. Int. Ed.* **2019**, *58*, 6230–6234.
[38] R. Aav, E. Shmatova, I. Reile, M. Borissova, F. Topić, K. Rissanen, *Org. Lett.* **2013**, *15*, 3786–3789.
[39] E. Prigorchenko, M. Öeren, S. Kaabel, M. Fomitšenko, I. Reile, I. Järving, T. Tamm, F. Topić, K. Rissanen, R. Aav, *Chem. Commun.* **2015**, *51*, 10921–10924.
[40] S. Kaabel, R. Aav, *Isr. J. Chem.* **2018**, *58*, 296–313.
[41] T. Kwon, B. Song, K. W. Nam, J. F. Stoddart, *J. Am. Chem. Soc.* **2022**, *144*, 12595–12601.
[42] A. M. Belenguer, G. I. Lampronti, N. De Mitri, M. Driver, C. A. Hunter, J. K. M. Sanders, *J. Am. Chem. Soc.* **2018**, *140*, 17051–17059.
[43] T. Friščić, S. L. Childs, S. A. A. Rizvi, W. Jones, *CrystEngComm* **2009**, *11*, 418–426.
[44] J. F. Reynes, V. Isoni, F. García, *Angew. Chem. Int. Ed.* **2023**, *62*, e202300819.
[45] D. E. Crawford, A. Porcheddu, A. S. McCalmont, F. Delogu, S. L. James, E. Colacino, *ACS Sustainable Chem. Eng.* **2020**, *8*, 12230–12238.
[46] R. Geib, E. Colacino, L. Gremaud, *ChemSusChem* **2024**, *17*, e202301921.
[47] R. S. Atapalkar, A. A. Kulkarni, *Chem. Commun.* **2023**, *59*, 9231–9234.
[48] R. R. A. Bolt, H. R. Smallman, J. A. Leitch, G. W. Bluck, F. Barreteau, A. V. Iosub, D. Constable, O. Dapremont, P. Richardson, D. L. Browne, *Angew. Chem. Int. Ed.* **2024**, *63*, e202408315.
[49] T. Dalidovich, J. V. Nallaparaju, T. Shalima, R. Aav, D. G. Kananovich, *ChemSusChem* **2022**, *15*, e202102286.
[50] J. V. Nallaparaju, R. Satsi, D. Merzhyievskyi, T. Jarg, R. Aav, D. G. Kananovich, *Angew. Chem. Int. Ed.* **2024**, *63*, e202319449.
[51] J. Varma Nallaparaju, T. Nikonovich, T. Jarg, D. Merzhyievskyi, R. Aav, D. G. Kananovich, *Angew. Chem. Int. Ed.* **2023**, *62*, e202305775.
[52] J. Andersen, J. Mack, *Green Chem.* **2018**, *20*, 1435–1443.
[53] J. E. Huheey, E. A. Keiter, R. L. Keiter, *Inorganic Chemistry: Principles of Structure and Rectivity*, HarperCollins College Publishers, Page 107, **1993**.
[54] O. F. Jafter, S. Lee, J. Park, C. Cabanetos, D. Lungerich, *Angew. Chem. Int. Ed.* **2024**, *63*, e202409731.
[55] C. R. McElroy, A. Constantinou, L. C. Jones, L. Summerton, J. H. Clark, *Green Chem.* **2015**, *17*, 3111–3121.

Manuscript received: October 31, 2024
Revised manuscript received: December 13, 2024
Accepted manuscript online: January 2, 2025
Version of record online: January 16, 2025

Curriculum vitae

Personal data

Name: Elina Suut-Tuule (Suut)
Date of birth: 11.02.1998
Place of birth: Tallinn, Estonia
Citizenship: Estonian

Contact data

E-mail: elina.suut@gmail.com

Education

2022–2026	Tallinn University of Technology, Chemistry and Biotechnology, PhD
2020–2022	Tallinn University of Technology, Applied Chemistry and Biotechnology, MSc (*cum laude*)
2017–2020	Tallinn University of Technology, Applied Chemistry, Food and Gene Technology, BSc (*cum laude*)
2014–2017	Pärnu Koidula Gymnasium, High school (silver medal)

Language competence

Estonian	native
English	fluent

Professional employment

2022–…	Tallinn University of Technology, School of Science, Department of Chemistry and Biotechnology, early-stage researcher

Honours and rewards

2026	Neo Performance Materials scholarship (The TalTech Development Fund, Estonia)
2024	Summer School on Organic Synthesis under Non-Classical Conditions Third Poster Prize, Warsaw, Poland
2022	Cambrex Tallinn Master Study Scholarship (The TalTech Development Fund, Estonia)

Supervised theses

2026	Eve Schults, MSc. *Mechanochemical methods for the synthesis of macrocycles and their intermediates* (Tallinn University of Technology, Department of Chemistry and Biotechnology)
2025	Julia Tkatšenko, BSc. *Mechanochemical defluorination of organic compounds* (Tallinn University of Technology, Department of Chemistry and Biotechnology)
2024	Eve Schults, BSc. *Biotin[6]uril mechanochemical synthesis* (Tallinn University of Technology, Department of Chemistry and Biotechnology)

Teaching experience

Spring 2025 and 2026	Analytical chemistry, practice and exercise tutorials (undergraduate course)
Fall 2023	Physical Organic Chemistry, exercise tutorials (graduate course)

Elulookirjeldus

Isikuandmed

Nimi: Elina Suut-Tuule (Suut)
Sünniaeg: 11.02.1998
Sünnikoht: Tallinn, Eesti
Kodakondsus: Eesti

Kontaktandmed

E-post: elina.suut@gmail.com

Hariduskäik

2022–2026	Tallinna Tehnikaülikool, Keemia ja biotehnoloogia, PhD
2020–2022	Tallinna Tehnikaülikool, Rakenduskeemia ja biotehnoloogia, MSc (*cum laude*)
2017–2020	Tallinna Tehnikaülikool, Rakenduskeemia, toidu- ja geenitehnoloogia, BSc (*cum laude*)
2014–2017	Pärnu Koidula Gümnaasium, keskharidus (hõbemedal)

Keelteoskus

Eesti	emakeel
Inglise	kõrgtase

Teenistuskäik

2022–…	Tallinna Tehnikaülikool, Loodusteaduskond, Keemia ja biotehnoloogia instituut, nooremteadur

Teaduspreemiad ja tunnustused

2026	Neo Performance Materials stipendium (TalTech Arengufond, Eesti)
2024	Suvekool “Organic Synthesis under Non-Classical Conditions” posterettekande auhind, Varssavi, Poola
2022	Cambrex Tallinn magistriõppe stipendium (TalTech Arengufond, Eesti)

Juhendatud lõputööd

2026	Eve Schults, MSc. *Mehhanokeemilised meetodid makrotsüklite ja nende vaheühendite sünteesiks* (Tallinna Tehnikaülikool, Keemia ja biotehnoloogia instituut)
2025	Julia Tkatšenko, BSc. *Orgaaniliste ühendite mehhanokeemiline defluorineerimine* (Tallinna Tehnikaülikool, Keemia ja biotehnoloogia instituut)
2024	Eve Schults, BSc. *Biotiin[6]uriili mehhanokeemiline süntees* (Tallinna Tehnikaülikool, Keemia ja biotehnoloogia instituut)

Õpetamiskogemus

Kevad 2025 ja 2026	Analüütiline keemia, praktikumid ja harjutustunnid (bakalaureuseõpe)
Sügis 2023	Füüsikaline orgaaniline keemia, harjutustunnid (magistriõpe)

ISSN 2585-6901 (PDF)
ISBN 978-9916-80-532-9 (PDF)